National Library of Canada
Bibliothèque nationale du Canada

Canadian Theses Service
Service des thèses canadiennes

Ottawa, Canada
K1A 0N4

NOTICE

The quality of this microform is heavily dependent upon the quality of the original thesis submitted for microfilming. Every effort has been made to ensure the highest quality of reproduction possible.

If pages are missing, contact the university which granted the degree.

Some pages may have indistinct print especially if the original pages were typed with a poor typewriter ribbon or if the university sent us an inferior photocopy.

Previously copyrighted materials (journal articles, published tests, etc.) are not filmed.

Reproduction in full or in part of this microform is governed by the Canadian Copyright Act, R.S.C. 1970, c. C-30.

AVIS

La qualité de cette microforme dépend grandement de la qualité de la thèse soumise au microfilmage. Nous avons tout fait pour assurer une qualité supérieure de reproduction.

S'il manque des pages, veuillez communiquer avec l'université qui a conféré le grade.

La qualité d'impression de certaines pages peut laisser à désirer, surtout si les pages originales ont été dactylographiées à l'aide d'un ruban usé ou si l'université nous a fait parvenir une photocopie de qualité inférieure.

Les documents qui font déjà l'objet d'un droit d'auteur (articles de revue, tests publiés, etc.) ne sont pas microfilmés.

La reproduction, même partielle, de cette microforme est soumise à la Loi canadienne sur le droit d'auteur, SRC 1970, c. C-30.

NL-339 (r. 88/04)

Canada

THE UNIVERSITY OF ALBERTA

THE TORSION OF MULTIPLY-CONNECTED INHOMOGENEOUS PRISMS

BY

(C) A. BOKHEUNG KIM

A THESIS

SUBMITTED TO THE FACULTY OF GRADUATE STUDIES AND RESEARCH

IN PARTIAL FULFILMENT OF THE REQUIREMENTS FOR THE DEGREE

OF

MASTER OF SCIENCE

DEPARTMENT OF MECHANICAL ENGINEERING

EDMONTON, ALBERTA

FALL, 1986

Permission has been granted to the National Library of Canada to microfilm this thesis and to lend or sell copies of the film.

The author (copyright owner) has reserved other publication rights, and neither the thesis nor extensive extracts from it may be printed or otherwise reproduced without his/her written permission.

L'autorisation a été accordée à la Bibliothèque nationale du Canada de microfilmer cette thèse et de prêter ou de vendre des exemplaires du film.

L'auteur (titulaire du droit d'auteur) se réserve les autres droits de publication; ni la thèse ni de longs extraits de celle-ci ne doivent être imprimés ou autrement reproduits sans son autorisation écrite.

ISBN 0-315-32318-3

THE UNIVERSITY OF ALBERTA

RELEASE FORM

Name of Author: *A. Bokheung Kim*

Title of Thesis: *The Torsion of Multiply-Connected Inhomogeneous Prisms*

Degree for which Thesis was Presented: *Master of Science*

Year This Degree Granted: *Fall, 1986*

Permission is hereby granted to The University of Alberta Library to reproduce single copies of this thesis and to lend or sell such copies for private, scholarly or scientific research purpose only.

The author reserves other publication rights, and neither the thesis nor extensive extracts from it may be printed or otherwise reproduced without the author's written permission.

Bokheung Kim

(*Signed*)

#280-9 Yongdu-2-ri, Sindo-eub
Koyang-kun, Kyungki-do 122-00
Republic of Korea

Date: April 23, 1986

THE UNIVERSITY OF ALBERTA

FACULTY OF GRADUATE STUDIES AND RESEARCH

The undersigned certify that they have read, and recommended to the Faculty of Graduate Studies and Research for acceptance, a thesis entitled **"The Torsion of Multiply-Connected Inhomogeneous Prisms,"** submitted by **A. Bokheung Kim** in partial fulfilment of the requirements for the degree of **Master of Science**.

(Supervisor)

Date: April 23, 1986

To My Family

ABSTRACT

The elastic torsion is characterized, mathematically, as one of the classical boundary value problems. Although well defined, it is generally not tractable by existing analytical methods for many practically important multiply-connected inhomogeneous cases. In the present study, the development of a solution method to cover more general types of such problem was first attempted, and then the optimal configuration of a prescribed cross-section maximizing the torsional rigidity under proportion constraints was considered.

The problem was formulated in terms of Prandtl stress function. As the solution procedure, the finite element method was employed in conjunction with a simple linear triangular element. For the treatment of general multiply-connected situations, two mathematical approaches were also introduced, those being the transformation and the superposition methods. The optimality conditions were determined through the method of numerical simulation of the membrane analogy. A computer algorithm was implemented based on the entire numerical procedure.

The accuracy as well as the reliability of the developed solution procedure was confirmed through various comparative numerical and experimental case studies. The results indicated that the numerical procedure is versatile and easily applicable to any arbitrary multiply-connected inhomogeneous situations and also that the optimization procedure is useable in an engineering sense. The solution procedure, thus verified, was then applied to some representative cases in torsion, and the optimal solutions obtained were presented both in the form of tables and figures.

It was observed from the results obtained that the optimalities of non-circular cross-sections tend to become as close as possible in shape to that of the circular case. For all cross-sections of different geometries in common, the optimalities of the cavity and the reinforcement were generally opposite to each other in their appearances.

The solution procedure and the result of the present study may be applied through analogies to the analysis of a number of other physical phenomena obeying similar linear partial differential equations.

ACKNOWLEDGEMENT

The author would like to express his sincere appreciation to both Dr. M. G. Faulkner and Dr. A. Mioduchowski for all their assistance and guidance in the successful completion of the present study; they have suggested the topic, provided financial support and supervised the progress of the research. The readability of this thesis, especially, is due to Dr. Faulkner who, despite his busy schedule as Chairman of the Department, made himself available for careful and patient review of each of the chapters.

To the Department of Mechanical Engineering, the author is thankful for the generous award of Teaching/Research Assistantships and a large sum of computing funds.

To Dr. T. M. Hrudey in the Department of Civil Engineering, the author extends his gratitude for his helpful comments.

To Chungang University, the author is indebted for helping him find an opportunity to further his studies at the University of Alberta.

To Luke and his family, the author offers his special thanks for their encouragement during his first years in Canada.

Most of all, the author reserves much of his thanks for his parents and family for their support throughout his academic career.

TABLE OF CONTENTS

Chapter		Page
1.	INTRODUCTION	1
	1.1 Historical Review on the Problem	1
	1.2 Preliminary to the Present Study	5
2.	STATEMENT OF THE PROBLEM	8
	2.1 Theoretical Background	8
	2.2 Optimization in Torsion	17
3.	PROCEDURE OF SOLUTION	19
	3.1 Finite Element Formulation	21
	3.2 Treatment of the Multiple-Connection	34
	3.2.1 The Transformation Method	39
	3.2.2 The Superposition Method	42
	3.3 Determination of the Optimality	53
	3.4 Organization of the Computer Program	57
4.	VERIFICATION OF THE SOLUTION PROCEDURE	61
	4.1 Test of the Numerical Procedure	62
	4.2 Test of the Optimization Procedure	75
5.	SOLUTIONS TO THE PROBLEM	83
	5.1 The Equilateral Triangular Cross-Section	90
	5.2 The Regular Square Cross-Section	94
	5.3 The Regular Hexagonal Cross-Section	98
6.	DISCUSSION	102
	6.1 Discussion of the Numerical Procedure	102
	6.2 Discussion of the Optimization Procedure	105
	6.3 Discussion of the Results	110
7.	CONCLUSIONS	116
	REFERENCES	119
	APPENDIX	127

LIST OF TABLES

Table		Page
3.1	General Relationship among Parameters Involved in the Superposition Method	43
3.2	Detailed Functions of the Torsional Optimization Computer Program Units	60
4.1	Comparison between the Analytical and the Present Finite Element Torsional Rigidity Solutions for a Solid Homogeneous Equilateral Triangular Cross-Section	63
4.2	Comparison between the Series and the Present Finite Element Torsional Rigidity Solutions for a Solid Homogeneous Regular Square Cross-Section	64
4.3	Comparison between the Previous and the Present Finite Element Torsional Rigidity Solutions for a Solid Inhomogeneous Regular Square Cross-Section at Three Representative Proportions of the Reinforcement	65
4.4	Comparison of the Boundary Constant Values Obtained by the Use of the Transformation and the Superposition Methods for a Doubly-Connected Homogeneous Square Cross-Section under Torsion	66
4.5	Comparison of the Contour Integral Values Resulted from the Use of the Transformation and the Superposition Methods for a Doubly-Connected Homogeneous Square Cross-Section under Torsion	67
4.6	Comparison between the Previous Hypercircle and the Present Finite Element Torsional Rigidity Solutions for a Doubly-Connected Homogeneous Square Cross-Section	67
4.7	Comparison of the Boundary Constant Values Obtained by the Use of the Transformation and the Superposition Methods for a Thin-Walled Homogeneous Hexagonal Cross-Section under Torsion	69
4.8	Comparison of the Contour Integral Values Resulted from the Use of the Transformation and the Superposition Methods for a Thin-Walled Homogeneous Hexagonal Cross-Section under Torsion	69
4.9	Comparison between the Approximate Membrane Analogy and the Present Finite Element Torsional Rigidity Solutions for a Thin-Walled Homogeneous Hexagonal Cross-Section	69

4.10 Comparison between the Exact and the Present Finite Element Torsional Rigidity Solutions for a Solid Homogeneous Circular Cross-Section · · · · · · · 77

4.11 Comparison between the Exact and the Present Finite Element Optimal Torsional Rigidity Solutions for a Hollow Homogeneous Circular Cross-Section at Three Representative Proportions of the Cavity · · · · · · · · 78

4.12 Comparison between the Exact and the Present Finite Element Optimal Torsional Rigidity Solutions for a Solid Composite Circular Cross-Section at Three Representative Proportions of the Reinforcement · · · · · · · · · · · · 78

4.13 Comparison between the Previous and the Present Finite Element Optimal Torsional Rigidity Solutions for a Solid Inhomogeneous Equilateral Triangular Cross-Section at Two Representative Proportions of the Reinforcement · · · · 80

4.14 Comparison between the Previous and the Present Finite Element Optimal Torsional Rigidity Solutions for a Solid Inhomogeneous Regular Square Cross-Section at Two Representative Proportions of the Reinforcement · · · · 82

5.1 Optimal Torsional Rigidity for the Hollow Composite Circular Cross-Section at Various Proportions of the Cavity and of the Reinforcement · · · · · · · · 86

5.2 Optimal Torsional Rigidity for the Hollow Composite Equilateral Triangular Cross-Section at Various Proportions of the Cavity and of the Reinforcement · 90

5.3 Optimal Torsional Rigidity for the Hollow Composite Regular Square Cross-Section at Various Proportions of the Cavity and of the Reinforcement · 94

5.4 Optimal Torsional Rigidity for the Hollow Composite Regular Hexagonal Cross-Section at Various Proportions of the Cavity and of the Reinforcement · 98

6.1 Variation of the Number of Contours for Some Typical Optimally-Shaped Hollow Homogeneous Regualr Cross-Sections at Various Proportions of the Cavity · 111

LIST OF FIGURES

Figure		Page
2.1	Torsion of a Multiply-Connected Inhomogeneous Prism	8
2.2	A Typical Hollow Composite Cross-Section under Torsion	17
3.1	Finite Element Representation of a Cross-Section under Torsion	21
3.2	A Generic Multiply-Connected Region	34
3.3	Schematic Diagram of the Transformation Method	40
3.4	Graphical Interpretation of the Concept of the Superposition Method	50
3.5	Schematic View of the Torsional Optimization in the Present Study	53
3.6	Four Different Paths Used to Ensure the Uniqueness of the Solution in the Present Optimization Procedure	56
3.7	Flow-Chart of the Main Torsional Optimization Program "TOROPT"	58
3.8	Organization of the Torsional Optimization Computer Program	59
4.1	A Solid Homogeneous Equilateral Triangular Cross-Section under Torsion	62
4.2	A Solid Homogeneous Regular Square Cross-Section under Torsion	63
4.3	A Solid Bi-Composite Regular Square Cross-Section under Torsion	64
4.4	A Doubly-Connected Homogeneous Regular Square Cross-Section under Torsion	66
4.5	A Thin-Walled Homogeneous Regular Hexagonal Tube under Torsion	68
4.6	A Hollow Composite Equilateral Triangular Cross-Section under Torsion	70
4.7	Display of the Stress Function Surface for a Hollow Composite Equilateral Triangular Cross-Section	71

4.8 Effect of the Number of Elements on the Convergence of the Finite Element Torsional Rigidity Solution for a Solid Homogeneous Square Cross-Section · · · · · · · · · · · · · · · 73

4.9 Optimal Configuration of the Hollow Composite Circular Cross-Section under Torsion · · · · · · · · · · · · · · · · · · · 76

4.10 Geometric Domain Substitution for the Finite Element Approximation of the Circular Cross-Section · · · · · · · · · · · · · · · 76

4.11 Two Different Optimal Configurations Obtained by the Previous and the Present Optimization Procedures for a Solid Inhomogeneous Equilateral Triangular Cross-Section under Torsion · · · · · · · · · · · · · · · · · 79

4.12 Two Different Optimal Configurations Obtained by the Previous and the Present Optimization Procedures for a Solid Inhomogeneous Regular Square Cross-Section under Torsion · 81

5.1 A Generic Finite Element Mesh for the Solutions of Various Regular-Shaped Cross-Sections under Torsion · · · · · · · · · · · · · 83

5.2 Three-Dimensional Display of the Relative Optimal Torsional Rigidity Values for the Hollow Composite Circular Cross-Section at Various Proportions of the Cavity and of the Reinforcement ($G_2/G_1=2, 5$) · 86

5.3 A Hollow Composite Regular Square Cross-Section under Torsion for the Determination of the Optimal Configuration · · · · · · · 88

5.4 An Example-Use of the Present Results for the Determination of the Optimal Configuration of a Hollow Composite Regular Square Cross-Section under Torsion · 89

5.5 Three-Dimensional Display of the Relative Optimal Torsional Rigidity Values for the Hollow Composite Equilateral Triangular Cross-Section at Various Proportions of the Cavity and of the Reinforcement ($G_2/G_1=2, 5$) · 90

5.6 Optimal Configuration of the Hollow Homogeneous Equilateral Triangular Cross-Section under Torsion at Various Proportions of the Cavity · · · · · · · 91

5.7 Optimal Configuration of the Solid Composite Equilateral Triangular Cross-Section under Torsion at Various Proportions of the Reinforcement ($G_2/G_1=2$) · 92

5.8 Optimal Configuration of the Solid Composite Equilateral Triangular Cross-Section under Torsion at Various Proportions of the Reinforcement ($G_2/G_1=5$) · 93

5.9 Three-Dimensional Display of the Relative Optimal Torsional Rigidity Values for the Hollow Composite Regular Square Cross-Section at Various Proportions of the Cavity and of the Reinforcement ($G_2/G_1=2, 5$) 94

5.10 Optimal Configuration of the Hollow Homogeneous Regular Square Cross-Section under Torsion at Various Proportions of the Cavity 95

5.11 Optimal Configuration of the Solid Composite Regular Square Cross-Section under Torsion at Various Proportions of the Reinforcement ($G_2/G_1=2$) 96

5.12 Optimal Configuration of the Solid Composite Regular Square Cross-Section under Torsion at Various Proportions of the Reinforcement ($G_2/G_1=5$) 97

5.13 Three-Dimensional Display of the Relative Optimal Torsional Rigidity Values for the Hollow Composite Regular Hexagonal Cross-Section at Various Proportions of the Cavity and of the Reinforcement ($G_2/G_1=2, 5$) 98

5.14 Optimal Configuration of the Hollow Homogeneous Regular Hexagonal Cross-Section under Torsion at Various Proportions of the Cavity 99

5.15 Optimal Configuration of the Solid Composite Regular Hexagonal Cross-Section under Torsion at Various Proportions of the Reinforcement ($G_2/G_1=2$) 100

5.16 Optimal Configuration of the Solid Composite Regular Hexagonal Cross-Section under Torsion at Various Proportions of the Reinforcement ($G_2/G_1=5$) 101

6.1 Relative Increment in the Torsional Rigidity of a Solid Regular Square Cross-Section with Each of the Constituent Elements Replaced by the Reinforcement ($G_2/G_1=3$) 106

6.2 Relative Decrement in the Torsional Rigidity of a Homogeneous Regular Square Cross-Section with Each of the Constituent Elements Replaced by the Cavity 107

6.3 Relative Optimal Torsional Rigidity Values for Some Typical Hollow and Composite Equal-Area Regular Cross-Sections at Various Proportions of the Cavity and of the Reinforcement 112

6.4 Relative Torsional Rigidity Values for Homogeneous Equal-Area n-Sided Regular Cross-Sections 114

1 INTRODUCTION

1.1 HISTORICAL REVIEW ON THE PROBLEM

[The Torsion Problem] Torsion is involved in a large class of engineering problems in a diversity of ways, and it is one of the well-defined classical problems in the field of applied mathematics.

Historically, the first mathematical model of the torsion problem was due to Coulomb [15][1] in 1784. The general applicability of this old theory of torsion, however, was put into question when Navier [55] later found that Coulomb's assumption led to erroneous results for non-circular cross-sections.

It was then by the introduction of so-called semi-inverse method that in 1853 Saint-Venant [78] extended Coulomb's theory and thereby established a concrete theoretical basis for the mathematical treatment of the problem. The conclusion arrived at by Saint-Venant was that the torsion problem can be reduced to a very commonly appearing Dirichlet type boundary value problem.

[Solutions to the Problem] Ever since the Saint-Venant's discovery, the torsion problem has drawn a great deal of attention not only from engineers because of the direct practical importance of application, but also from mathematicians because of the purely theoretical importance in relation to some other physical problems in the same mathematical category.

As a result of these continued efforts by various investigators through the history of classical theory of elasticity, solutions to most of the practical problems are now available for many simply-connected, isotropic, homogeneous, elastic, prismatic and regular

[1] *refers to the literature number in the References.*

cross-sections. Nonetheless, there still remain to be solved a number of problems involving multiple-connection, anisotropy, inhomogeneity, plasticity, nonprismacy and/or geometric irregularity.

The major approaches in the analysis of the torsion problem have been first to find analytical solutions, and then experimental and numerical.

[Analytical Approaches] Analytical methods were employed from the very beginning as the most natural way of obtaining solutions to the torsion problem.

One of the first major advances in this direction was providing the theory of torsion with more mathematical completeness. This was accomplished in 1871 when Boussinesq [8] derived the integral condition which is indispensable for the treatment of more general multiply-connected cross-sections. Following this was the development of a series of exact solutions for various simple problems as is well summarized by Timoshenko [77] or Love [49].

General accounts of the theory for the torsion of cross-sections involving inhomogeneity and anisotropy were also given by Muskhelishvili [53] and by Lekhnitskii [47], respectively. More recently, a solution for the torsion of multi-layered rectangular cross-section was presented by Booker and Kitipornchai [6], and the torsion of the circular bar having multiple rings of circular holes was considered by Kuo and Conway [45] using the hypercircle method.

Generally, the existing analytical solutions are confined to rather trivial cases of geometry and inhomogeneity without even considering the multiple-connection. This is due mainly to the mathematical difficulties involved in dealing with the governing differential equations. As a result, any further development in this direction in the solution of the torsion problem seems very unlikely.

[Experimental Approaches] With the realization of the limitations of the analytical methods available for the solution of the torsion problem, experimental efforts were

employed based on various analogies.

Most widely used among these was the membrane analogy which originally was suggested by Prandtl [62] in 1903. The practical applicability of this analogy to the elastic torsion problem was confirmed first by Anthes [1]; this was soon followed by systematic applications to simply- and then finally to multiply-connected cross-sections by Taylor and Griffith [75,76].

As an alternative to the membrane analogy, a hydrodynamic analogy was also presented by Pestel [7]. For the plastic torsion problem, Nádai [54] proposed the sand-hill analogy, which later was combined with the membrane analogy to cover the elastic-plastic torsion problem. Extension of this sand-hill analogy for the fully plastic torsion of multiply-connected sections was due to Sadowsky [68].

While still of much importance especially in connection with the visualization of the problem, the experimental methods for the solution of the torsion problem are now essentially obsolete in practice because of the unavoidable experimental difficulties and errors involved.

[**Finite Difference Approach**] The first numerical technique employed for the approximate solution of the torsion problem was the finite difference method.

Christopherson and Southwell [11] became the pioneer investigators in this direction when, in 1938, they adopted this numerical approach for the solution of the elastic-plastic torsion problem of simply-connected cross-sections. The basis of their approach was borrowed from the previous experimental methods. More extensive application of the numerical technique to homogeneous cross-sections with both simply- and multiply-connected boundaries was due to Shaw [70]. Recent progress in this category includes the examination of both homogeneous and inhomogeneous cross-sections with simply- and multiply-connected boundaries by Ely and Zienkiewicz [20].

Although being powerful enough for simpler classes of problems, the finite difference method is generally believed not to be very suitable for the analysis of more advanced

types of problems, and hence not preferred as a general method of solution. In particular for the torsion problem, this is because of the unique difficulties arising from the special requirements in treating complicated geometries, multiple-connections and/or inhomogeneities of the cross-section.

[Finite Element Approach] An alternative numerical technique applied to the approximate solution of the torsion problem was the finite element method, which offered much more versatility in many ways than the rival finite difference method.

The first introduction of this method to the solution of the torsion problem was by Courant [16] in 1943 for the torsion of a simply-connected cross-section. Following this, there was a sequence of suggestions and developments of various finite element models for the analysis of many different types of problems in torsion. A piecewise linear stress function approach was devised by Synge and Cahill [74] for the solution of a hollow square prism. Zienkiewicz and Cheung [83] made a more general and systematic application of the same approach to the solution of homogeneous and inhomogeneous sections with isotropy. Based on the warping function approach, a displacement formulation was also developed by Herrmann [33] and applied extensively by Hodge et al. [36] in their study of the elastic-plastic torsion of prisms with both simply- and multiply-connected cross-sections. More recently, in an effort to overcome some of the deficiencies arising from the use of either the stress function or the displacement formulation, a hybrid stress approach was devised by Pian [59,60] and further developed by Yamada et al. [82]. As well, a mixed approach was introduced by Noor and Andersen [56] with the same purpose in mind.

Not only because of its flexibility in the mapping of more realistic complex boundaries, but also because of the ease of treating inhomogeneity and multiple-connection, the finite element method is considered to be the best approach available for the solution of the torsion problem; therefore, this numerical technique serves presently as the most widely used approximation procedure for the analysis of the torsion problem.

1.2 PRELIMINARY TO THE PRESENT STUDY

[Torsion as an Optimization Problem] It is often the case that the optimization of a certain engineering system can be considered rigorously only after a sufficient background knowledge on the subject has been established. Of no less importance in this regard is the availability of parallel developments in a wide variety of other related fields.

Unlike many other optimization problems in the same area of solid mechanics, the ultimate optimal solution to the torsion problem was, in a way, known already and had been applied accordingly to the structure mechanics even long before the problem was precisely formulated; the simple circular shape is the one that provides an isotropic cross-section with the maximum torsional rigidity under the area constraint.

[Renewed Interest on the Torsional Optimization] While the early realization that the circle is optimum among various cross-sectional shapes may be part of the answer to why the optimization problem for non-circular sections has not yet been fully examined, the more obvious reason is the absence of general mathematical methods available for the treatment of this type of problems. As structural elements which are complicated in geometry as well as in composition are already in very common use, the investigation of optimization problems of this sort becomes much more important.

[Various Studies on the Torsional Optimization] The optimization of many different aspects of the torsion problem have been considered by using several different methods at various stages during the theoretical development of the problem.

The first recorded investigators in this direction are Polya et al. [61], who in 1951 considered the optimal shape of the external boundary of a solid elastic prism under torsion; they thereby made a theoretical confirmation that the circular prism has the maximum torsional rigidity among all the isotropic solid ones of the equal cross-sectional

area. A graphical method was introduced by Mioduchowski [50] for the determination of the optimal inhomogeneity of a perfectly plastic prismatic bar. Klosowicz and Lurie [43] also examined the optimal inhomogeneity of an elastic prism made of two materials which are different in shear modulus. In the investigation of the optimization problems of anisotropic elastic bars and of homogeneous bars with multiply-connected sections, Banichuk [3] employed a perturbation technique and as a result revealed that for elastic bars of transverse anisotropy the elliptic cross-section has the maximum torsional rigidity among all the sections of the same area. Recently, a complex potential method was used by Kurszin and Onoprijenko [46] to find the optimal shape of the external boundary of an isotropic bar, while a shape parameter method was applied by Dems [17] to determine the optimal shape of the internal and the external boundaries of an elastic bar. Very recently, in the study of the optimal jump inhomogeneity of composite bars, Faulkner, Mioduchowski and Hong [21,22] used the finite element method based on the hybrid stress approach. In this case, the optimization problem was formulated as a variational problem to derive a necessary condition for the optimality.

While the optimal inhomogeneity of a cross-section under torsion has been examined extensively, no optimal multiple-connection of such a problem has yet been investigated not to mention the optimality with both the inhomogeneity and the multiple-connection together. The resolution of these unsolved problems is entirely dependent upon the development of versatile mathematical means for the treatment of multiple-connection—in mathematical terms, a method to deal with the multiple boundary value problem.

[The Present Study] The present study is concerned with the problem of optimization of a multiply-connected inhomogeneous cross-section which with a prescribed shape of the external boundary is subject to elastic torsion.

Considered first in the study is the theoretical aspect together with the general formulation of the problem. The solution procedure employs the finite element approach based on the stress function formulation in close conjunction with the membrane analogy.

As well, two mathematical methods for the treatment of multiple-connection are introduced in the present study, those being the transformation and the superposition methods. The condition of optimality is determined through the implementation of numerical simulation of the membrane analogy. A computer algorithm is also developed accordingly on the basis of the foregoing procedure.

In order to verify the solution procedure developed, it is applied to several example problems which either have analytical solutions or have been solved using numerical approximation techniques by previous investigators. Optimal solutions to a few selected typical cross-sections of practical importance are then obtained by using the procedure for some representative shear modulus ratios. Being compared with those of the circular case, these numerical results are summarized both in the form of tables and figures. The limitations of the solution method and of the results are detailed in the discussion part, which is followed by overall conclusions drawn from the present study.

2 STATEMENT OF THE PROBLEM

2.1 THEORETICAL BACKGROUND

[Mathematical Model of the Problem] Shown in Figure 2.1.1, a long, isolated prism is subject to a pure torque applied at its both ends in a rectangular cartesian coordinate system (x,y,z). It is assumed that the prism has no variation of its geometry and of material properties along the entire length and that it behaves only within the elastic range.

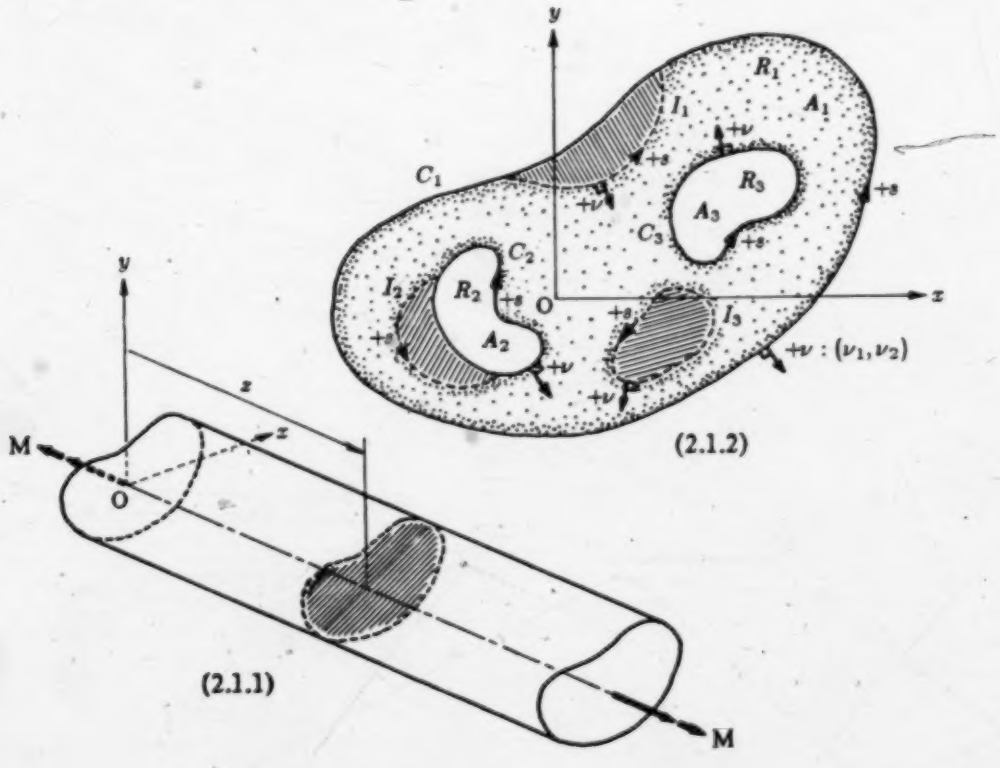

Figure 2.1: Torsion of a Multiply-Connected Inhomogeneous Prism

The cross-section of the prism may have any arbitrary shape, be multiply-connected, and include inhomogeneities. Each of the materials composing the cross-section is considered to be isotropic and to have constant but distinct shear modulus:

$$G \equiv G(x,y) = G_i \qquad (x,y) \in R_i, \quad i = 1,2 \cdots NR \tag{2.1}$$

The application of Saint-Venant's principle allows the details of the end load condition to be ignored. As a result, the state of the deformation of the prism may be assumed to be independent of location along the axis of twist with the result that the problem simplifies mathematically to a two-dimensional one. It follows, therefore, that the behaviour of the prism under torsion can be described completely by examination of any generic cross-section such as the one illustrated in Figure 2.1.2.

[Formulation of the Problem] As is generally the case for all elasticity problems, it is necessary that an acceptable solution to this torsion of a prism should also simultaneously satisfy the six strain–displacement relations, the six stress–strain relations, the three equations of equilibrium and possibly the six compatibility equations. In addition, the interface and the boundary conditions particular to this problem must be considered at the same time.

With the general formulation based solely on these equations and conditions, considerable mathematical difficulties are unavoidable for a direct solution. In order to bypass these difficulties, the semi-inverse formulation of Saint-Venant will be employed. Under this hypothesis, the cross-section experiences a combined deformation of both in-plane rotation and out-of-plane distortion, in which the latter part is characterized by the unknown warping function:

$$\psi \equiv \psi(x,y) \tag{2.2}$$

This leads to the assumption of the displacement vector $\lfloor \underline{u} \;\; \underline{v} \;\; \underline{w} \rfloor$ in the form:

$$\begin{Bmatrix} u \\ v \\ w \end{Bmatrix} \equiv \begin{Bmatrix} u(y,z) \\ v(x,z) \\ w(x,y) \end{Bmatrix} = \alpha \begin{Bmatrix} -yz \\ xz \\ \psi \end{Bmatrix} \tag{2.3}$$

where α denotes the angle of twist per unit length of the prism.

The formulation of the problem hereafter is based on this pre-determined form of displacement vector. As a consequence, the need to check the six compatibility equations is eliminated, and the following can be identified as the equations and conditions to be satisfied by the assumed displacement solution:

EQUATIONS OF ELASTICITY

(1) Cauchy's Strain–Displacement Relations.

(2) Generalized Hooke's Law.

(3) Navier's Equations of Equilibrium.

INTERFACE CONDITIONS

(4) Static Equilibrium at Each of the Interfaces.

(5) Displacement Continuity across Each of the Interfaces.

BOUNDARY CONDITIONS

(6) No Traction on Every Free Surface.

(7) Single-Valued Displacement along Each of the Contours.

(8) No Resultant Force on the Cross-Section.

(9) Resultant Moment—Applied Torque Equivalence on the Cross-Section.

[Strain–Displacement Relations] The six strain–displacement relations, when combined with the displacement expression of Equation 2.3, reduce to:

$$\begin{Bmatrix} \epsilon_{xz} \\ \epsilon_{yz} \end{Bmatrix} = \frac{1}{2} \begin{bmatrix} \frac{\partial}{\partial x} & 0 & \frac{\partial}{\partial z} \\ 0 & \frac{\partial}{\partial z} & \frac{\partial}{\partial y} \end{bmatrix} \begin{Bmatrix} u \\ v \\ w \end{Bmatrix} = \frac{\alpha}{2} \begin{Bmatrix} -y + \frac{\partial \psi}{\partial x} \\ x + \frac{\partial \psi}{\partial y} \end{Bmatrix} \tag{2.4}$$

where ϵ_{xz} and ϵ_{yz} are the two non-vanishing components of the strain tensor.

[Stress–Strain Relations] Substitution of Equation 2.4 into the six elastic stress–strain relations gives:

$$\begin{Bmatrix} \tau_{zx} \\ \tau_{yz} \end{Bmatrix} \equiv \begin{bmatrix} G & 0 \\ 0 & G \end{bmatrix} \begin{Bmatrix} \epsilon_{zx} \\ \epsilon_{yz} \end{Bmatrix} = G\alpha \begin{Bmatrix} -y + \dfrac{\partial \psi}{\partial x} \\ x + \dfrac{\partial \psi}{\partial y} \end{Bmatrix} \tag{2.5}$$

where τ_{zx} and τ_{yz} are the corresponding stress tensor components.

[Governing Differential Equation] Under the assumption that the inertia effects and the body forces applied to the prism are negligible, the three equations of equilibrium together with Equation 2.5 then yield the following Laplace equation:

$$\Delta \psi \equiv \nabla^2 \psi \equiv \frac{\partial^2 \psi}{\partial x^2} + \frac{\partial^2 \psi}{\partial y^2} = 0 \tag{2.6}$$

An alternative form of this expression—the Poisson's type—furnishes several distinct advantages such as the considerably simplified boundary conditions and the availability of various analogies for the visualization of the problem. This can be obtained through the introduction of the Prandtl stress function:

$$\phi \equiv \phi(x, y) \tag{2.7}$$

In this case, the two non-zero components of the stress tensor are defined as first derivatives of the stress function in such a way that the equations of equilibrium are all automatically satisfied:

$$\begin{Bmatrix} \tau_{zx} \\ \tau_{yz} \end{Bmatrix} \equiv \begin{Bmatrix} \dfrac{\partial \phi}{\partial y} \\ -\dfrac{\partial \phi}{\partial x} \end{Bmatrix} = G\alpha \begin{Bmatrix} -y + \dfrac{\partial \psi}{\partial x} \\ x + \dfrac{\partial \psi}{\partial y} \end{Bmatrix} \tag{2.8}$$

The magnitude and the direction of the resultant stress at any point thus are given respectively by:

$$|\tau| \equiv \sqrt{\tau \cdot \tau} = \sqrt{\left(\frac{\partial \phi}{\partial x}\right)^2 + \left(\frac{\partial \phi}{\partial y}\right)^2} \tag{2.9}$$

and

$$\angle\tau = \tan^{-1}\left[-\frac{\partial\phi}{\partial y} \Big/ \frac{\partial\phi}{\partial x} \right] \tag{2.10}$$

Combination of Equations 2.3, 2.5 and 2.7, and elimination of the warping function from these by appropriate differentiation and subtraction yield the following linear partial differential equation of elliptical type:

$$\frac{\partial}{\partial x}\left(\frac{1}{G}\frac{\partial\phi}{\partial x}\right) + \frac{\partial}{\partial y}\left(\frac{1}{G}\frac{\partial\phi}{\partial y}\right) + 2\alpha = 0 \tag{2.11}$$

This is the governing differential equation of the torsion of a prism in terms of the Prandtl stress function. In the event of the homogeneous cross-section, it can be easily seen that this reduces to a familiar Poisson's equation:

$$\Delta\phi \equiv \nabla^2\phi \equiv \frac{\partial^2\phi}{\partial x^2} + \frac{\partial^2\phi}{\partial y^2} = -2\alpha G \tag{2.12}$$

The analogy of Equation 2.12 to the one that represents the inflated surface of a thin elastic membrane is now apparent by identifying:

$$\varphi \equiv \phi, \quad p \equiv 2\alpha \quad \& \quad T \equiv \frac{1}{G} \tag{2.13}$$

where φ is the transverse deflection of the membrane surface, p the external pressure applied on it, and T the tension per unit length of the membrane.

[Equilibrium at Interfaces] At each of the interfaces where discontinuous variations of the material properties occur, the condition of static equilibrium requires that the stress components normal to the interface be equal not only in magnitude but also in direction, i.e.:

$$\frac{\partial\phi}{\partial s}\Big)_{-} = \frac{\partial\phi}{\partial s}\Big)_{+} \qquad (x,y) \in I_i, \quad i = 1,2\cdots \mathrm{NI} \tag{2.14}$$

where s is taken along the path of the curve; and the subscripts, $-$ and $+$, imply the inward and the outward directions to the surface, respectively. It may be shown that this condition can be satisfied easily by making:

$$\phi)_- = \phi)_+ \qquad (x,y) \in I_i, \quad i = 1,2 \cdots \mathrm{NI} \tag{2.15}$$

[Displacement Continuity across Interfaces] Because a perfect bonding is assumed to exist at each of the interfaces, there is an additional requirement for the continuity of axial displacements:

$$\frac{\partial w}{\partial s}\Big)_- = \frac{\partial w}{\partial s}\Big)_+ \qquad (x,y) \in I_i, \quad i = 1,2 \cdots \mathrm{NI} \tag{2.16}$$

Upon substitution of Equations 2.3, 2.5 and 2.7, this expression becomes equivalent to:

$$\frac{1}{G}\frac{\partial \phi}{\partial \nu}\Big)_- = \frac{1}{G}\frac{\partial \phi}{\partial \nu}\Big)_+ \qquad (x,y) \in I_i, \quad i = 1,2 \cdots \mathrm{NI} \tag{2.17}$$

where ν is the unit normal vector directed outwards to the interface.

[No Traction on Free Surfaces] The condition that every free lateral surface of the prism is subject to no normal component of the resultant shear stress yields:

$$\tau \cdot \nu = \left[\frac{\partial \phi}{\partial y} \quad -\frac{\partial \phi}{\partial x} \right] \begin{Bmatrix} \frac{dy}{ds} \\ -\frac{dx}{ds} \end{Bmatrix} = \frac{d\phi}{ds} = 0 \tag{2.18}$$

or equivalently:

$$\phi = \text{Constant} \qquad (x,y) \in C_i, \quad i = 1,2 \cdots \mathrm{NC} \tag{2.19}$$

The shear stress distribution across the cross-section is not affected by the value of each of these contour constants. Hence, there is no loss of generality even though one of the constants is set to zero such that:

$$\phi = \begin{cases} 0 & (x,y) \in C_i, \quad i = 1 \\ \phi_i & (x,y) \in C_i, \quad i = 2,3 \cdots \text{NC} \end{cases} \tag{2.20}$$

where ϕ_i are unknown boundary constants.

In the membrane analogy, this requirement imposes a constant deflection on the inflated surface along each of the boundary contour curves. It happens that every one of the internal contours encloses the cavity regions; within each of these regions, the shear modulus can be assumed to be zero, hence the stress function accordingly being constant everywhere. It follows, therefore, that this condition further relates to the weightless flat plates which with the same boundary shapes as the respective internal contours are floating horizontally on the top of the membrane surface.

[Single-Valued Displacements along Contours] In order that the axial displacement is single-valued along each of the boundary contour lines, it is necessary that the following line integral condition hold:

$$\oint dw = \oint \left(\frac{\partial w}{\partial x} dx + \frac{\partial w}{\partial y} dy \right) = 0 \qquad (x,y) \in C_i, \quad i = 1,2 \cdots \text{NC} \tag{2.21}$$

By the use of Equations 2.3, 2.5 and 2.7, this can be shown to result in:

$$\oint \frac{1}{G} \tau_s ds \equiv \oint \frac{1}{G} \left(-\frac{\partial \phi}{\partial \nu} \right) ds = 2\alpha A_i \qquad (x,y) \in C_i, \quad i = 1,2 \cdots \text{NC} \tag{2.22}$$

where τ_s is the tangential component of the shear stress along the path, and A the area of the region bounded by the closed curve.

In terms of the membrane analogy, this expression can be interpreted as the condition of vertical static equilibrium of the floating plate which was mentioned previously.

[No Resultant Force on the Cross-Section] . The resultant shear force vector V acting on the cross-section under torsion can be determined by:

$$V \equiv \iint \lfloor \tau_{zx} \quad \tau_{yz} \rfloor \, dx\, dy = \iint \lfloor \frac{\partial \phi}{\partial y} \quad -\frac{\partial \phi}{\partial x} \rfloor \, dx\, dy \qquad (x,y) \in R_1 \tag{2.23}$$

where R_1 is the region enclosed by the external boundary curve C_1. With the assistance of Green's theorem, the result of this integration may be shown to be:

$$V \equiv \lfloor V_x \quad V_y \rfloor = 0 \tag{2.24}$$

thus confirming that the no-resultant-force condition is always satisfied on the cross-section.

[Resultant Moment—Applied Torque Equivalence] Finally, the requirement that the resultant moment M acting on the cross-section should be equal in magnitude to the applied torque gives:

$$M \equiv \iint \lfloor \tau_{zx} \quad \tau_{yz} \rfloor \begin{Bmatrix} -y \\ x \end{Bmatrix} dx\, dy = \iint \lfloor \frac{\partial \phi}{\partial y} \quad -\frac{\partial \phi}{\partial x} \rfloor \begin{Bmatrix} -y \\ x \end{Bmatrix} dx\, dy \qquad (x,y) \in R_1 \tag{2.25}$$

Again, application of Green's theorem yields:

$$M = 2\left[\iint \phi \, dx\, dy + \sum_{i=2}^{NC} \phi_i A_i\right] \qquad (x,y) \in R_1 \tag{2.26}$$

From the viewpoint of the membrane analogy, it can be easily concluded that this is equal in magnitude to twice the volume bounded between the inflated surface and the xy plane.

On the other hand, this torsional moment is linearly related to the angle of twist per unit length of the prism through:

$$Z \equiv \frac{M}{\alpha} = \frac{2}{\alpha}\left[\iint \phi \, dx\, dy + \sum_{i=2}^{NC} \phi_i A_i\right] \qquad (x,y) \in R_1 \tag{2.27}$$

where Z is defined as the torsional rigidity of the cross-section.

[Summary of the Formulation] In formulating the torsion of a prism by end couples, a mode of deformation was assumed. It was shown, as a consequence, that the solution of the torsion problem amounts to the finding of the Prandtl stress function which satisfies an elliptic partial differential equation. For the unique solution of the problem, a sufficient number of interface and boundary conditions were also derived accordingly. With the stress function solution obtained, the state of stress and the torque can be readily determined.

Most of all, visualization of the problem was found possible by the introduction of the analogy of the inflated membrane, which may be further extended to various field problems such as the potential flow, the seepage, the conduction heat transfer, the electric conduction, etc..

2.2 OPTIMIZATION IN TORSION

[A Hollow Composite Cross-Section] Figure 2.2 illustrates a generic hollow composite cross-section under torsion.

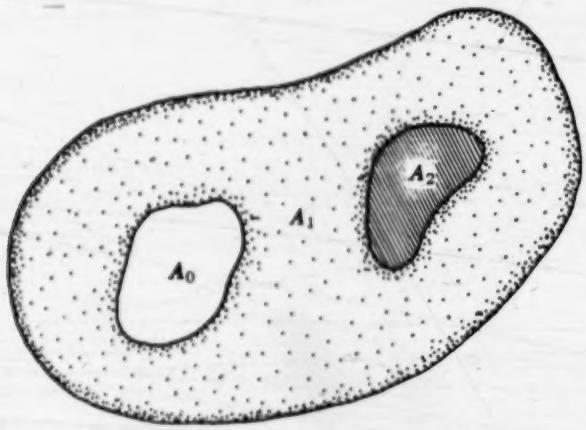

Figure 2.2: A Typical Hollow Composite Cross-Section under Torsion

[The Mathematical Model] In mathematically modelling the multiply-connected composite cross-section above, it is assumed that the shear modulus function varies in the following jump-like manner:

$$G \equiv G(x,y) = \begin{cases} G_0 & (x,y) \in A_0 \\ G_1 & (x,y) \in A_1 \\ G_2 & (x,y) \in A_2 \end{cases} \qquad (2.28)$$

where

$$0 \simeq G_0 < G_1 < G_2 \qquad (2.29)$$

and

$$A = A_0 + A_1 + A_2 \qquad (2.30)$$

[Torsional Optimization] The optimization aspect of the torsion problem derives from the fact that the torsional rigidity of a cross-section varies depending on the composition and also on the geometric configuration. The objective of general torsional optimizations, therefore, is to find the cross-sectional shape for which the torsional rigidity attains the maximum value possible, i.e.:

$$Z(G) \xrightarrow{\text{Maximum}} Z^*(G^*) \tag{2.31}$$

[Various Constraints Applicable] With no constraints applied to the above cross-section at all, the optimal configuration will simply be a circular one having the cavity and the reinforcement at the core and at the outer layer, respectively. Otherwise, however, the optimal solutions will take different forms depending on the nature of the constraints imposed.

There are indeed a number of conditions that can be used alone or in combination as such constraints. These include the shape, the number and the location of the internal and/or the external boundary contours, and the material interfaces. As well, the proportions of the cavity and of the reinforcement can be varied, and these will result in different optimal solutions.

[The Constraints Considered in the Present Study] Among all the above possibilities, two of the more fundamental constraints that yet best describe many of the common practical situations are considered in the present study; the shape of the external boundary is prescribed, while the proportions of the cavity and the reinforcement are fixed.

The problem is, therefore, equivalent to seeking the optimal distribution of the cavity and of the reinforcement inside the specified external boundary so that the amount of the materials can be utilized most effectively while producing the maximum torsional rigidity possible.

3 PROCEDURE OF SOLUTION

It has been shown in the previous chapter that, mathematically, the solution of the torsion problem is equivalent to seeking Prandtl stress function over the cross-section under consideration. In finding the explicit form of this function, however, there is as yet no known general analytical approach that is equally applicable to any type of assigned cross-section. This is principally due to the mathematical difficulties in simultaneously satisfying the governing differential equation with the interface and the boundary conditions.

[Finite Element Approach] Through the history of torsional analysis, there have emerged nevertheless several methods of solution. The most powerful among these, as was remarked earlier, is the finite element approach. Indeed, for the particular problem of torsion, this elementwise-formulated numerical technique as applied to the exact theory provides a number of advantages over any other methods. These include:

(1) No restriction on the geometric configuration of the cross-section which can be dealt with.

(2) No special treatment necessary for inhomogeneous as well as for multiply-connected situations.

(3) No consideration of interface conditions required because of identical satisfaction.

(4) No limitation on the freedom of choice of element shapes for various problems of different characteristics.

[Selection of the Element] As for the selection of the element type in connection with the finite element approach, there are basically two alternatives. Either of these two options—a large number of simple elements or a smaller number of higher-order elements—leads to about the same level of accuracy in approximation. However, for

more general torsion problems in which complicated irregularity of geometry, interface and multiple-connection are involved, it can be concluded that the former alternative, i.e. using a linear triangular element for instance, is much better suited. This is especially the case because not only the discretization of the cross-section into more elements means better modelling of curved interfaces and boundaries, but it also helps later in obtaining better approximated optimal solutions of inhomogeneity and of multiple-connection.

[The Present Solution Procedure] In accordance with the preceding considerations, the present study employs as a solution procedure the finite element approach using a linear constant-strain triangular element.

In this connection, the first section following is concerned with the transformation of the previous exact formulation into a series of appropriate finite element relationships. As an important supplement to this, the next section is devoted to the mathematical methods for the treatment of multiple-connection. Then, also described is the procedure adopted for the determination of the optimality conditions with inhomogeneity and multiple-connection. The last section presents the organization of the computer program that carries out the entire numerical procedure implemented for the solution of the problem.

3.1 FINITE ELEMENT FORMULATION

[Discretization of the Solution Domain] As illustrated in Figure 3.1.1, a typical cross-section under torsion is subdivided into a series of small triangular elements. In this finite element division, each of the constituent elements and also each of the associated nodal points are numbered arbitrarily 1 to NE and 1 to NP, respectively.

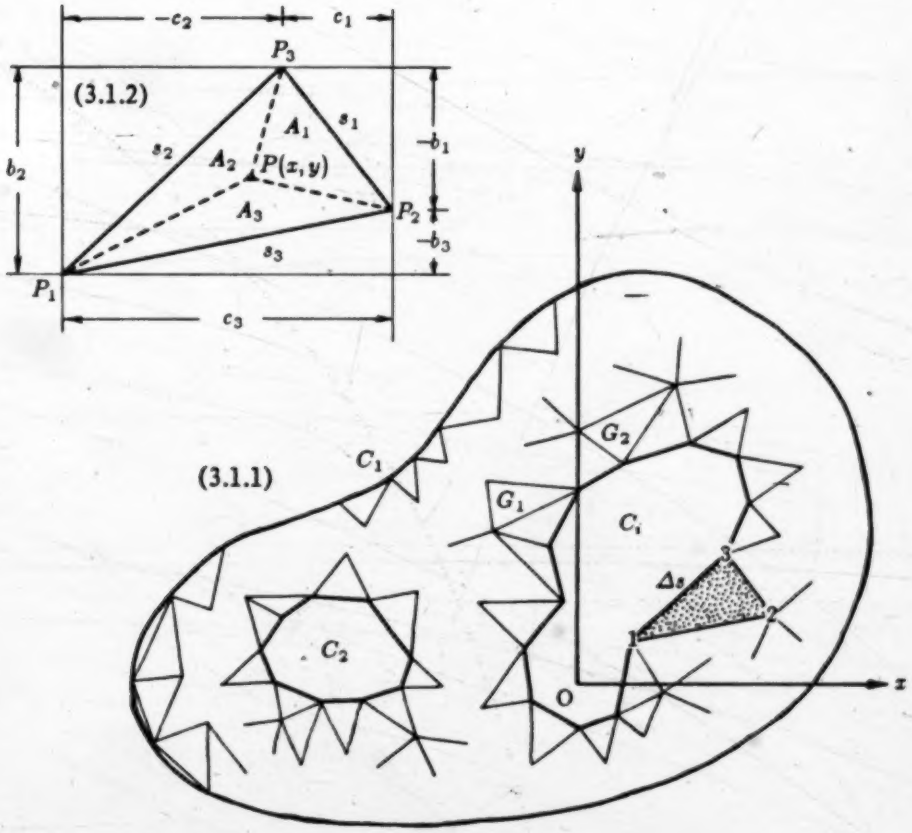

Figure 3.1: Finite Element Representation of a Cross-Section under Torsion

The discretization of the region is performed in such a way that there is no discontinuous variation of material properties within any of the elements. As a result, each of the interfaces or the boundary curves can be easily approximated by a simple sequential connection of the relevant element edges. Moreover, it can be noted consequently that the region may include as many different inhomogeneities and possibly cavities as the number of the total and the inner elements, respectively.

[Area Coordinate System] Consider an isolated generic triangular element in Figure 3.1.2, and let its three nodal points—P_1, P_2 and P_3—be numbered in a counterclockwise manner 1 to NN, respectively.

In establishing the stiffness relationship of this element, it is more convenient to work with a local coordinate system. Such is precisely the case with the area coordinates, in which the three non-dimensional components— $\mathcal{L}_1$, $\mathcal{L}_2$ and $\mathcal{L}_3$ —are defined as:

$$\lfloor \mathcal{L} \rfloor \equiv \lfloor \mathcal{L}_1 \;\; \mathcal{L}_2 \;\; \mathcal{L}_3 \rfloor \equiv \left\lfloor \frac{A_1}{A} \;\; \frac{A_2}{A} \;\; \frac{A_3}{A} \right\rfloor \tag{3.1}$$

where A_1, A_2 and A_3 are the subdivided areas; and A is the total area of the element:

$$A = \frac{1}{2} \det \begin{bmatrix} 1 & x_1 & y_1 \\ 1 & x_2 & y_2 \\ 1 & x_3 & y_3 \end{bmatrix} \tag{3.2}$$

From the above definition of the new natural coordinate system, it can be easily observed that each of the components takes up any value always between zero and unity. Furthermore, it follows immediately that:

$$\sum_{i=1}^{NN} \mathcal{L}_i = 1 \tag{3.3}$$

As an essential part of the definition of the new coordinate system, the Cartesian coordinates are now linearly related to the area coordinates through the following set of transformations:

$$\begin{aligned} x &\equiv [\mathcal{L}]\{x\} \\ y &\equiv [\mathcal{L}]\{y\} \end{aligned} \tag{3.4}$$

where (x,y) is the location of an arbitrary point within the element; and $\{x\}$ and $\{y\}$ are the corresponding nodal coordinate vectors:

$$[x] \equiv [\, x_1 \;\; x_2 \;\; x_3 \,]$$

$$[y] \equiv [\, y_1 \;\; y_2 \;\; y_3 \,]$$

Combination of Equations 3.3 and 3.4, and then inversion of the resulting set of linear simultaneous equations yield:

$$\begin{Bmatrix} \mathcal{L}_1 \\ \mathcal{L}_2 \\ \mathcal{L}_3 \end{Bmatrix} = [T] \begin{Bmatrix} 1 \\ x \\ y \end{Bmatrix} \tag{3.5}$$

This equation describes the linear transformation between the Cartesian and the area coordinate systems with [T] as the coordinate transformation matrix:

$$[T] \equiv \frac{1}{2A} \begin{bmatrix} a_1 & b_1 & c_1 \\ a_2 & b_2 & c_2 \\ a_3 & b_3 & c_3 \end{bmatrix} = \frac{1}{2A} \begin{bmatrix} x_2y_3 - x_3y_2 & y_2 - y_3 & x_3 - x_2 \\ x_3y_1 - x_1y_3 & y_3 - y_1 & x_1 - x_3 \\ x_1y_2 - x_2y_1 & y_1 - y_2 & x_2 - x_1 \end{bmatrix} \tag{3.6}$$

[Finite Element Equation] Being rewritten in matrix notation, the governing differential equation to be transformed into a finite element equation appears as:

$$\lfloor \nabla \rfloor \frac{1}{G} \{\nabla\} \phi + 2\alpha = 0 \qquad (x,y) \in E_i, \quad i = 1,2 \cdots \mathrm{NE} \tag{3.7}$$

where

$$\lfloor \nabla \rfloor \equiv \lfloor \frac{\partial}{\partial x} \quad \frac{\partial}{\partial y} \rfloor$$

Assume now that the discretized elements in Figure 3.1 are all sufficiently small in size. Then, the variation of stress function ϕ within each of them may consequently be approximated by the following linear trial function:

$$\phi \equiv \phi(x,y) = \lfloor N \rfloor \{\phi\} \qquad (x,y) \in E_i, \quad i = 1,2 \cdots \mathrm{NE} \tag{3.8}$$

in which $\lfloor N \rfloor$ is the shape function vector that describes the nature of change in the stress function, and $\{\phi\}$ the nodal stress function vector of the element:

$$\lfloor N \rfloor^T \equiv \lfloor N_1 \quad N_2 \quad N_3 \rfloor$$

$$\{\phi\}^T \equiv \lfloor \phi_1 \quad \phi_2 \quad \phi_3 \rfloor$$

Under the further assumption that, within the element, the shape functions take the same form as the area coordinates:

$$\lfloor N \rfloor = \lfloor L \rfloor \tag{3.9}$$

Since the stress function expression in Equation 3.8 not being an exact solution, when it is substituted into Equation 3.7, the right-hand-side of the governing differential equation becomes not necessary zero. Instead, an error function R which is termed as the Residual occurs such that:

$$R = \lfloor \nabla \rfloor \frac{1}{G} \{\nabla\} \lfloor N \rfloor \{\phi\} + 2\alpha \qquad (x,y) \in E_{rr} \quad i = 1,2 \cdots \mathrm{NE} \tag{3.10}$$

In order that this residual is relaxed in an average sense within the element region, the weighted residual methods require that:

$$\iint WR\,dA = 0 \qquad (x,y) \in E_i, \quad i = 1,2 \cdots \mathrm{NE} \tag{3.11}$$

in which W is a set of appropriate weighting functions. Depending on the choice of this weightings, there are in reality several different approaches available to achieve the requirement: Collocation, Subdomain, Least Square, Moments, Galerkin's, etc.. With being chosen to be used over others, the Bubnov-Galerkin method enforces:

$$W = \{N\} \tag{3.12}$$

Thus, from Equations 3.10, 3.11 and 3.12:

$$\iint WR\,dA = \iint \{N\}\left[\lfloor\nabla\rfloor\frac{1}{G}\{\nabla\}\lfloor N\rfloor\{\phi\} + 2\alpha\right] dA = 0 \tag{3.13}$$

In this equation, however, evaluation of the integral requires the application of the first identity of Green's theorem, which states:

$$\iint \omega(\nabla\cdot\Omega)\,dA = \oint \omega(\Omega\cdot\nu)\,ds - \iint (\Omega\cdot\nabla\omega)\,dA \qquad (x,y) \in R \tag{3.14}$$

where ω and Ω are respectively any appropriate scalar and vector functions defined continuously within the region, and ν the outward-drawn unit normal vector:

$$\omega \equiv \omega(x,y)$$

$$\Omega \equiv \lfloor\, \Omega_x \quad \Omega_y \,\rfloor$$

and

$$\nu \equiv \lfloor\, \frac{\partial x}{\partial \nu} \quad \frac{\partial y}{\partial \nu} \,\rfloor$$

As a result, it may be shown that Equation 3.13, with some rearrangement, is equivalent to:

$$\left[\iint \frac{1}{G}[B]^T[B]\,dA\right]\{\phi\} = \left\{2\alpha\iint\{N\}\,dA\right\} + \left\{\oint\{N\}\frac{1}{G}[\nu][B]\{\phi\}\,ds\right\} \quad (3.15)$$

in which [B] is a usual transformation matrix:

$$[B] \equiv \{\nabla\}\{N\} = \begin{bmatrix} \frac{\partial N_1}{\partial x} & \frac{\partial N_2}{\partial x} & \frac{\partial N_3}{\partial x} \\ \frac{\partial N_1}{\partial y} & \frac{\partial N_2}{\partial y} & \frac{\partial N_3}{\partial y} \end{bmatrix} = \frac{1}{2A}\begin{bmatrix} b_1 & b_2 & b_3 \\ c_1 & c_2 & c_3 \end{bmatrix} \quad (3.16)$$

Equation 3.15 is the generalized matrix stiffness relation sought for the finite element, which in a compact form is:

$$[K]\{\phi\} = \{Q\}_A + \{Q\}_S \qquad (x,y) \in E_i, \quad i = 1,2\cdots \mathrm{NE} \quad (3.17)$$

In this finite element equation, [K] is the generalized element stiffness matrix representing the stiffness contribution of each of the elements:

$$[K] \equiv \iint \frac{1}{G}[B]^T[B]\,dA = \frac{1}{4A^2}\begin{bmatrix} b_1^2+c_1^2 & b_1b_2+c_1c_2 & b_1b_3+c_1c_3 \\ \cdot & b_2^2+c_2^2 & b_2b_3+c_2c_3 \\ sym. & \cdot & b_3^2+c_3^2 \end{bmatrix} \quad (3.18)$$

$\{Q\}_A$ a generalized element load vector due to the external forcing parameter over the element region, which with the assistance of the integral formula:

$$\iint N_1^l N_2^m N_3^n\,dA = \frac{2\,l!m!n!}{(l+m+n+2)!}A \qquad (x,y) \in E_i, \quad i = 1,2\cdots \mathrm{NE} \quad (3.19)$$

becomes equal to:

$$\{Q\}_A \equiv 2\alpha \iint \{N\}\, dA = \frac{2}{3}\alpha A \begin{Bmatrix} 1 \\ 1 \\ 1 \end{Bmatrix} \qquad (x,y) \in E_i, \quad i = 1,2 \cdots \text{NE} \qquad (3.20)$$

and, finally, $\{Q\}_S$ another generalized element load vector due to the internal reaction parameter along the neighboring element interfaces:

$$\{Q\}_S \equiv \oint \{N\} \frac{1}{G} \left(\frac{\partial \phi}{\partial \nu} \right) ds = -\frac{1}{G} \oint \{N\} \tau_s \, ds \qquad (x,y) \in E_i, \quad i = 1,2 \cdots \text{NE} \qquad (3.21)$$

The shear-strain circulation round the element boundary is what is represented by this term; it is nevertheless an unknown of which the explicit evaluation is possible only after the $\{\phi\}$ is obtained.

Physical interpretation of the behaviour of the global assemblage of these terms for the entire solution domain reveals some interesting general characteristics of this particular portion of the load vector, and in this case it can be viewed clearly in terms of the smoothness of the approximated stress function surface—more specifically, the continuity of the element used.

If the element used is one that satisfies C^1-continuity such that the slope of the approximated surface is continuous and uniquely defined everywhere across the element interfaces, the reactions present between the two adjoining elements will be the same in magnitude and the opposite in direction with the reason being that the magnitude of the tangential component of the shear stress on the element boundary is directly proportional to the slope of the surface in the normal direction. It follows therefore that, when the $\{Q\}_S$ terms are all assembled into the global load vector, the contribution from an interior element is cancelled by similar contributions from other adjoining elements for all the interior nodes of the solution domain. Because the external elements, however, are those with no such adjoining elements, these $\{Q\}_S$ terms for the external nodes, unlike those for the internal ones, will not be cancelled even after the assemblage, and thus will result in

non-zero values regardless of the continuity of the element. Since every one of those external nodes, though, happens to coincide with one of the boundary curves along which boundary values are all prescribed, the $\{Q\}_S$ terms for the external nodes, on the other hand, will be all removed while those essential boundary conditions are being introduced. As a result, no consideration of the $\{Q\}_S$ terms in the global matrix stiffness equation is necessary if at least C^1-continuity is satisfied by the element used.

Unfortunately, the linear triangular element which is being used in the present formulation lacks such a C^1-continuity, and therefore, for the internal nodes, the $\{Q\}_S$ terms will not necessarily be cancelled out when assembled into the global load vector. Even for this most coarse linear triangular element, however, it may still be possible to assume, as long as the mesh used is reasonably fine, that the C^1-continuity is satisfied in an approximate sense; this will become even more realistic, as the mesh gets finer. When the finite element mesh using the triangular element is sufficiently fine, the order of magnitude of the $\{\{Q\}\}_S$ also is very small as compared with that of the $\{\{Q\}\}_A$ with the result that its influence on the final solution vector $\{\{\phi\}\}$ is nearly negligible.

For the reasons detailed above, the $\{Q\}_S$ terms are not included in the subsequent consideration as well as in the actual computation. In fact, regardless of the type of the element used, the $\{Q\}_S$ term never appears if the finite element equation is derived from the variational principle rather than from the weighted residual method as in the present formulation.

Over the entire cross-sectional region, there are NE elements in total with each of the elements possessing its matrix stiffness contribution as is given by Equation 3.17. Therefore, for the whole region, assembly of all of these contributions into a set of system matrix stiffness equations leads to:

$$[[K]]\{\{\phi\}\} = \{\{Q\}\} \qquad (x, y) \in R_1 \tag{3.22}$$

This is the generalized global matrix stiffness equation of NP degrees of freedom. In the equation, [[K]] is the generalized global stiffness matrix:

$$[[K]] \equiv \sum_{i=1}^{NE} [K]_i \tag{3.23}$$

{{ ϕ }} the global nodal stress function vector:

$$\{\{\phi\}\} \equiv \sum_{i=1}^{NE} \{\phi\}_i \tag{3.24}$$

and {{Q}} the generalized global load vector:

$$\{\{Q\}\} \equiv \sum_{i=1}^{NE} \{Q\}_{A_i} \tag{3.25}$$

The assembly of the above system matrix equation can be performed by the usual superposition technique. After inclusion of all the necessary constraints into this system equation, the resulting linear simultaneous equations can be solved by any standard methods such as Gaussian elimination or Gauss-Seidel iteration:

$$\{\{\phi\}\} = [[K]]^{-1}\{\{Q\}\} \qquad (x, y) \in R_1 \tag{3.26}$$

thus eventually obtaining the unknown global nodal stress function vector explicitly.

[Interface Conditions] In the torsion problem, these conditions are essentially to make sure that there are both static equilibrium at, and displacement continuity across the inhomogeneity interfaces. As can be concluded from the previous formulation, both of these requirements are always satisfied if the stress function is continuous and uniquely defined along each of the interface curves.

On the other hand, such is the case with the finite element approach if there is C^0-continuity at element interfaces. It happens that, with the finite element approach,

C^0-continuity is not particularly difficult to achieve; so is with the linear constant-strain triangular element which is used herein. As a result, for the present finite element formulation, the interface conditions are always satisfied identically, hence requiring no special consideration.

[**Boundary Conditions**] With boundary values prescribed, the boundary conditions appearing in torsional analyses are basically all of essential type. The same is also true for the problems involving multiple-connection although for such cases a further study has to be accompanied on how to determine the unknown boundary values.

In almost all cases of torsional analyses, the finite element process can easily handle the prescribed boundary conditions by simply inserting the values into the appropriate locations in the system matrix equation.

[**Stress Components**] The conversion of the stress components for the continuum into equivalent discretized elemental values follows a series of straightforward algebraic manipulations. In this case, the final expression of the stress tensor components may be obtained in terms of both the nodal coordinate and the nodal stress function values for the respective elements:

$$\{\tau\}_i = \begin{Bmatrix} \dfrac{\partial \phi}{\partial y} \\ \\ -\dfrac{\partial \phi}{\partial x} \end{Bmatrix}_i = [C]_i \begin{Bmatrix} \phi \end{Bmatrix}_i \qquad i = 1, 2 \cdots \mathrm{NE} \tag{3.27}$$

where $[C]_i$ is the stress–stress function transformation matrix:

$$[C]_i \equiv \frac{1}{2A_i} \begin{bmatrix} c_1 & c_2 & c_3 \\ \\ -b_1 & -b_2 & -b_3 \end{bmatrix}_i \tag{3.28}$$

As what follows the above, the expressions of the magnitude and the direction of the resultant stress on each of the elements may also be rewritten as:

$$|\tau|_i = \sqrt{\tau_i \cdot \tau_i} = \frac{1}{2A_i}\sqrt{\left(\sum_{j=1}^{NN} b_j\phi_j\right)^2 + \left(\sum_{j=1}^{NN} c_j\phi_j\right)^2} \qquad i = 1,2\cdots NE \qquad (3.29)$$

and:

$$\angle\tau_i = \tan^{-1}\left[-\frac{\sum_{j=1}^{NN} c_j\phi_j}{\sum_{j=1}^{NN} b_j\phi_j}\right]_i \qquad (3.30)$$

From the matrix stress tensor relation of Equation 3.27, it may be noticed immediately that the assumption of the linear variation of the stress function in Equation 3.8 gives rise to constant shear stresses everywhere within the respective elements with the constant stress/strain triangular element as the result.

[**Integral Conditions**] The finite element reformulation of the integral conditions involves the transformation of the line integral into an equivalent line summation:

$$\sum_{i=1}^{NS}\frac{1}{G_i}\tau_{s_i}\Delta s_i = 2\alpha A_j \qquad j = 1,2\cdots NC \qquad (3.31)$$

In this altered form of the integral conditions, the summation is taken along the NS element edges that coincide with each of the NC approximated contour lines. On these element sides, Δs is the line length measured in a counterclockwise manner:

$$\Delta s = \sqrt{(\Delta x)^2 + (\Delta y)^2}$$

and τ_s the corresponding tangential component of the element shear stress, which in combination with Equation 3.27 is:

$$\tau_s = \lfloor \cos\theta \quad \sin\theta \rfloor \begin{Bmatrix} \tau_{zx} \\ \tau_{yz} \end{Bmatrix} = \begin{bmatrix} \frac{\Delta x}{\Delta s} & \frac{\Delta y}{\Delta s} \end{bmatrix} [C] \{\phi\} \tag{3.32}$$

Upon substitution of Equation 3.32 into Equation 3.31, the final transformed integral conditions are:

$$\sum_{i=1}^{NS} \frac{1}{G_i} \lfloor \Delta x \quad \Delta y \rfloor_i [C]_i \{\phi\}_i = 2\alpha A_j \qquad j = 1, 2 \cdots NC \tag{3.33}$$

[Torsional Rigidity] For the torsional rigidity equation, as well, the conversion requires that the area integral over the entire cross-sectional region be transformed into an equivalent algebraic summation of piecewise numerical area integrations performed on each of the elements. This yields:

$$Z \equiv \frac{M}{\alpha} = \frac{2}{\alpha} \left[\sum_{i=1}^{NC} \phi_i A_i + \sum_{i=1}^{NE} \iint \lfloor N \rfloor_i \{\phi\}_i dA_i \right] \tag{3.34}$$

By making use of the integral formula in Equation 3.19, the elemental area integral in this equation may be evaluated explicitly as:

$$\iint \lfloor N \rfloor \{\phi\} dA = \frac{1}{3} \left(\sum_{i=1}^{NN} \phi_i \right) A$$

With substitution of this result, the transformed expression of the torsional rigidity now becomes:

$$Z = \frac{2}{\alpha}\left[\sum_{i=1}^{NC}\phi_i A_i + \frac{1}{3}\sum_{i=1}^{NE}\sum_{j=1}^{NN}\phi_j A_i\right] \tag{3.35}$$

It happens with the optimization procedure used in the present study that all elements within the region are of equal cross-sectional area. In such an event, this equation may also be written alternatively as:

$$Z = \frac{2}{\alpha}\left[\sum_{i=1}^{NC}\phi_i A_i + \frac{1}{3}A\sum_{i=1}^{NP}w_i\phi_i\right] \tag{3.36}$$

where A is the constant element area, and w the stress function weighting factor which represents the number of elements joining at the nodal point concerned.

3.2 TREATMENT OF THE MULTIPLE-CONNECTION

Shown in Figure 3.2 is a generic cross-section of a prism under torsion. It is similar in nature to the one upon which the formulation was based previously. With possible inclusion of inhomogeneities inside, the cross-section is bounded first externally by a closed contour C_1. Enclosed interior to this outer boundary curve are a number of non-intersecting internal contours C_2, C_3, · · · · and C_{NC}.

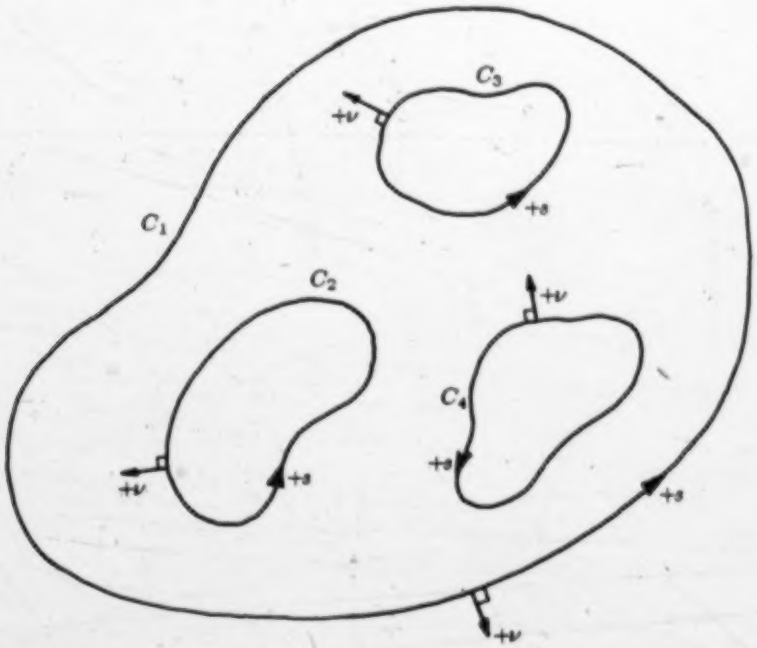

Figure 3.2: A Generic Multiply-Connected Region

[The Problem of Multiple-Connection] As was revealed from the formulation, the solution of this type of torsion problem can be made equivalent to the finding of the stress function over the cross-section. To be more specific, the stress function solution to be acceptable must first of all satisfy everywhere within the region the equation:

$$\frac{\partial}{\partial x}\left(\frac{1}{G}\frac{\partial \phi}{\partial x}\right)+\frac{\partial}{\partial y}\left(\frac{1}{G}\frac{\partial \phi}{\partial y}\right)+2\alpha=0 \qquad (x,y)\in R_1 \tag{3.37}$$

At the same time, the solution has to be one that allows constant stress function values along all of the NC boundary curves:

$$\phi=\phi_i \qquad (x,y)\in C_i, \quad i=1,2\cdots \mathrm{NC} \tag{3.38}$$

Among these constants, the one on the external boundary can be set arbitrarily to zero as was noted earlier; then the internal ones are all remained to be determined as part of the solution:

$$\phi=\begin{cases} 0 & (x,y)\in C_i, \quad i=1 \qquad (3.39)\\ \phi_i & (x,y)\in C_i, \quad i=2,3\cdots \mathrm{NC} \qquad (3.40)\end{cases}$$

In this case, the NC-1 unknown boundary constants are to be found in such a way that the following integral conditions are satisfied on each of the regions encompassed by the contours:

$$\oint \frac{1}{G}\tau_s\, ds \equiv \oint \frac{1}{G}\left(-\frac{\partial \phi}{\partial \nu}\right) ds = 2\alpha A_i \qquad (x,y)\in C_i, \quad i=1,2\cdots \mathrm{NC} \tag{3.41}$$

[Approaches for the Solution] It is fundamentally the constant boundary value and its related integral conditions on the internal boundary contours that require further consideration when multiple-connection is included within the region. For this

mathematically more involved situation, however, there is no general analytical method yet devised for the simultaneous solution with the governing differential equation. Therefore, treatment of these types of problems has nearly always been done by experimental or numerical methods. None of the approaches in either of these two categories, however, are without deficiencies deriving from their own characteristics.

[Experimental Approach] The membrane or soap-film analogy is the first and, perhaps at the same time, the only experimental method used in the treatment of multiple-connection in elastic torsion.

In this approach, an interior closed contour is analogous to a floating weightless flat disc which takes up an equilibrium position when placed horizontally-constrained on the top of an inflated membrane surface; from the analogy's point of view, this means the automatic satisfaction of the integral condition. The unknown boundary constant can then be determined from direct measurement of the vertical displacement of the disc.

In practice, however, this soap-film analogy appears not to work quite satisfactorily. The problem with it in the first place is that the force involved within the film surface is much too small in magnitude. As a consequence, it is never easy for the soap-film to overcome the gravity and the friction forces which are unavoidable in actually performing the floating disc experiment. Since it is thus almost impossible in reality to make the behaviour of the disc determined by the static equilibrium only, the true satisfaction of the integral condition in such case also is always somewhat dubious.

Yet, what is even more discouraging than this is the actual formation of the soap-film over a multiply-bounded cross-section; even when it is successful, with the pressure applied to it, the soap-film surface remains stable only for a very short period of time. It was particularly in this connection that the zero-pressure film was concluded to be much more efficient for such experimentation by Taylor and Griffith [76].

In addition to these intrinsic disadvantages, the inevitable experimental errors are still present. It is interesting after all of these difficulties that, until numerical methods came

into use, this extended membrane analogy was the only way available to deal with the multiply-connected torsion problems.

[Numerical Approaches] With numerical methods gaining wide-spread application in the solutions of various engineering problems, such efforts have also been directed to the problem of treatment of multiple-connection in torsion. The series of numerical attempts in this direction may be divided broadly into two groups: trial-and-error and iterative approaches.

On one hand, this categorization may seem appropriate if based on the way the undetermined boundary values are found. On the other hand, however, these two approaches are essentially the same; this is because they all start initially with arbitrarily chosen boundary values and then attempt to relax the resulting imbalance in the integral conditions by means of some numerical treatment. In this case, the numerical process is repeated until at some point the balance becomes stationary. Then, the boundary values which were used for the computation of the finally balanced integral conditions are the undetermined boundary constants sought.

In addition, another characteristic which is common to the two types of numerical techniques is that both are all established solely on the more commonly appearing doubly-connected situations and that, for such cases at least, they work reasonably well. Unfortunately however, serious difficulties being unavoidable when there are more than two boundaries present within the region, the numerical approaches in both categories mentioned above are not generally applicable to any given number of multiple-connections.

[Torsion as a Multiple Boundary Value Problem] It is of great importance to have a mathematical method—analytically, experimentally or numerically oriented—that can deal with multiple-connection problems regardless of the number of boundaries involved; from a purely mathematical view, this means solution of the multiple boundary value problem.

Later, such a situation will be encountered when the torsional optimalities of multiply-connected cross-sections are found; in these cases, it is not predictable how many boundaries to appear in the process of the optimization.

[Approaches in the Present Study] In what follows, two mathematical methods that can handle general multiply-connected situations will be introduced; these are the transformation and the superposition methods.

While the former of these has been used from time to time to simplify the problem by previous investigators, e.g. [83], the latter—the concept of which was originally suggested as a means to support the soap-film experimentation [76]—is introduced in an extended and modified form to the present finite element procedure.

3.2.1 THE TRANSFORMATION METHOD

This is one of the widely adapted numerical approaches for the treatment of multiple-connection problems in torsion. Conventional as the technique is, it lacks a clear theoretical basis. However, this method can be applied to any type of multiply-connected situations regardless of how many boundary curves are involved. Because of its particular suitability, on the other hand, it has been used in almost exclusive connection with the finite element procedure alone.

[The Transformation] Generally speaking, the transformation method does not, in fact it cannot, put any emphasis on determining the unknown boundary constants while satisfying the integral conditions. Instead, the fundamental idea behind this approach is to transform the given multiply-connected problem somehow into its singly-connected equivalent. It goes without saying that this transformation is intended primarily to obviate as much mathematical difficulty in the solution process as there is such a difference in between the conversion. Thus, with this approach, the boundary and the integral conditions are only secondary in consideration.

[Numerical Approximation of the Cavity] Although seemingly somewhat complicated, the whole procedure for the transformation method is rather straightforward. In its application, the discretization of the solution domain concerned is first extended into the multiply-connected region. Subsequently, the newly created cavity elements are then assumed simply as consisting of extremely weak material such that its shear strength as compared to that of the base material—G_0/G_1—is approximately:

$$\frac{G_0}{G_1} = O\left(10^{-9} \sim 10^{-10}\right) \tag{3.42}$$

The concept used in this approach is shown schematically in Figure 3.3. Once the above procedure is completed, the entire region can then be treated as a singly-connected composite cross-section.

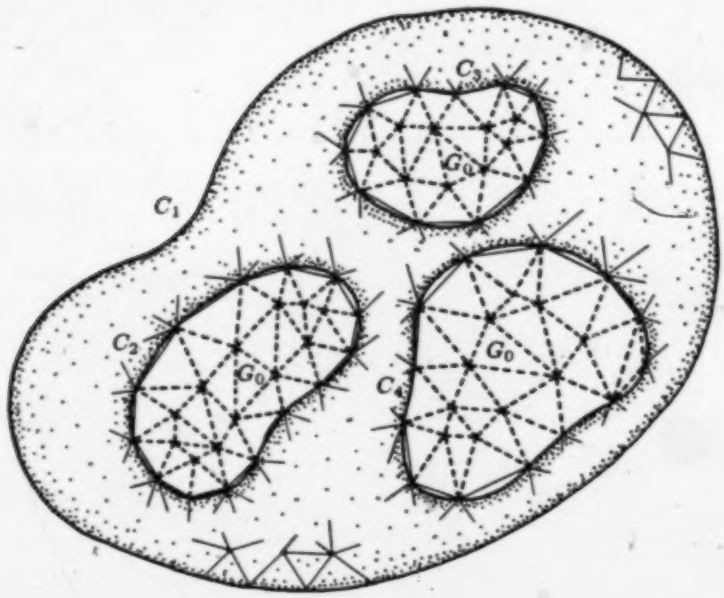

Figure 3.3: Schematic Diagram of the Transformation Method

[Mathematical Simplification] It should be pointed out that what actually happens in the foregoing procedure is that any cavity within the region is replaced with an inhomogeneity. As a result of this, any multiply-connected situation reduces always to a simply-connected one with the introduction of a new inhomogeneity. From another point of view, it can be also said that, by the same procedure, multiple-connection is treated as a limiting case of simple-connection with internal inhomogeneities.

In either case, what eventually follows the application of the procedure is that the internal boundary conditions of Equation 3.40 and the related integral conditions of Equation 3.41 are all automatically eliminated as intended at the beginning. Therefore,

with this approach, all that need be considered for the treatment of multiple-connection are Equations 3.37 and 3.39 of the first part; these can be usually solved with no particular difficulties.

[Mathematical Incompleteness] The transformation method, since it never considers the integral as well as the related boundary conditions, results in only approximate satisfaction of these conditions for the original multiply-connected problem.

In terms of the membrane problem, on the other hand, it may be assumed that the tension within the cavity area, which is analogous to the material compliance in the torsion problem, tends to become infinite in magnitude. The higher tension thus automatically generating a flatter region on the appropriate soap-film surface, this method still allows the application of the floating disc analogy. In this case, however, the floating discs provided by the method will not necessarily be precisely in static equilibrium.

Therefore, with this approach, it turns out that the boundary and the integral conditions are all, rather than requirements, secondary considerations upon which no control is given.

[Summary of the Transformation Method] The transformation method is characterized first of all by its uncomparable simplicity. This conciseness naturally suggests its advantage in terms of the numerical computation time. Furthermore, it allows any standard computer program, usually developed only for the treatment of singly-connected situations, to be applied without any modification directly to the solution of the multiply-connected problem as well.

From a mathematical point of view, however, this method is not nearly as attractive. The main reason for this, of course, is that in the solution procedure this transformation method completely disregards some of the necessary conditions and as a result satisfies them only in an approximate sense.

3.2.2 THE SUPERPOSITION METHOD

Earlier, a linear elliptic partial differential equation was found to govern the elastic torsion problem. Since the governing differential equation is "linear" in this case, it follows that the principle of superposition or linear combination holds. In the way in which the multiply-connected situation is treated, the superposition method depends on this linear characteristic of the governing equation.

At present, it appears to be the only known approach which determines the unknown boundary constants as simultaneously satisfying all the integral conditions.

[The Trial Solution] The superposition method, first of all, assumes for the given problem a form of general solution by which most of the required equations and conditions can be simultaneously satisfied. Let such a trial solution φ be expressed in the following linear combination form:

$$\varphi = \sum_{i=1}^{NC} f_i \varphi^{(i)} \tag{3.43}$$

On the right-hand-side of this equation of superposition, $\varphi^{(i)}$ are the linearly independent mode solutions to the problem, and f_i the undetermined coefficients or weighting factors to the mode solutions.

[Requirements for the Trial Solution] The basic requirement for the individual mode solutions in Equation 3.43 is that they all satisfy the governing differential equation of Equation 3.37, and the boundary conditions of Equation 3.38 within the region concerned. Note that Equation 3.39—the condition of zero boundary value on the external contour—is not yet imposed. It is also not necessary at this point that the integral conditions be satisfied by these mode solutions.

However, another global requirement for these mode solutions is that they should be all mathematically unique and distinct. It is implied by this additional condition that the

respective mode solutions must be linearly independent of one another so that no combination among them can possibly yield any one of them.

On the other hand, the undetermined coefficients introduced in the same Equation 3.43 will be later determined in such a way that the summation of these weighted mode solutions satisfies all the remaining integral conditions. Then, with the application of the last zero boundary value condition at the outer contour, the resulting linear combination will become the final solution to the given multiply-connected problem. To make the equation of superposition more definite, Table 3.1 establishes a general relationship among those parameters involved therein.

Table 3.1: General Relationship among Parameters Involved in the Superposition Method

SOLUTION DOMAIN	[2]NO	[3]NM	[4]NW	[5]φ
[1]NC-tuply-connected	NC−1	NC	NC	$\sum_{i=1}^{NC} f_i \varphi^{(i)}$

[1] *The number of contour curves over the region.*
[2] *The number of cavity areas included.*
[3] *The number of linearly independent mode solutions deducible.*
[4] *The number of necessary undetermined coefficients.*
[5] *The corresponding form of the general solution.*

According to this table, the superposition method needs, for the treatment of an NC-tuply-connected cross-section inside which NC−1 cavity areas are contained, to form at least as many as NC mode solutions with introduction of NC undetermined weighting coefficients.

[The Mode Solutions] From consideration of the linear independence of the NC mode solutions in Equation 3.43, it might be concluded that, except those boundary constants, there are no other parameters that could possibly yield such characteristics. In fact, for the uniqueness of these mode solutions, it is not only necessary but also sufficient that the corresponding boundary value sets all be linearly independent.

This requirement may be seen more clearly from the trial boundary constant matrix $[\kappa]$ given in Equation 3.44. Represented by each column of this square matrix is a set of boundary values for the related mode of solutions. It is convenient that, with this matrix, the uniqueness and distinctiveness of each column vector itself is directly related to the linear independence of the corresponding boundary constant set, and therefore to the mode solution as well.

$$
[\kappa] \equiv
\begin{array}{c}
\begin{array}{ccccccc}
\varphi^{(1)} & \varphi^{(2)} & \varphi^{(3)} & & \cdots & \varphi^{(NC)} & \\
\downarrow & \downarrow & \downarrow & & & \downarrow &
\end{array} \\
\left[\begin{array}{ccccccc}
\kappa_{11} & \kappa_{12} & \cdot & & \cdots & \kappa_{1NC} & \leftarrow \varphi_1 \\
\kappa_{21} & \kappa_{22} & \cdot & & \cdots & \kappa_{2NC} & \leftarrow \varphi_2 \\
\cdot & \cdot & \kappa_{33} & & & \cdot & \leftarrow \varphi_3 \\
\cdot & \cdot & & \cdot & & \cdot & \cdot \\
\cdot & \cdot & & & \cdot & \cdot & \cdot \\
\cdot & \cdot & & & & \cdot & \cdot \\
\kappa_{NC1} & \kappa_{NC2} & \cdot & & \cdots & \kappa_{NCNC} & \leftarrow \varphi_{NC}
\end{array}\right]
\end{array}
\qquad (3.44)
$$

Every element of this matrix, i.e. the boundary constants, can take completely arbitrary values as long as the resulting column vectors remain all linearly independent to one another. Notice, in this connection, that the boundary constant matrix happens to be square. As a result, linear independence either row- or columnwise implies that the determinant should be non-zero. By applying this principle conversely to the matrix concerned, i.e., in other words, by making sure that its determinant does not vanish, its

constituent column vectors can be arbitrarily made linearly independent. Needless to say, this general condition means that there exist an infinite number of such possible matrices. However, it is apparent that among all these possibilities the diagonal one is the easiest and also the most convenient matrix with which to deal. Therefore:

$$\kappa_{ij}\begin{cases} = 0 & i \neq j \\ \neq 0 & i = j \end{cases} \qquad i,j = 1,2 \cdots \mathrm{NC} \tag{3.45}$$

Even at this stage, the surviving diagonal terms can still be any freely chosen non-zero constants. Hence, no generality is lost even if, for the sake of convenience, these diagonal terms are all assigned identical values or, one step further, taken as unities thus producing normal modes; as a result, the boundary constant matrix becomes a scalar matrix, and then a unit matrix. In this connection, while the original notation being kept for more generality, it will be hereafter assumed implicitly that all non-zero elements of the matrix under consideration are of unit value. Therefore:

$$[\kappa] = \begin{bmatrix} \kappa_{11} & 0 & 0 & \cdots & 0 \\ 0 & \kappa_{22} & 0 & \cdots & 0 \\ 0 & 0 & \kappa_{33} & & \cdot \\ \cdot & \cdot & & \cdot & \cdot \\ \cdot & \cdot & & \cdot & \cdot \\ \cdot & \cdot & & \cdot & \cdot \\ 0 & 0 & \cdot\ \cdot & \cdot\ \cdot & \kappa_{\mathrm{NCNC}} \end{bmatrix} \tag{3.46}$$

From this explicit diagonalized boundary constant matrix, it can be seen that the i-th mode solution $\varphi^{(i)}$ is to be formed with a non-zero boundary value on the i-th contour C_i only, and with zero values everywhere else. It should be recognized that with this arrangement the originally intended columnwise uniqueness is also achieved.

For each set of the boundary constants above, the governing differential equation can now be satisfied over the entire region concerned, thus yielding a series of NC linearly independent mode solutions. Since the boundary values are all prescribed at this time, the whole such procedure can be done usually with no particular difficulties.

[The Weightings] Once the NC mode solutions are all obtained, it is then necessary that their respective weightings be found. As was mentioned before, these weightings are to be determined such that the integral conditions are all satisfied by the linear combination of those weighted mode solutions.

In order to have this condition satisfied, Equation 3.43 can be substituted into Equation 3.41. With a proper rearrangement, the result becomes:

$$\sum_{i=1}^{NC} f_i \oint \frac{1}{G} \frac{\partial \varphi^{(i)}}{\partial \nu} ds = -2\alpha A_j \qquad j = 1, 2 \cdots NC \tag{3.47}$$

There are NC such independent equations—one for every boundary curves over the region. Certainly, this is not only a necessary but also a sufficient number of equations for the determination of the NC unknown coefficients. In an explicit matrix form, Equation 3.47 turns into:

$$\begin{bmatrix} \oint_{C_1} \frac{1}{G} \frac{\partial \varphi^{(1)}}{\partial \nu} ds & \oint_{C_1} \frac{1}{G} \frac{\partial \varphi^{(2)}}{\partial \nu} ds & \cdots & \oint_{C_1} \frac{1}{G} \frac{\partial \varphi^{(NC)}}{\partial \nu} ds \\ \oint_{C_2} \frac{1}{G} \frac{\partial \varphi^{(1)}}{\partial \nu} ds & \oint_{C_2} \frac{1}{G} \frac{\partial \varphi^{(2)}}{\partial \nu} ds & \cdots & \\ \cdots & \cdots & \oint_{C_3} \frac{1}{G} \frac{\partial \varphi^{(3)}}{\partial \nu} ds & \cdots \\ \cdots & \cdots & \cdots & \cdots \\ \oint_{C_{NC}} \frac{1}{G} \frac{\partial \varphi^{(1)}}{\partial \nu} ds & \cdots & \cdots & \oint_{C_{NC}} \frac{1}{G} \frac{\partial \varphi^{(NC)}}{\partial \nu} ds \end{bmatrix} \begin{Bmatrix} f_1 \\ f_2 \\ \cdot \\ \cdot \\ \cdot \\ f_{NC} \end{Bmatrix} = \begin{Bmatrix} -2\alpha A_1 \\ -2\alpha A_2 \\ \cdot \\ \cdot \\ \cdot \\ -2\alpha A_{NC} \end{Bmatrix} \tag{3.48}$$

or equivalently:

$$[S]\{f\} = \{R\} \tag{3.49}$$

with

$$S_{i,j} = \oint_{C_i} \frac{1}{G} \frac{\partial \varphi^{(j)}}{\partial \nu} ds \qquad i,j = 1,2 \cdots \text{NC}$$

and

$$R_i = -2\alpha A_i \qquad i = 1,2 \cdots \text{NC}$$

Equation 3.48 or 3.49 is the matrix integral condition derived specifically from the application of the superposition method. Elements of both the [S] matrix and the {R} vector above can be all evaluated explicitly by performing contour integrals on the NC mode solutions obtained previously. In the matrix relationship, while those elements in a particular row are computed all from the same corresponding contour, those in a column are all from the same mode solution.

With these [S] matrix and {R} vector known, Equation 3.49 can then be inverted; thus, eventually, the NC weighting factors can be determined explicitly:

$$\{f\} = [S]^{-1}\{R\} \tag{3.50}$$

[The General and the Final Solutions] As expressed by Equation 3.43, the superposition method started with an assumption for the form of the general solution. It was then found that the NC linearly independent mode solutions necessary to support this hypothesis were obtainable. A matrix integral condition was also derived for the proper determination of the weighting coefficients for these mode solutions.

With these two necessary parameters—the mode solutions and their corresponding weightings—all known, it is then possible to determine the general solution. There

appear to be two practicable ways to accomplish this:

One approach is to follow exactly the definition of the linear combination as indicated by Equation 3.43—the individual mode solutions are all actually weighted and then added up to yield the general solution. With the other alternative, however, Equation 3.43 is used only for the determination of the correct boundary constant values. In this case, it is then by simultaneous solution of these exact boundary values with the governing differential equation that the final solution is obtained.

[Direct Superposition Approach] According to the direct superposition approach, i.e. the first alternative mentioned above, φ the general solution is given through the following weighted linear combination form:

$$\varphi = \sum_{i=1}^{NC} f_i \varphi^{(i)} \tag{3.51}$$

At this point, however, it must be remembered that the boundary condition upon which the superposition-method was based is simply a constant value along each of the contours; the zero boundary function value on the external contour is not yet imposed specifically.

It follows therefore that, depending on what the weighting of the first mode solution is, the general solution resulting from the above linear combination will not necessarily have a zero value on the external boundary. This is due to the fact that the first mode solution—in fact, only this mode—happens to be formed with a non-zero boundary-constant on the external contour. The zero external boundary value condition, nevertheless, can still be applied to the general solution, and in this case ϕ the final solution to the problem is obtained by:

$$\phi = \varphi - f_1 \kappa_{11} \tag{3.52}$$

In terms of the membrane analogy, this equation can be interpreted as the shifting down of the entire membrane surface by $f_1 \kappa_{11}$, thus adjusting the external boundary deflection to zero.

[Re-Solution Approach] With the above approach to obtaining the final solution, there was no need to evaluate explicitly the correct boundary values. The other alternative, in contrast, begins with finding these exact boundary constants. Since each of the boundary contours as in Equation 3.46 has been assigned a non-zero boundary value once only with a particular mode of the solutions, it is not surprising that the general boundary constant vector $\{\varphi\}_C$ is obtainable from Equation 3.43 in the following compact form:

$$\begin{Bmatrix} \varphi_1 \\ \varphi_2 \\ \cdot \\ \cdot \\ \cdot \\ \varphi_{NC} \end{Bmatrix}_C = \begin{Bmatrix} f_1\kappa_{11} \\ f_2\kappa_{22} \\ \cdot \\ \cdot \\ \cdot \\ f_{NC}\kappa_{NCNC} \end{Bmatrix} \tag{3.53}$$

Notice, though, that the external boundary constant φ_1 here again, as was so with the foregoing alternative, turns out to be non-zero. Therefore, setting this outer boundary value to zero in a manner similar to that in the previous approach, the final boundary constant vector $\{\phi\}_C$ is given by:

$$\begin{Bmatrix} \phi_1 \\ \phi_2 \\ \cdot \\ \cdot \\ \cdot \\ \phi_{NC} \end{Bmatrix}_C = \{\varphi\}_C - \{f_1\kappa_{11}\} = \begin{Bmatrix} 0 \\ f_2\kappa_{22} - f_1\kappa_{11} \\ \cdot \\ \cdot \\ \cdot \\ f_{NC}\kappa_{NCNC} - f_1\kappa_{11} \end{Bmatrix} \tag{3.54}$$

Once these exact boundary values are all determined, the final solution can then be obtained by solving them simultaneously with the governing differential equation.

[Visualization of the Superposition Procedure] Illustrated in Figure 3.4 in terms of the membrane analogy is the graphical interpretation of the general procedure for the superposition method. The example happens to be based only on a triply-connected

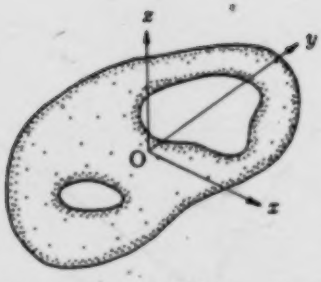

A Triply-Connected Solution Domain

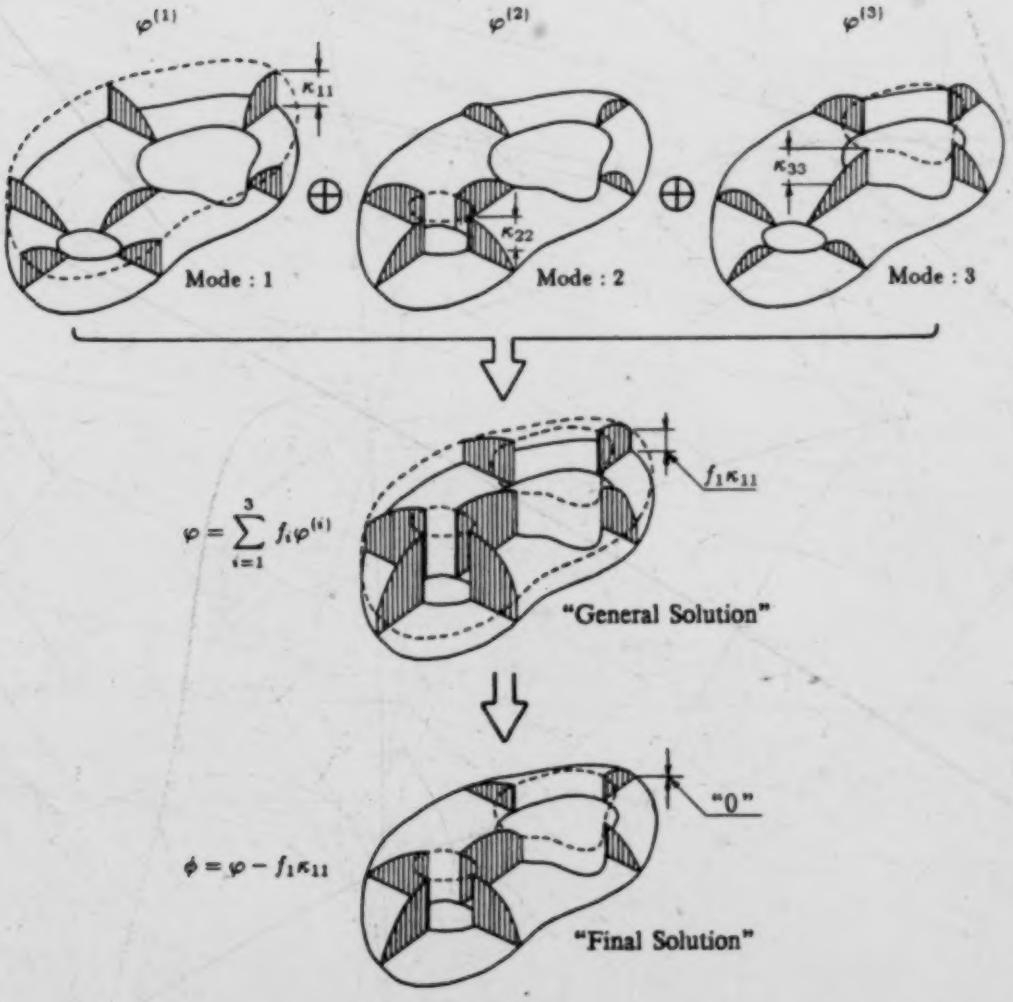

Figure 3.4: Graphical Interpretation of the Concept of the Superposition Method

cross-section, but, even if otherwise, the fundamental structure of the procedure is essentially the same. Moreover, despite the fact that there are two different approaches in obtaining the final solution, the main steps demonstrated in the schematic diagram are also more or less common to the both.

[Usability of the Superposition Approach] It is noteworthy that the superposition method is, unlike the transformation method, compatible with any major experimental or numerical technique.

Such is also true with the finite element method which is employed in the present study. In particular with this numerical approach, each of the mode solutions in the trial function is represented by a column vector of size NP, containing stress function values at every nodal points over the region. As well, with the same numerical method, it is computationally very much advantageous to introduce multiple right-hand-side to the global matrix stiffness equation. It is then not necessary to assemble the same global stiffness matrix everytime when one of the mode solutions is formed; in fact, it is instead possible to obtain the whole set of mode solutions at once.

The matrix integral condition also can be reformulated specifically for the finite element procedure by rewriting the contour integral elements as:

$$S_{i,j} = \left(\sum_{k=1}^{NS} \frac{1}{G_k} [\, \Delta x \;\; \Delta y \,]_k |C|_k \{\varphi\}_k \right)_i^{(j)} \qquad i,j = 1,2 \cdots NC \tag{3.55}$$

[Summary of the Superposition Method] In connection with the multiple boundary value problem, the superposition method attempts to determine the unknown boundary constants as simultaneously satisfying the integral conditions, the governing differential equation, and the boundary conditions.

Generally, the method is capable of dealing with any type of multiply-connected situations regardless of the number of boundary contours involved therein. As was

developed above, it is necessary, for the determination of these boundary constants, to form a series of different mode solutions. A solution obtained by an appropriate linear combination of these modes satisfies the required governing equation as well as other conditions all simultaneously. In terms of the membrane analogy, the floating discs over the multiply-connected regions, therefore, will be also all truly in static equilibrium.

Furthermore, the method developed is not restricted in its extend of application to any particular type of solution method as much as it is not so to any special class of governing equation—such as Poisson's in the present study. Instead, this superposition method can be applied to any type of multiple boundary value problem of which the governing differential equation is linear.

3.3 DETERMINATION OF THE OPTIMALITY

Shown in Figure 3.5 is a schematic diagram of the optimization in the present study as defined earlier. The objective is to determine the optimal shape and the corresponding optimal torsional rigidity of the given cross-section for the points in the A_0-A_2 plane.

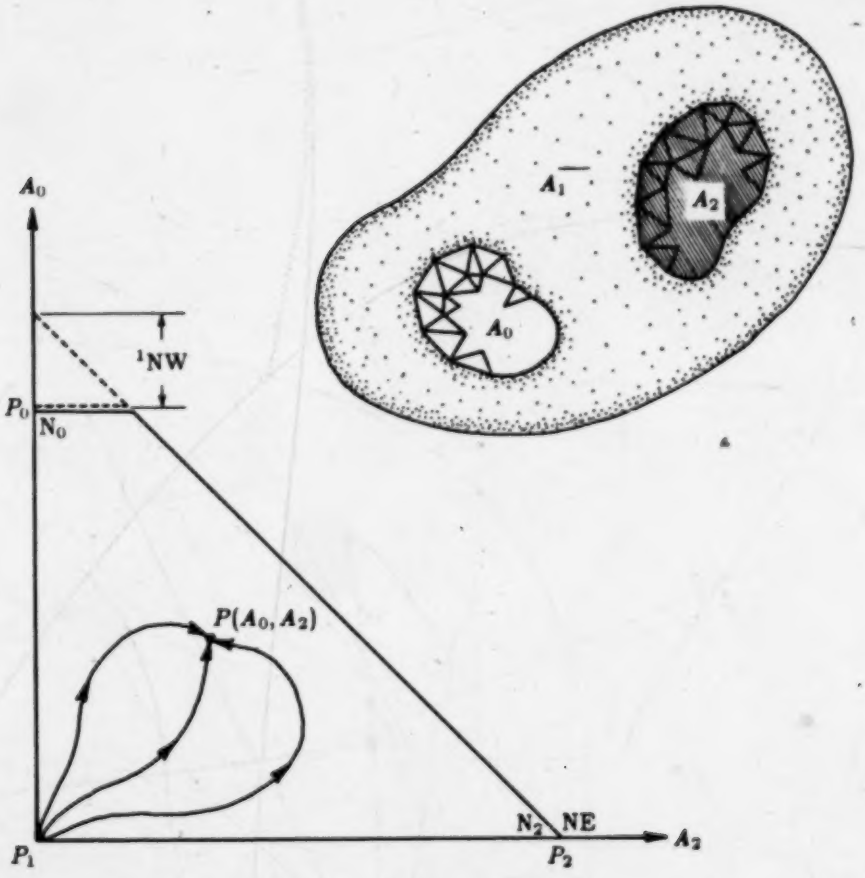

[1] *The number of wall elements.*

Figure 3.5: Schematic View of the Torsional Optimization in the Present Study

[Limitation of Analytical Methods] The solution for this shape optimization problem, except for a very few cases such as the circular cross-section, is generally intractable with analytical methods. It is, therefore, very important to develop a suitable numerical procedure that will allow solutions for other common practical problems involving non-circular geometries.

[A Previous Approach] In this connection, an iterative technique has been used previously by Faulkner, Mioduchowski and Hong [22] for the optimization of an inhomogeneous cross-section. In this case, the optimality has been reached by continually interchanging higher-stressed base material elements with lower-stressed reinforcement elements within the region, until the torsional rigidity value becomes stationary.

Unfortunately, however, this method is not directly applicable to the present problem in which cavity elements with zero shear stress are introduced in addition, and thus no appropriate comparison of the stress values is possible in the procedure.

[The Present Approach] The present study employs as an optimization procedure the numerical simulation of the membrane analogy; this is equally applicable to the optimization with the cavity and also with the reinforcement. With this analogy used in this connection, the relation between the local variation of the tension within the membrane surface over the region and twice the resulting change in volume under the surface is analogous to the relation between the variation in element material compliance and double the resulting change in torsional rigidity of the cross-section.

In order to account for the same amount of materials or cavities in this procedure, the domain under consideration is divided into equal-area elements which, though, are not required to be of the same shape. The shear modulus can be specified independently for each of these elements.

The actual optimization then proceeds based on the following three assumptions which are all derived from the circular case:

[Assumption I] *Since the system under consideration is linear, the idea of superposition also holds for the variation of torsional rigidity with respect to that of shear modulus, i.e.:*

$$\Delta Z\left(\sum \tilde{G}_i\right) = \sum \Delta Z\left(\tilde{G}_i\right) \tag{3.56}$$

where $\tilde{G}_i$ are independent shear modulus functions for the entire cross-section.

At each stage of the optimization, the present procedure computes the volume under the membrane surface adjusting the tension within the individual base material elements. Upon completion of the computation, the contributions of the respective elements to the volume are sorted in an ascending order of magnitude. It is at this time that this assumption allows the choice of the last few elements as the locations for the optimal interchange of the cavity or the reinforcement.

[Assumption II] *The optimal torsional rigidity functional is continuous and monotonic such that the optimality of a higher proportion always include those of every possible combination of lower proportions.*

This assumption is necessary for the sequential determination of the optimality. Without this, every different proportion will have to be treated totally independently.

[Assumption III] *The optimalities of the cavity and the reinforcement are independent of each other.*

According to this assumption, the problem which originally involves three parameters—A_0, A_1 and A_2—can be transformed into an equivalent pair of problems with each containing only two parameters of either A_0-A_1 or A_1-A_2. Therefore, it follows that, for a general multiply-connected inhomogeneous case, the optimalities of A_0 and A_1 can be considered separately, fixing one of them while the other one is being optimized.

[Uniqueness of the Optimality] Note, again, that for the circular case all of these three assumptions are always true over the whole region in the A_0-A_2 plane above. However, it is expected that such will not be the case for non-circular cases especially in the region where the influence of one parameter is particularly dominant compared with that of the other. For such cases, depending on the path taken, the three assumptions made above might lead erroneously to different optimalities for a point on the A_0-A_2 plane; this is certainly not acceptable.

In order to have such path-dependency detected and thereby ensure the uniqueness of the optimal solutions, the present optimization procedure considers for the same problem four different paths as shown in Figure 3.6. From the results obtained, only the parts that are essentially identical in these four cases are then accepted as the final optimal solution.

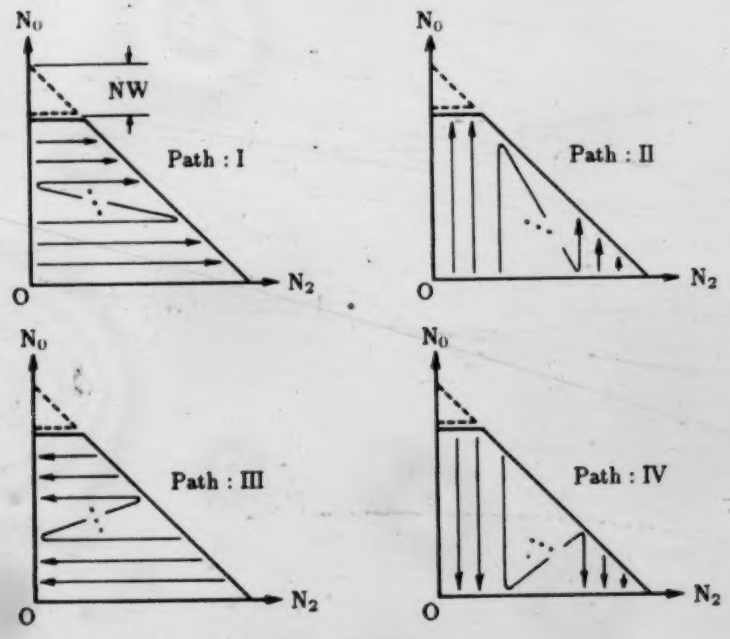

Figure 3.6: Four Different Paths Used to Ensure the Uniqueness of the Solution in the Present Optimization Procedure

3.4 ORGANIZATION OF THE COMPUTER PROGRAM

On the basis of the foregoing solution procedure, a computer algorithm was developed as outlined in the following.

Figure 3.7 shows the flowchart of the main program "TOROPT" which controls the entire optimization procedure, while Figure 3.8 illustrates the schematic diagram of the organization of the main program and the twenty-one subprograms. The functions of the individual program units are all detailed in Table 3.2.

The computer program is written specifically for the *FORTRANVS compiler on MTS system at The University of Alberta, and it is fully documented in the Appendix.

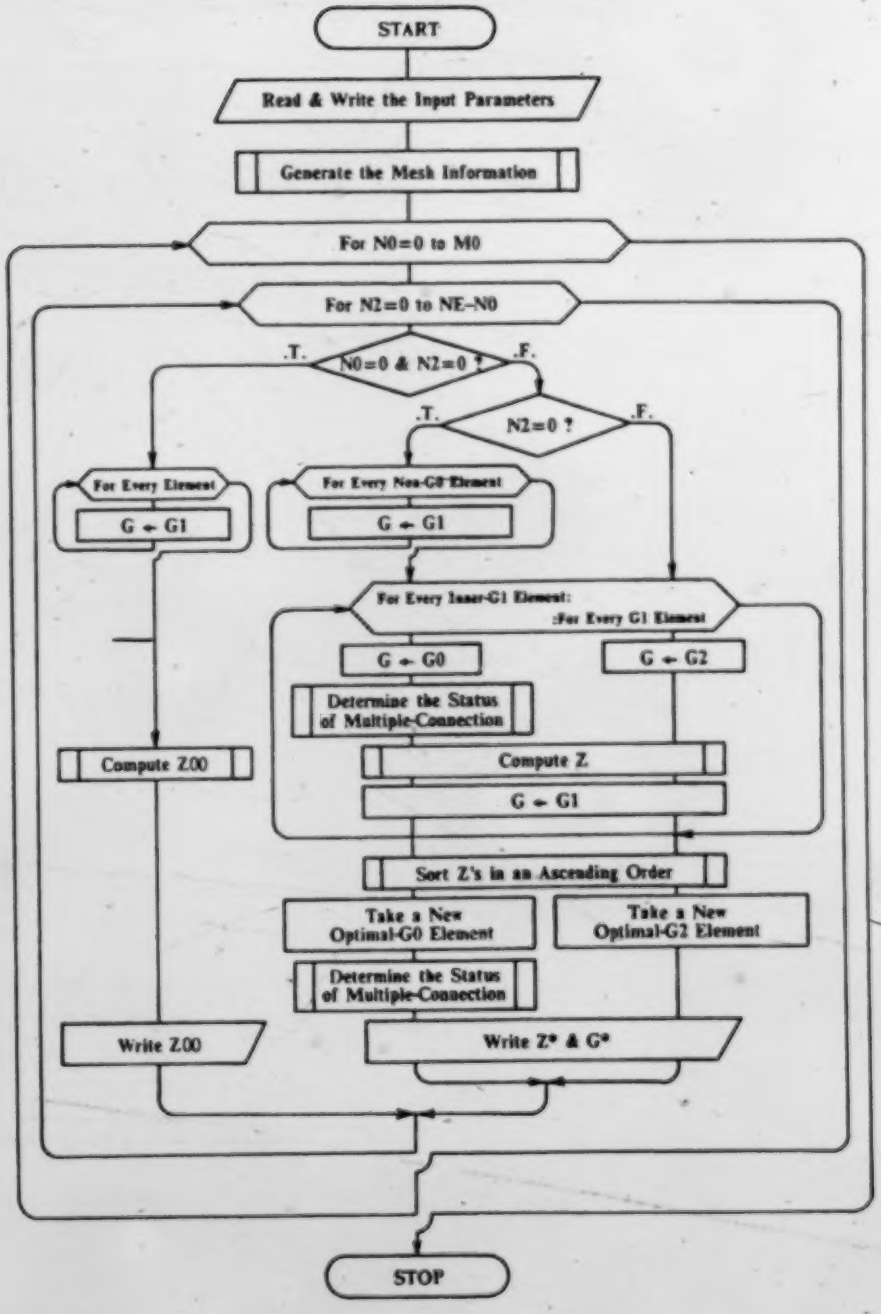

Figure 3.7: Flow-Chart of the Main Torsional Optimization Program "TOROPT"

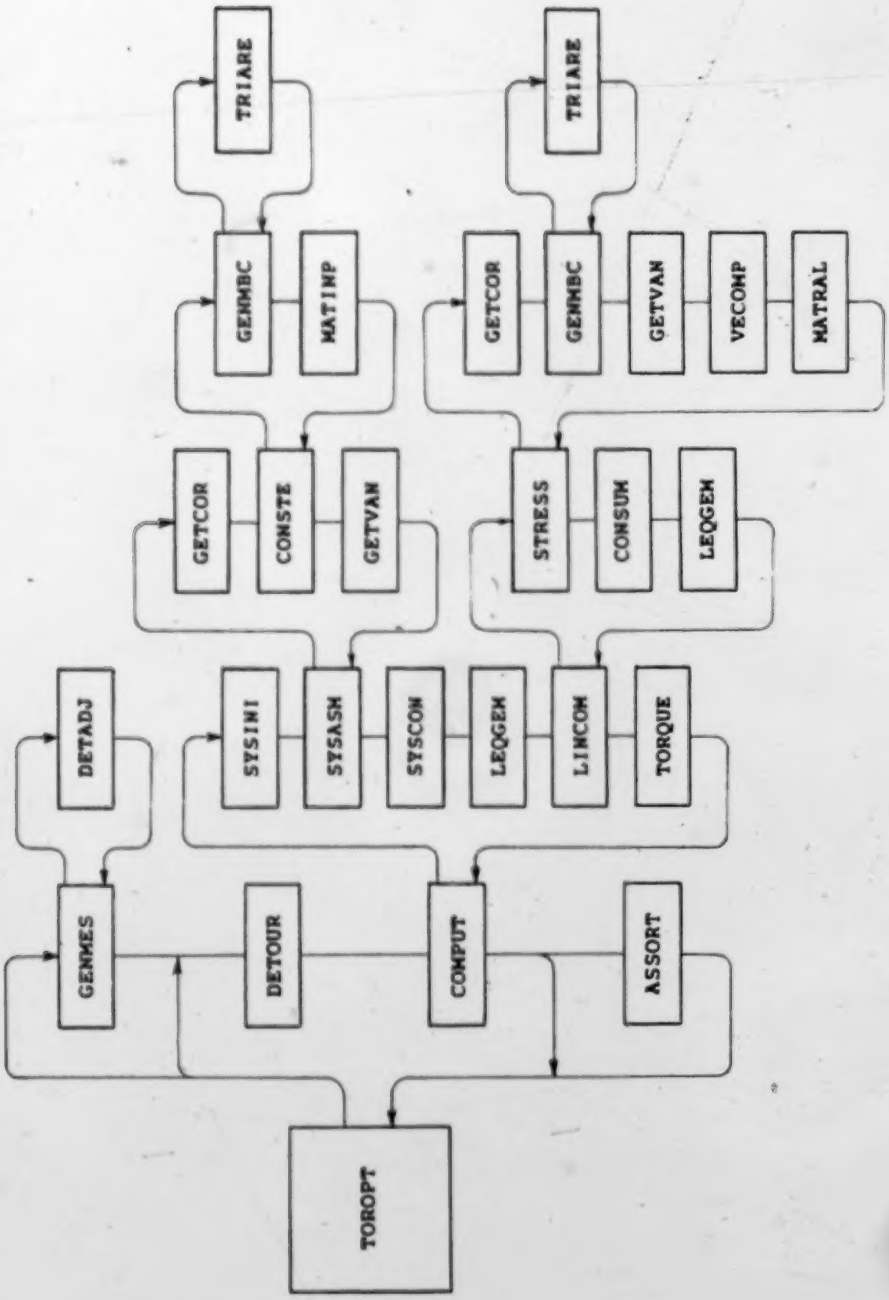

Figure 3.8: Organization of the Torsional Optimization Computer Program

Table 3.2: Detailed Functions of the Torsional Optimization Computer Program Units

MAIN	[0]	TOROPT	Controls the Entire Optimization Procedure
SUBPROGRAMS	[1]	ASSORT	Sorts Torsional Rigidity Values in an Ascending Order
	[2]	COMPUT	Hosts Computation of the Torsional Rigidity Value
	[3]	CONSTE	Generates the Linear Triangular Element Stiffness Matrix
	[4]	CONSUM	Evaluates the Contour Integral Value
	[5]	DETADJ	Determines the Adjacent Elements
	[6]	DETOUR	Determines the Status of Multiple-Connection
	[7]	GENMBC	Generates the [B] or the [C] Transformation Matrix
	[8]	GENMES	Generates the Mesh Information
	[9]	GETCOR	Returns Element Coordinate Information
	[10]	GETVAN	Returns Element Node Variable Names
	[11]	LEQGEM	Performs Gaussian Elimination
	[12]	LINCOM	Performs the Linear Combination
	[13]	MATINP	Performs Matrix Inner-Production
	[14]	MATRAL	Performs Matrix Linear Transformation
	[15]	STRESS	Computes Element Stress Components
	[16]	SYSASM	Assembles System Matrices
	[17]	SYSCON	Applies System Constraints
	[18]	SYSINI	Initializes the System Matrices
	[19]	TORQUE	Returns the Torque Value
	[20]	TRIARE	Returns the Area of a Triangular Element
	[21]	VECOMP	Returns Vector Components

4 VERIFICATION OF THE SOLUTION PROCEDURE

Based on the formulation before, a complete finite element solution procedure was developed in the preceding chapter for the torsion and its optimization problem. In view of the complexity of the entire procedure, it seems desirable to assess the accuracy and/or the dependability of the scheme before applications to any new problems are made. As is usual, this evaluation can be conducted by applying the procedure to some typical cases with known solutions and comparing thereby obtained results. Naturally, any problems for which either analytical or numerical solutions are available may be selected for this purpose.

In the following two sections, the verification of the solution procedure is considered first for the numerical treatment of the torsion problem itself and then for its optimization. For both of these cases, the various numerical studies carried out indicate that the overall reliability of the developed solution procedure is excellent. Although not presented here, an independent experimental verification of the identical numerical procedure also confirmed the same.

4.1 TEST OF THE NUMERICAL PROCEDURE

As an essential part of the verification of the method of solution, this section is concerned with the test of the finite element procedure by analyzing known solutions of several torsion problems. Considered in what follows for this are: Checks on accuracy of the numerical results in comparative case studies including those of homogeneous, inhomogeneous and multiply-connected cross-sections; also on the formation of the stress function surface; and, finally, on the numerical convergence.

It can be seen from the various numerical studies conducted in this section that the results obtained by the present numerical method compare very favorably with previous counterparts. As can be concluded thereby, the finite element numerical part of the developed solution procedure works satisfactorily in all practical situations.

[A Homogeneous Triapgular Cross-Section] Illustrated in Figure 4.1 is the first example, i.e., a homogeneous equilateral triangular cross-section and its mesh division for the finite element analysis; only one-sixth of the entire region needs to be considered due to the symmetry.

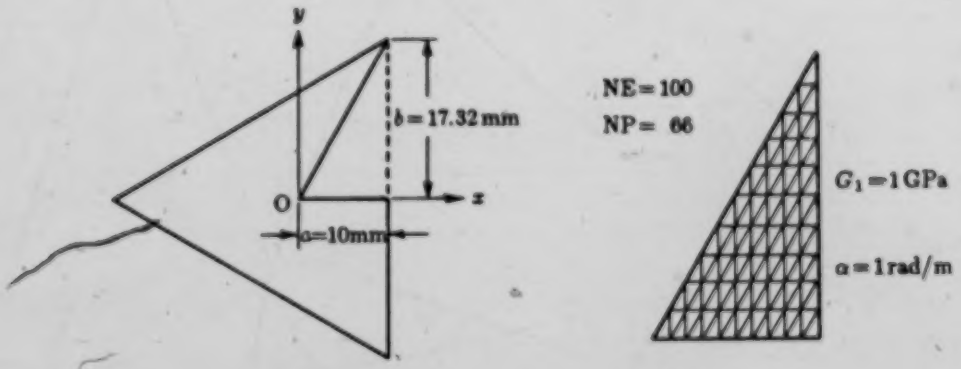

Figure 4.1: A Solid Homogeneous Equilateral Triangular Cross-Section under Torsion

For this case, the exact solution of the torsional rigidity is available [67], i.e.:

$$Z = \frac{9\sqrt{3}}{5} G a^4 \tag{4.1}$$

The torsional rigidity values for the above cross-section are obtained from Equation 4.1 as well as from the present numerical procedure and are summarized in Table 4.1 showing very good agreement.

Table 4.1: Comparison between the Analytical and the Present Finite Element Torsional Rigidity Solutions for a Solid Homogeneous Equilateral Triangular Cross-Section

Z, TORSIONAL RIGIDITY, Nm^2/rad		
ANALYTICAL	PRESENT	DISCREPANCY
31.1769	31.0335	−0.46 %

[A Homogeneous Square Cross-Section] Another homogeneous case studied is that of the regular square cross-section as shown in Figure 4.2.

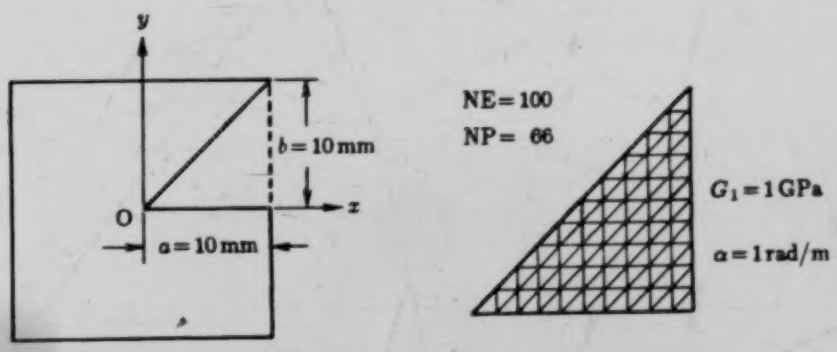

Figure 4.2: A Solid Homogeneous Regular Square Cross-Section under Torsion

The torsional rigidity of this case is known in the following form of a series solution [77]:

$$Z = \frac{16}{3} G a^4 \left(1 - \frac{192}{\pi^5} \sum_{k=1,3,5\cdots}^{\infty} \frac{1}{k^5} \tanh \frac{k\pi}{2} \right) \tag{4.2}$$

Table 4.2 compares the torsional rigidity values computed through the use of Equation 4.2 and the present approximation method. The agreement is again reasonably good.

Table 4.2: Comparison between the Series and the Present Finite Element Torsional Rigidity Solutions for a Solid Homogeneous Regular Square Cross-Section

Z, TORSIONAL RIGIDITY, Nm^2/rad		
ANALYTICAL	PRESENT	DISCREPANCY
22.4923	22.3895	−0.46 %

[An Inhomogeneous Square Cross-Section] In order to test the capability of the developed numerical procedure in an inhomogeneous situation, the bi-composite square cross-section as detailed in Figure 4.3 is examined.

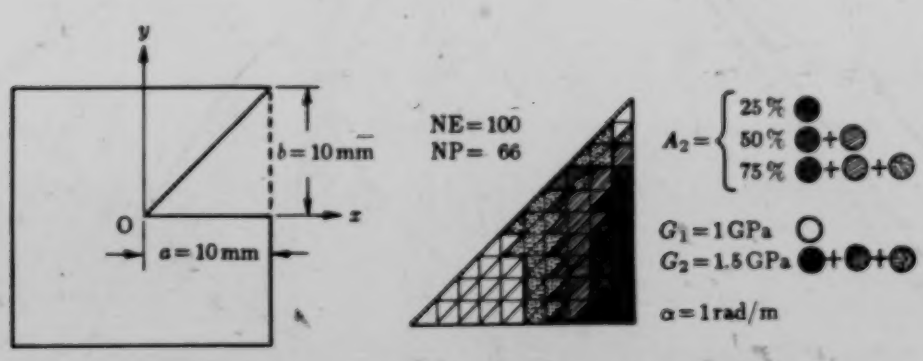

Figure 4.3: A Solid Bi-Composite Regular Square Cross-Section under Torsion

This problem has been dealt with previously using a hybrid finite element approach [22]. Three different compositions of the cross-section—25, 50 and 75 percents of the reinforcement with the shear modulus ratio G_2/G_1 of 1.5—are considered as the study case. Given in Table 4.3 is the comparison of the results obtained by the previous and the present approaches.

Table 4.3: Comparison between the Previous and the Present Finite Element Torsional Rigidity Solutions for a Solid Inhomogeneous Regular Square Cross-Section at Three Representative Proportions of the Reinforcement

[1]REINFORCEMENT A_2/A	Z, TORSIONAL RIGIDITY, Nm²/rad		
	[2]PUBLISHED	PRESENT	DISCREPANCY
25 %	27.84	27.66	−0.65 %
50 %	30.88	30.60	−0.91 %
75 %	32.96	32.82	−0.43 %

[1] $\gamma = G_2/G_1 = 1.5$; $G_1 = 1\,\text{GPa}$

[2] *A hybrid finite element solution by* Faulkner, Mioduchowski and Hong [22].

Both of the finite element procedures use the same number of elements, and the results show excellent agreement.

[A **Doubly-Connected Square Cross-Section**] Consider the homogeneous square cross-section with a square cutout as shown in Figure 4.4.

An extensive numerical investigation carried out on the same problem can be found in [74]. In this case, the approach employed was the hypercircle method, and according to the published approximate solution the torsional rigidity for the specific case above is given in the range:

$$Z = (\,2.02090016 \sim 2.11228368\,)Ga^4 \qquad (4.3)$$

Figure 4.4: A Doubly-Connected Homogeneous Regular Square Cross-Section under Torsion

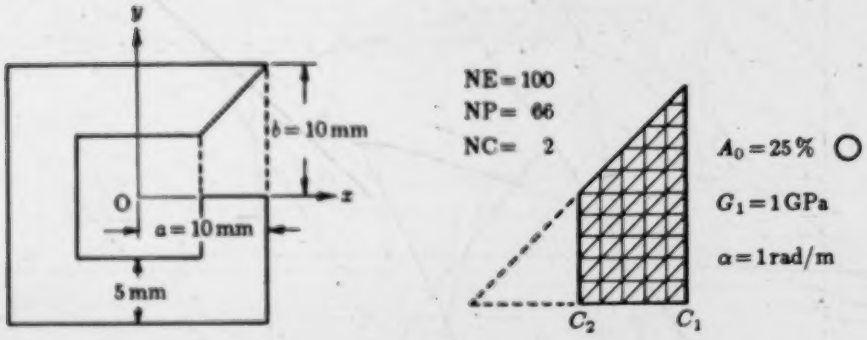

For the treatment of the double-connection problem involved in this case, both the transformation and the superposition methods were applied. In what follows, some of the intermediate results from these treatments are tabulated in order to demonstrate the performance of the two approaches.

Table 4.4 first compares the boundary constants obtained by the methods.

Table 4.4: Comparison of the Boundary Constant Values Obtained by the Use of the Transformation and the Superposition Methods for a Doubly-Connected Homogeneous Square Cross-Section under Torsion

CONTOUR $(x,y) \in C_i$	ϕ_i, BOUNDARY CONSTANT, kN/m by the method of	
	TRANSFORMATION	SUPERPOSITION
$i = 1$	0	0
$i = 2$	41.5634	41.0512

In addition, summarized in Table 4.5 are the contour integral values corresponding to each of the above boundary constant sets.

Table 4.5: Comparison of the Contour Integral Values Resulted from the Use of the Transformation and the Superposition Methods for a Doubly-Connected Homogeneous Square Cross-Section under Torsion

CONTOUR $(x,y) \in C_i$	$\oint \frac{1}{G}\left(-\frac{\partial \phi}{\partial \nu}\right) ds$, CONTOUR INTEGRAL, μm		
	EXACT $2\alpha A_i$	DISCREPANCY with the method of	
		TRANSFORMATION	SUPERPOSITION
$i = 1$	100.	−3.62 %	0 %
$i = 2$	25.	+12.26 %	0 %

The results of torsional rigidity values are also given along with the previous approximate solution in Table 4.6.

Table 4.6: Comparison between the Previous Hypercircle and the Present Finite Element Torsional Rigidity Solutions for a Doubly-Connected Homogeneous Square Cross-Section

Z, TORSIONAL RIGIDITY, Nm^2/rad		
[1]PUBLISHED	by the method of	
	TRANSFORMATION	SUPERPOSITION
20.2090~21.1228	20.4909	20.5548

[1] *Obtained by* Synge and Cahill [74] *using hypercircle method* (n=8).

[A Thin-Walled Hexagonal Cross-Section] Figure 4.5 below illustrates a cross-section of a hollow homogeneous hexagonal tube under torsion. It is intended to use this particular case to test further the developed numerical procedure in similar limiting situations.

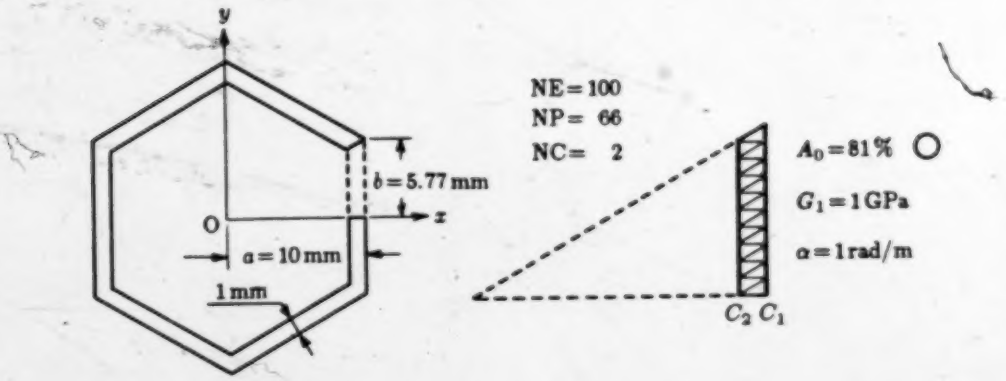

Figure 4.5: A Thin-Walled Homogeneous Regular Hexagonal Tube under Torsion

The membrane analogy, as is well known, provides a general approximate solution for problems of this nature [67]. For the particular case above, application of this analogy yields the following expression for the torsional rigidity:

$$Z = \frac{4\bar{A}G\delta}{S} \tag{4.4}$$

In this equation, $\bar{A}$ denotes the mean value of the areas enclosed by the external and the internal boundary contours of the cross-section, δ the uniform wall thickness, and S the length of the centerline of the ring section.

The finite element solution procedure for this study example employed, as was done so with the previous doubly-connected case, the both methods in its treatment of the double-boundary problem. The numerical values of the boundary constants and the

Table 4.7: Comparison of the Boundary Constant Values Obtained by the Use of the Transformation and the Superposition Methods for a Thin-Walled Homogeneous Hexagonal Cross-Section under Torsion

CONTOUR $(x,y) \in C_i$	ϕ_i, BOUNDARY CONSTANT, kN/m	
	by the method of	
	TRANSFORMATION	SUPERPOSITION
$i = 1$	0	0
$i = 2$	9.5085	9.7280

Table 4.8: Comparison of the Contour Integral Values Resulted from the Use of the Transformation and the Superposition Methods for a Thin-Walled Homogeneous Hexagonal Cross-Section under Torsion

CONTOUR $(x,y) \in C_i$	$\oint \frac{1}{G}\left(-\frac{\partial \phi}{\partial \nu}\right) ds$, CONTOUR INTEGRAL, μm		
	EXACT $2\alpha A_i$	DISCREPANCY with the method of	
		TRANSFORMATION	SUPERPOSITION
$i = 1$	58.00	−5.35 %	0 %
$i = 2$	46.98	+5.17 %	0 %

Table 4.9: Comparison between the Approximate Membrane Analogy and the Present Finite Element Torsional Rigidity Solutions for a Thin-Walled Homogeneous Hexagonal Cross-Section

Z, TORSIONAL RIGIDITY, Nm^3/rad		
[1]THEORY	by the method of	
	TRANSFORMATION	SUPERPOSITION
5.9401	5.9509	6.0882

[1] *Based on approximate membrane analogy* [67].

contour integrals obtained are given in Tables 4.7 and 4.8, respectively. As well, the torsional rigidity values from the approximate theory and also from the present numerical solution procedure are summarized in Table 4.9.

[The Stress Function Surface] This example is intended for the visual verification of the numerical procedure. As detailed in Figure 4.6, an equilateral triangular cross-section containing both the inhomogeneity and the multiple-connection simultaneously is considered for the demonstration.

Because of the symmetry, the analysis can be restricted to only one-sixth of the entire cross-section. As a consequence, the number of contours which originally is eight for the whole region is reduced to four.

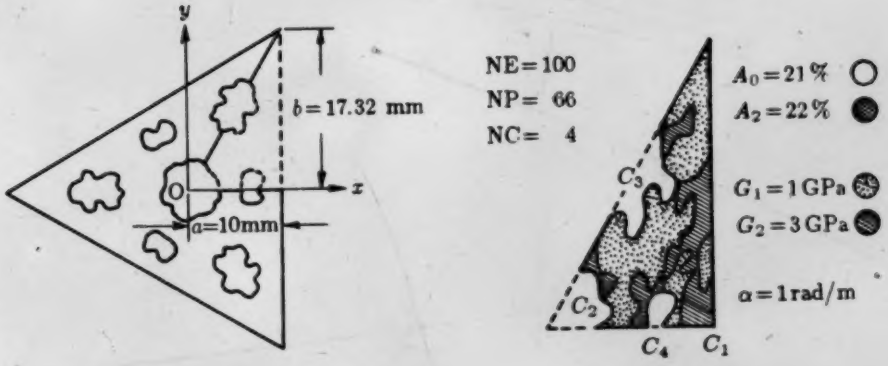

Figure 4.6: A Hollow Composite Equilateral Triangular Cross-Section under Torsion

The finite element mesh discretization used for the approximate solution and thereby obtained stress function surface are shown in Figure 4.7. From the three-dimensional plot, the noticeable large changes in the stress function surface over the reinforced regions can be observed. It can be seen, in addition, that the boundary conditions are all

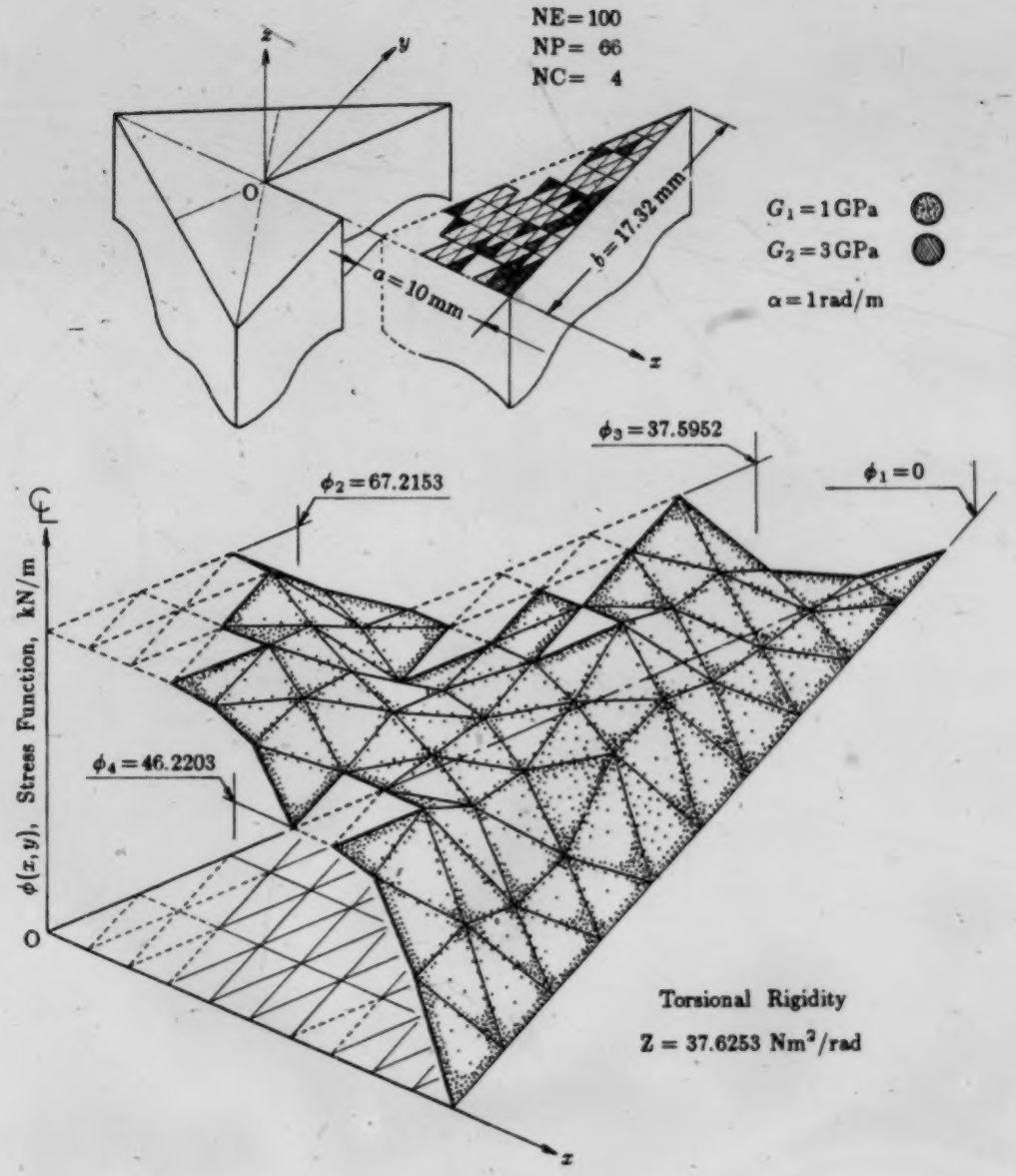

Figure 4.7: Display of the Stress Function Surface for a Hollow Composite Equilateral Triangular Cross-Section

satisfied by the zero and the constant stress function values along the external and the internal contours, respectively. Also seen on the membrane surface are the three flat areas generated above the cavity regions; they confirm the validity of the floating disc analogy. Because the multiple-connection is so treated using the superposition technique, the corresponding integral conditions are also all met.

The final boundary constants and the torsional rigidity obtained for this particular case are given on the figure.

[**Convergence of the Torsional Rigidity Solution**] The tests of the developed numerical procedure up to this point have been carried out only with fixed numbers of elements for the given cross-sections. Even though those finite element meshes used in most of these cases were rather coarse, the results obtained for the various examples indicated that the approximations were on the whole quite reasonable.

It is then also appropriate at this stage to examine the global reliability of the numerical method. As is usual, this purpose can be best served by the convergence test, which is to ensure that for a given problem better accuracy of approximation is obtainable by the use of a more refined mesh. For the present case, the same type of convergence is demonstrated for a homogeneous square cross-section as in Figure 4.8. One of the advantages of working with the regular square cross-section as in this case is the fact that it is the one which, when triangulated, allows lowest aspect ratios for the elements; it is generally in such situations particularly with triangular elements that the finite element procedure operates most stably, and therefore that its convergence also is most accurately estimatable.

As for the actual test, twenty different mesh divisions—from the most coarse to the finest—have been considered. The number of elements NE in this case ranges from 1^2 to 20^2 for the one-eighth of the square cross-section. For each of these NE values, the corresponding torsional rigidity Z_{NE} has been computed and then compared with Z_∞ the analytical series solution.

Figure 4.8: Effect of the Number of Elements on the Convergence
of the Finite Element Torsional Rigidity Solution
for a Solid Homogeneous Square Cross-Section

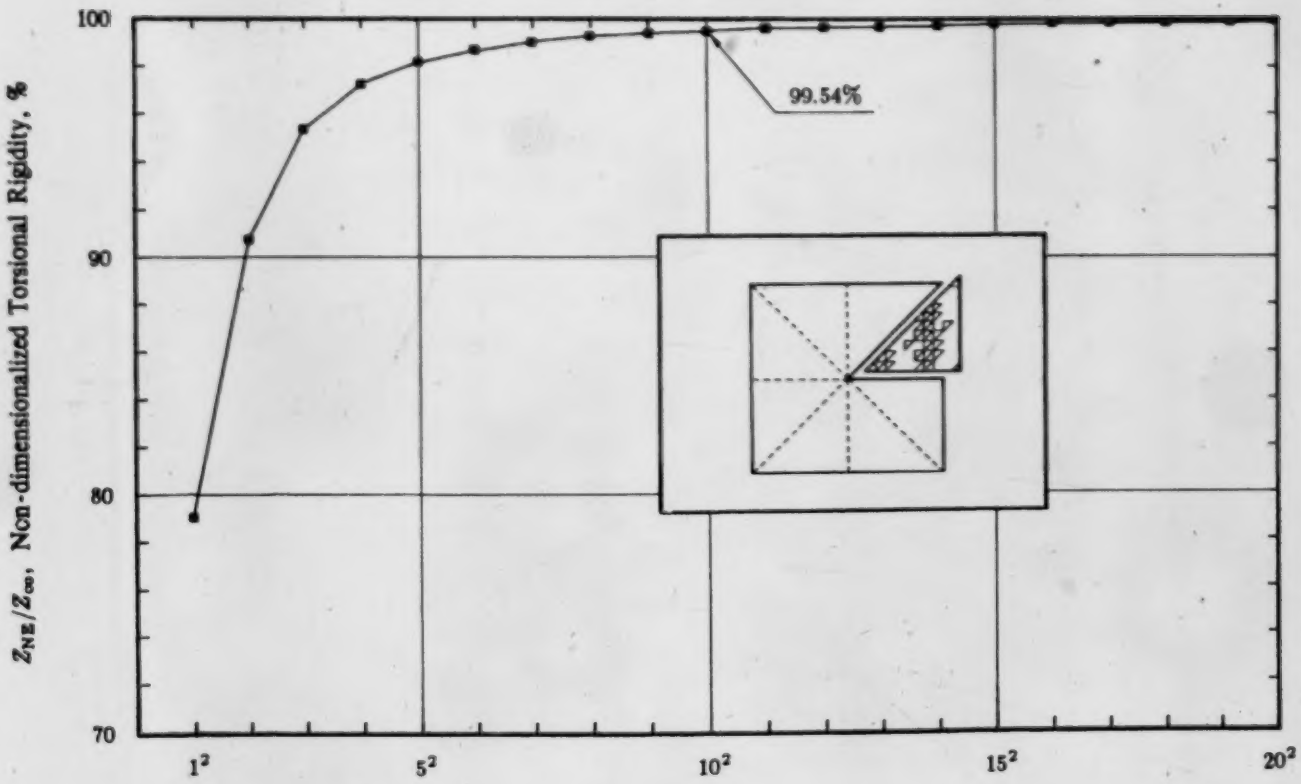

Figure 4.8 summarizes the results in a non-dimensionalized format. From the figure, it can be seen immediately that the convergence is quite rapid and monotonic, and as well that, as the NE value increases, the approximate solution gradually becomes identical with the analytical one. Evidently, the error involved, thus, can be made arbitrarily small by representing the body by a sufficiently large number of elements. For the specific case with 100 elements for instance, the discrepancy between the two solutions is already well below 0.5%.

The same figure, on the other hand, reveals another general characteristic of the stress function formulation: The approximations are all lower bounds to the exact solution, and this is in agreement with what was observed by Desai [18]; the warping function approach, to the contrary, is known to yield only upper bound solutions.

4.2 TEST OF THE OPTIMIZATION PROCEDURE

In confirming the dependability of the solution method developed in the present study, the previous section has been devoted exclusively to the testing of the finite element numerical treatment part alone. This section deals with the remaining portion of the test, which is that of the torsional optimization scheme.

Since the circular cross-section is known to be optimal, it is used as the first example. Also studied subsequently are a few more cases of optimal inhomogeneity. As there are unfortunately no known solutions of optimally shaped cavities for non-circular cross-sections, no comparative studies on such cases are possible. However, because the technique used for determining the optimal cavity shape is by all means the same as that used for the optimal inhomogeneity, it is to be expected that the optimization procedure will likewise work for the cavity optimization as it appears to for the inhomogeneity cases.

The various case studies carried out in the following indicate that the present procedure yields improved optimal solutions compared to the previous results.

[The Circular Cross-Section] In the torsional optimization problem, the isotropic circular cross-section holds a somewhat unique position in that it is the only case whose optimal solution is self-evident and, moreover, analytically defined. Figure 4.9 shows such an optimal configuration along with Equation 4[illegible] for its optimal torsional rigidity Z^*.

As can be seen, the torsional rigidity of a hollow inhomogeneous circular cross-section is maximum when the cavity and the more rigid portions are placed, respectively, at the closest and at the furthest distances possible from the axis of rotation. On the other hand, this is also the only case in which the optimality of the reinforcement is entirely independent of the ratio of shear modulii.

Figure 4.9: Optimal Configuration of the Hollow Composite Circular Cross-Section under Torsion

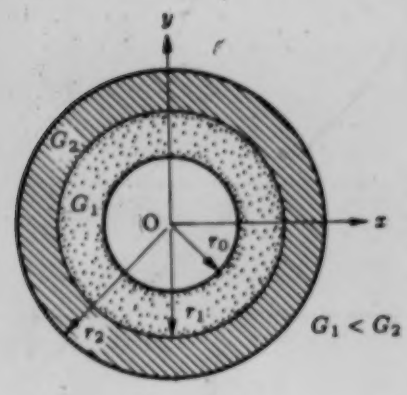

$$Z^* = G_1 J_1 + G_2 J_2 \qquad (4.5)$$
$$= \frac{\pi}{2}\left[\, G_1(r_1^4 - r_0^4) + G_2(r_2^4 - r_1^4) \,\right]$$

These distinct characteristics of the circular cross-section make it useful as a measure for the performance of the developed optimization procedure. The actual specimen used for such a numerical test is detailed in Figure 4.10, where the circular cross-section is replaced by a regular sixty-sided polygon and owing to the symmetry only a one-hundred-and-twentieth of it is taken for the analysis. The isolated sector is then divided into equal-area triangular elements representing the same amounts of materials.

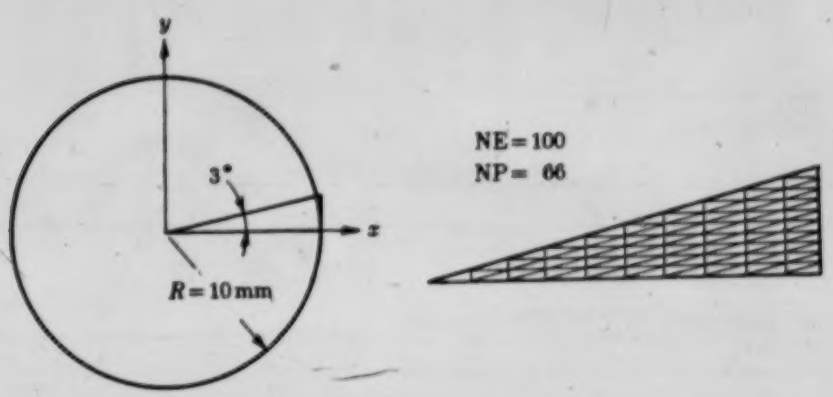

Figure 4.10: Geometric Domain Substitution for the Finite Element Approximation of the Circular Cross-Section

In an effort to assess, first of all, the suitability of this geometric domain-substitution, the torsional rigidity for the homogeneous case is computed from the mesh, and the value is compared with the analytical one. Table 4.10 indicates that, despite the unusually yet unavoidably large aspect ratios of the elements used, the result obtained is in excellent agreement with that from the exact solution.

Table 4.10: Comparison between the Exact and the Present Finite Element Torsional Rigidity Solutions for a Solid Homogeneous Circular Cross-Section

[1] Z, TORSIONAL RIGIDITY, Nm^3/rad		
ANALYTICAL	PRESENT	DISCREPANCY
15.7080	15.7079	−0.001 %

[1] $G_1 = 1\,GPa$; $\alpha = 1\,rad/m$

Since the geometric approximation thus appeared to be reasonable, the optimalities for both A_0 and A_2 were then determined by employing the optimization procedure. Satisfactorily enough, the results obtained were also very close to the above exact optimal solution. To be more specific, the results obtained were such that the first optimal elements for the G_0(*cavity*) and G_2(*reinforcement*) were found to be located respectively at the innermost and at the outermost part of the cross-section. As the amount of A_0 or A_2 gradually increased thereafter, the A_0 formed an inner cavity core, while the A_2 built up an outer ring.

The numerical values for the optimal torsional rigidity at various proportions of the cavity and of the reinforcement are given in Tables 4.11 and 4.12 for comparison with the exact solutions.

Table 4.11: Comparison between the Exact and the Present Finite Element Optimal Torsional Rigidity Solutions for a Hollow Homogeneous Circular Cross-Section at Three Representative Proportions of the Cavity

CAVITY A_c / A	Z^*, OPTIMAL TORSIONAL RIGIDITY, Nm^3/rad		
	ANALYTICAL	[1]PRESENT	DISCREPANCY
9 %	15.5807	15.6487	+0.44 %
25 %	14.7262	14.8364	+0.75 %
49 %	11.9365	12.0139	+0.65 %

[1] *by the Transformation Method*

Table 4.12: Comparison between the Exact and the Present Finite Element Optimal Torsional Rigidity Solutions for a Solid Composite Circular Cross-Section at Three Representative Proportions of the Reinforcement

[1]REINFORCEMENT A_2 / A	Z^*, OPTIMAL TORSIONAL RIGIDITY, Nm^3/rad		
	ANALYTICAL	PRESENT	DISCREPANCY
19 %	26.5119	26.5139	+0.01 %
36 %	34.2559	34.2636	+0.02 %
51 %	39.5809	39.5911	+0.03 %

[1] $\gamma = G_2/G_1 = 3$; $G_1 = 1\,GPa$

[A Triangular Cross-Section] As the first example that involves non-circular geometry, consider the optimal distribution of the inhomogeneity over the triangular cross-section in Figure 4.11.

Figure 4.11: Two Different Optimal Configurations Obtained by the Previous and the Present Optimization Procedures for a Solid Inhomogeneous Equilateral Triangular Cross-Section under Torsion

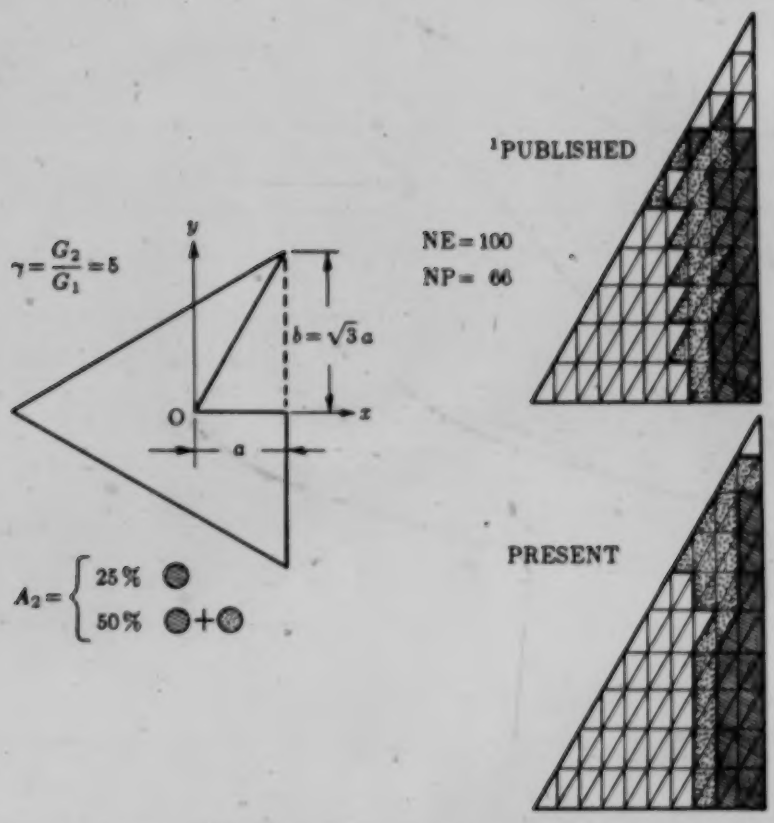

[1] *by* Faulkner, Mioduchowski and Hong [22].

The same problem was treated numerically by previous investigators [22], who published optimal solutions for various shear modulus ratios and proportions of reinforcement. Of these, however, only two cases—25 and 50 percents of reinforcements with the shear modulus ratio of 5—are examined in this case study. The previously and the presently obtained optimal solutions for the cases selected are shown simultaneously in the above figure.

As one way of verifying the dependability of the present optimization procedure, the torsional rigidities for both of the solutions were calculated, and comparison between the two obtained values is made in Table 4.13. For the sake of consistency, all computations were performed employing the present numerical procedure only.

Table 4.13: Comparison between the Previous and the Present Finite Element Optimal Torsional Rigidity Solutions for a Solid Inhomogeneous Equilateral Triangular Cross-Section at Two Representative Proportions of the Reinforcement

[1]REINFORCEMENT A_1 / A	Z^*, OPTIMAL TORSIONAL RIGIDITY, Nm^2/rad		
	[2]PUBLISHED	PRESENT	IMPROVEMENT
25 %	79.0955	85.7122	+8.37 %
50 %	118.1491	118.8082	+0.56 %

[1] $\gamma = G_2/G_1 = 5$; $G_1 = 1\,GPa$

[2] *by* Faulkner, Mioduchowski and Hong [22].

From the table, it can be observed that the torsional rigidity values of the new solution are somewhat larger in magnitude than that previous and therefore that, for the particular problem considered herein at least, the present optimization procedure yields a better approximation to the real optimal solution.

The comparison of the results in the same table, on the other hand, reflects the effect of the intrinsic difficulties encountered in the optimization procedure used for the previous solutions [22]. The control of the optimization in this case was based on the shear stress values of the elements, and therefore large mesh sizes and also large shear modulus ratios, which both usually lead to coarsely approximated shear stresses, caused instability in the performance of the procedure.

[A Square Cross-Section] Shown in Figure 4.12 is a regular square cross-section which is similar in nature to the one in the previous study case. The two solutions of optimal inhomogeneity obtained by using different approaches are also given together.

While the upper of the two solutions given above is from [22], the lower is from the present optimization procedure. The compositions of the stiff material for the particular case being considered are 25 and 50 percents with shear modulus ratio of 2. Table 4.14 shows small improvements in the torsional rigidity values calculated.

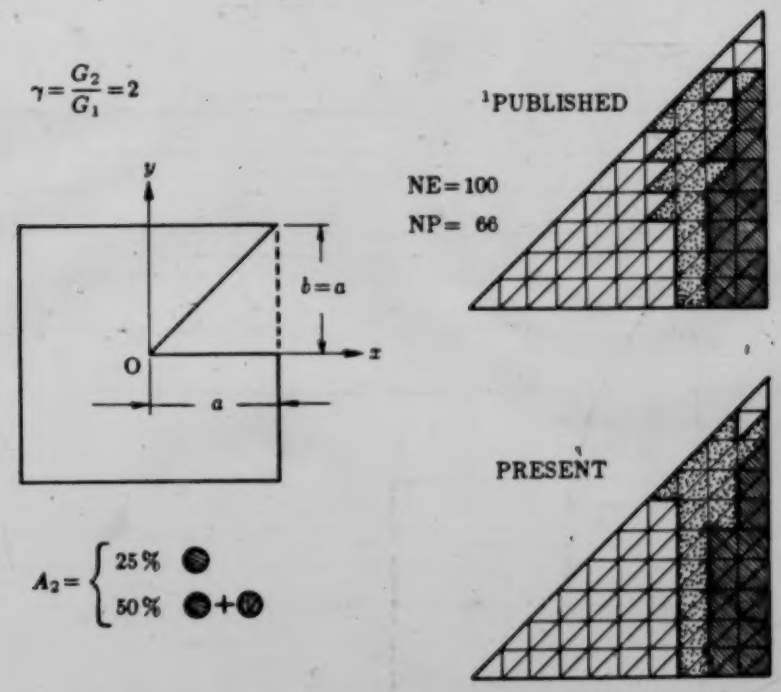

[1] *by* Faulkner, Mioduchowski and Hong [22].

Figure 4.12: Two Different Optimal Configurations Obtained by the Previous and the Present Optimization Procedures for a Solid Inhomogeneous Regular Square Cross-Section under Torsion

Table 4.14: Comparison between the Previous and the Present Finite Element Optimal Torsional Rigidity Solutions for a Solid Inhomogeneous Regular Square Cross-Section at Two Representative Proportions of the Reinforcement

[1]REINFORCEMENT A_1 / A	Z^*, OPTIMAL TORSIONAL RIGIDITY, Nm^3/rad		
	[2]PUBLISHED	PRESENT	IMPROVEMENT
25 %	32.5183	32.5495	+0.10 %
50 %	38.6928	38.9493	+0.66 %

[1] $\gamma = G_2/G_1 = 2$; $G_1 = 1\,GPa$

[2] *by* Faulkner, Mioduchowski and Hong [22].

5 SOLUTIONS TO THE PROBLEM

The developed solution procedure of the present study, which was tested in the previous chapter, can now be applied to various types of torsion and its optimization problems including those with irregularly-shaped geometries. This chapter will show several new examples of the application of the procedure to some selected typical regularly-shaped cross-sections for the determination of optimal distribution of the cavity and the reinforcement within the prescribed boundary.

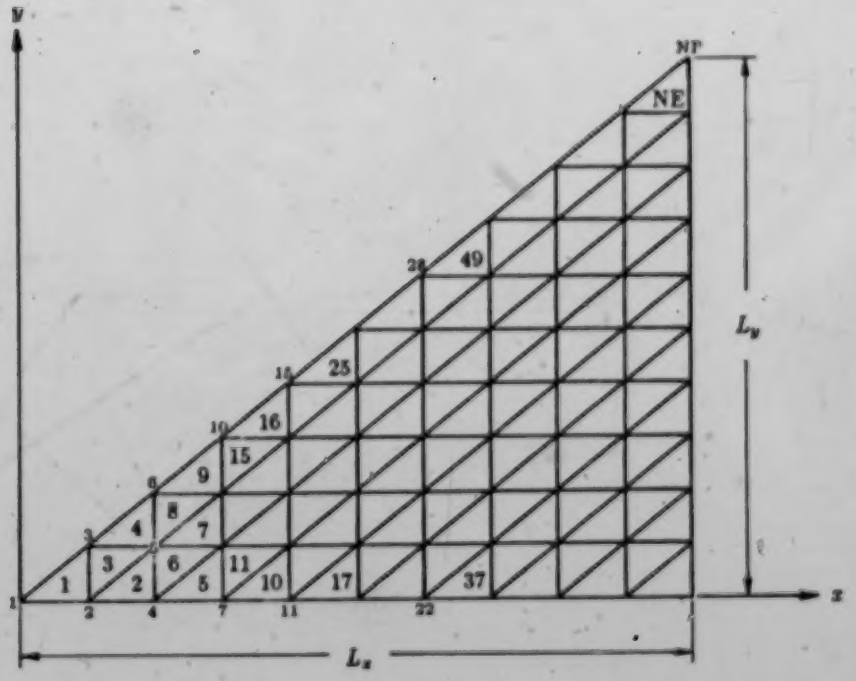

Figure 5.1: A Generic Finite Element Mesh for the Solutions of Various Regular-Shaped Cross-Sections under Torsion

[The Finite Element Mesh Used] As often is the case for regularly-shaped cross-sections, symmetry allows the analysis to be confined only to a certain triangular sector of the entire region. Illustrated in Figure 5.1 is such a generic domain, which is divided, as required by the developed optimization procedure, into a number of equal-area elements and nodal points, being numbered from 1 to NE and NP, respectively.

While the numbering can be done totally arbitrarily in general, the above particular numbering scheme, in which all the prescribed external boundary constants are arranged to be assembled later at the bottom part of the system matrix equation, is computationally advantageous as it enables the matrix equation, when partitioned, to be reduced considerably in size.

The work required in preparing the mesh information was eliminated by the adoption of an automatic mesh generation scheme. This scheme, covering almost all possible regular cross-sections, generates all the necessary mesh information, given the following three parameters of L_x, L_y, and NH the number of divisions in either direction of the triangular sector.

For the particular mesh division above, it is easy to show that the following relations hold:

$$\begin{aligned} NE &= NH^2 \\ NP &= \frac{1}{2}(NH^2 + 3NH + 2) \end{aligned} \tag{5.1}$$

Because the increase in computation time necessary is substantial for larger numbers of elements, and also because it is a much easier number to handle the obtained results statistically with, all results in the present study were obtained using NH=10, thus making NE=100 and NP=66. The number of elements for the entire cross-section in this case is still as many as 2·NS·NE with NS being the number of sides of the original cross-section. This is considered to be quite reasonable for a good approximation accuracy.

[The Circular Case] Since the circular case, as shown in Figure 5.2, is quite standard among regular cross-sections, it is considered first. Again, the optimal solution for the circular case is trivial as can be seen from the figure; not only the optimal shape for this case is independent of the ratio of shear modulii G_2/G_1, but as well is the torsional rigidity given in an exact form.

Given in Table 5.1 are the relative optimal torsional rigidity values as function of proportions of both the cavity and the reinforcement. The same information is then also shown plotted in three dimensions. In both the table and the diagram, the torsional rigidity values are all non-dimensionalized relative to that of the homogeneous case, which allows easy comparison of the results. Two values for the ratio of shear modulii, i.e. 2 and 5, have been considered and are represented by the lower and the upper surfaces in the plot, respectively.

For the circular case, close observation reveals that the optimality condition of a multiply-connected inhomogeneous case is simply the linear combination of those for two separate cases of the multiple-connection and the inhomogeneity. Therefore, for more general cases, the analysis of optimization can be done independently for the multiple-connection and the inhomogeneity. As given in Table 5.1 are the results showing the decrements and the increments in torsional rigidity from the homogeneous case's, resulting from optimally replacing some part of the original cross-section with the cavity or the reinforcement; these are given in the rows and columns, respectively.

Thus, for a general multiply-connected inhomogeneous case which is represented by any point in the A_0-A_2 plane, the linear combination principle can be used not only for obtaining the optimal shape, but also for determining its corresponding torsional rigidity value. In fact, the circular cross-section is the only case with which such superposition is possible over the entire A_0-A_2 plane.

Table 5.1: Optimal Torsional Rigidity for the Hollow Composite Circular Cross-Section at Various Proportions of the Cavity and of the Reinforcement

$\%A_2$ / G_2/G_1 / $\%A_1$		0	5	10	15	20	25	30	35	40	50	60	70	80	90	100
0		100.00	-0.25	-1.00	-2.25	-4.00	-6.25	-9.00	-12.25	-16.00	-25.00	-36.00	-49.00	-64.00	-81.00	-100.00
5	2	+9.75														
	5	+39.00														
10	2	+19.00														
	5	+76.00														
15	2	+27.75														
	5	+111.00														
20	2	+36.00														
	5	+144.00														
25	2	+43.75														
	5	+175.00														
30	2	+51.00														
	5	+204.00														
35	2	+57.75														
	5	+231.00														
40	2	+64.00														
	5	+256.00														
50	2	+75.00														
	5	+300.00														
60	2	+84.00														
	5	+336.00														
70	2	+91.00														
	5	+364.00														
80	2	+96.00														
	5	+384.00														
90	2	+99.00														
	5	+396.00														
100	2	+100.00														
	5	+400.00														

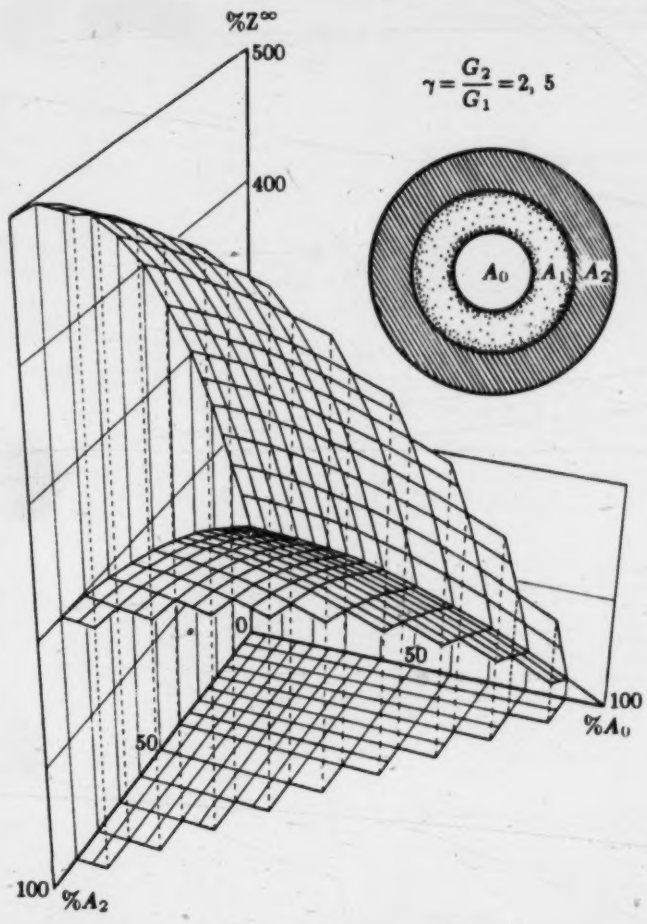

Figure 5.2: Three-Dimensional Display of the Relative Optimal Torsional Rigidity Values for the Hollow Composite Circular Cross-Section at Various Proportions of the Cavity and of the Reinforcement ($G_2/G_1=2, 5$)

[Non-Circular Cases] For non-circular regular cross-sections, the triangle, the square, and the hexagon are considered in the following.

As was so with the foregoing circular case, for each of these three geometries, optimal solutions are obtained for shear modulus ratios of 2 and 5, and for proportions of both the cavity and the reinforcement from 0 to 100 percents. The solutions are presented in the following in a manner similar to that of the circular case. The results presented for each of the cases include: the table and the three-dimensional plot of the torsional rigidity, followed by the three corresponding optimal configurations of the cross-section, respectively; for the cavity and for the inhomogeneities with shear modulus ratios of 2 and 5.

Similar principles as those with the circular case are applicable in the interpretation of the results except that, for these non-circular cases, the surfaces of the torsional rigidity are plotted only in a certain area of the A_0-A_2 plane. Those plotted areas are approximately where the principle of linear combination as outlined for the circular case is applicable; elsewhere, the actual optimalities are different from what may be obtained by the superposition.

Fortunately enough, though, the plotted, rather narrow particular region in which the simple linear combination technique can be used coincides with the area where the engineering interest lies, and furthermore the optimization itself is also in real necessity.

[Computation of the Results] For those cases examined herein, the results were all obtained using the developed program "TOROPT" on an Amdahl 5870 Computer.

The determination of the optimal shapes and the corresponding torsional rigidities required considerable computing time; for each of the geometries considered, the optimization process took approximately 812 CPU seconds following each of the four paths concerned. In fact, for 100 elements, the number of membrane surfaces formed reached as many as 165,345.; this is not even taking the number of the mode solutions for each of the membranes into account.

[An Example-Use of the Results] — As an example of using the results obtained, consider the multiply-connected inhomogeneous square cross-section in Figure 5.3. It is composed of 5% cavity and 10% stiffer material with $G_2/G_1=2$.

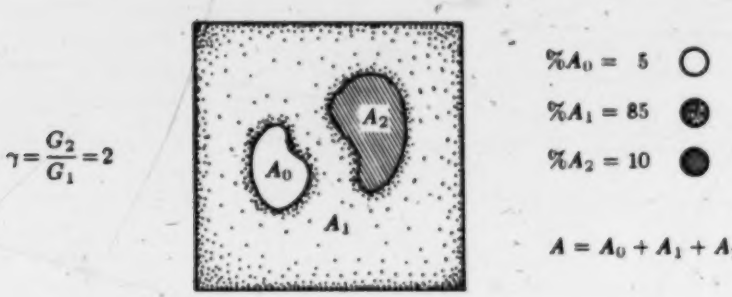

Figure 5.3: A Hollow Composite Regular Square Cross-Section under Torsion for the Determination of the Optimal Configuration

The optimal torsional rigidity and the optimal distribution of the cavity as well as of the reinforcement of the given cross-section can be determined by the linear combination of the optimal cavity and the optimal inhomogeneity.

Since the $(\%A_0,\%A_2)=(5,10)$ is within the plotted region in Figure 5.9, the result obtained is applicable, and the optimal torsional rigidity $\%Z^{iv.2}_{5.10}$ is therefore:

$$\%Z^{iv.2}_{5.10} = \%Z^{iv}_{0.0} + \Delta Z^{iv}_{5.0} + \Delta Z^{iv.2}_{0.10} \qquad (5.2)$$

No. of Sides — G_2/G_1 — *Homogeneous*

$\%A_0$ — $\%A_2$ — *by Cavity* — *by Reinforcement*

or, equivalently, from Table 5.3:

$$121.22\% = 100\% - 0.61\% + 21.83\%$$

In the optimal configuration, the hollow composite square cross-section concerned thus has 121.22% the torsional rigidity of the homogeneous one of the same size. The configuration of the one-eighth cross-section for the above maximum torsional rigidity can be also determined by overlapping the appropriate results given in Figures 5.10 and 5.11:

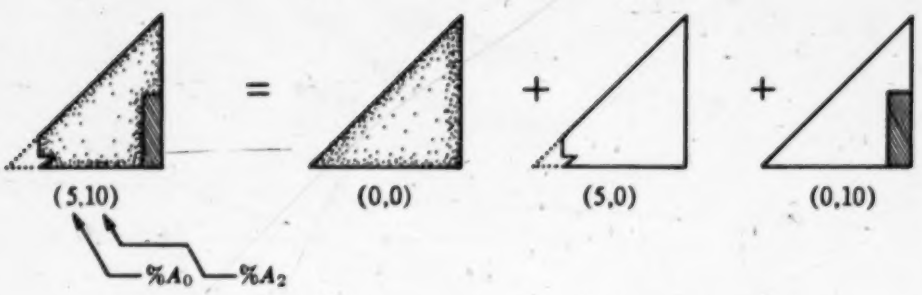

Figure 5.4: An Example-Use of the Present Results for the Determination of the Optimal Configuration of a Hollow Composite Regular Square Cross-Section under Torsion

5.1 THE EQUILATERAL TRIANGULAR CROSS-SECTION

Table 5.2: Optimal Torsional Rigidity for the Hollow Composite Equilateral Triangular Cross-Section at Various Proportions of the Cavity and of the Reinforcement

$\%A_0$ / G_2/G_1 / $\%A_2$		0	5	10	15	20	25	30	35	40	50	60	70	80	90	100
0		100.00	-0.72	-2.24	-4.17	-6.04	-10.80	-13.56	-18.33	-25.54	-36.46	-45.25	-62.51	-71.24	-86.32	-100.00
5	2	+13.39														
	5	+27.51														
10	2	+25.26														
	5	+69.01														
15	2	+34.47														
	5	+104.41														
20	2	+43.84														
	5	+139.51														
25	2	+50.86														
	5	+176.19														
30	2	+56.87														
	5	+197.90														
35	2	+63.10														
	5	+217.64														
40	2	+67.68														
	5	+239.61														
50	2	+76.42														
	5	+282.84														
60	2	+84.27														
	5	+318.71														
70	2	+90.99														
	5	+352.70														
80	2	+95.27														
	5	+378.46														
90	2	+98.85														
	5	+393.55														
100	2	+100.00														
	5	+400.00														

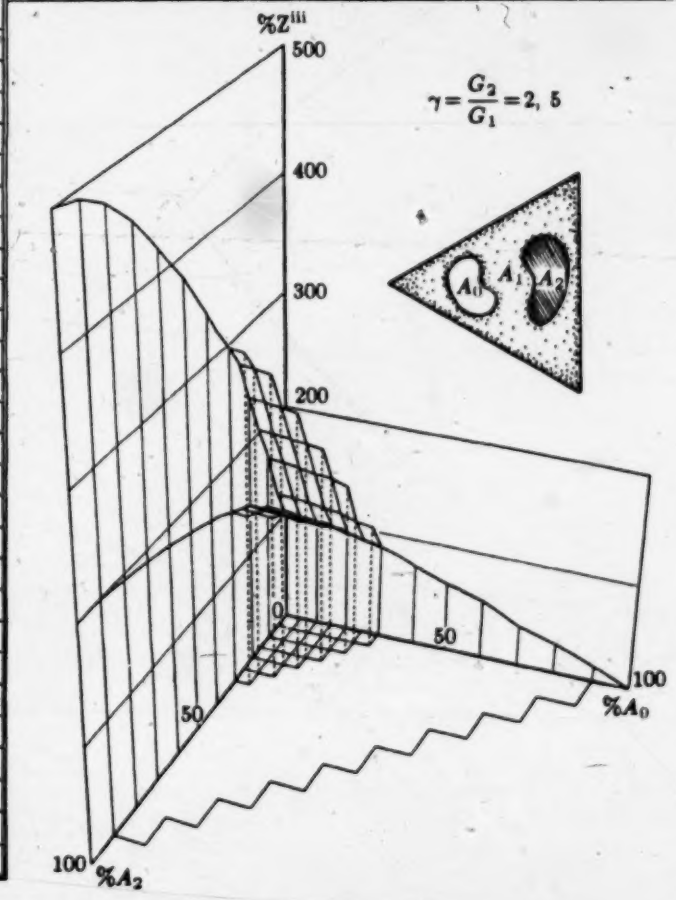

Figure 5.5: Three-Dimensional Display of the Relative Optimal Torsional Rigidity Values for the Hollow Composite Equilateral Triangular Cross-Section at Various Proportions of the Cavity and of the Reinforcement ($G_2/G_1=2, 5$)

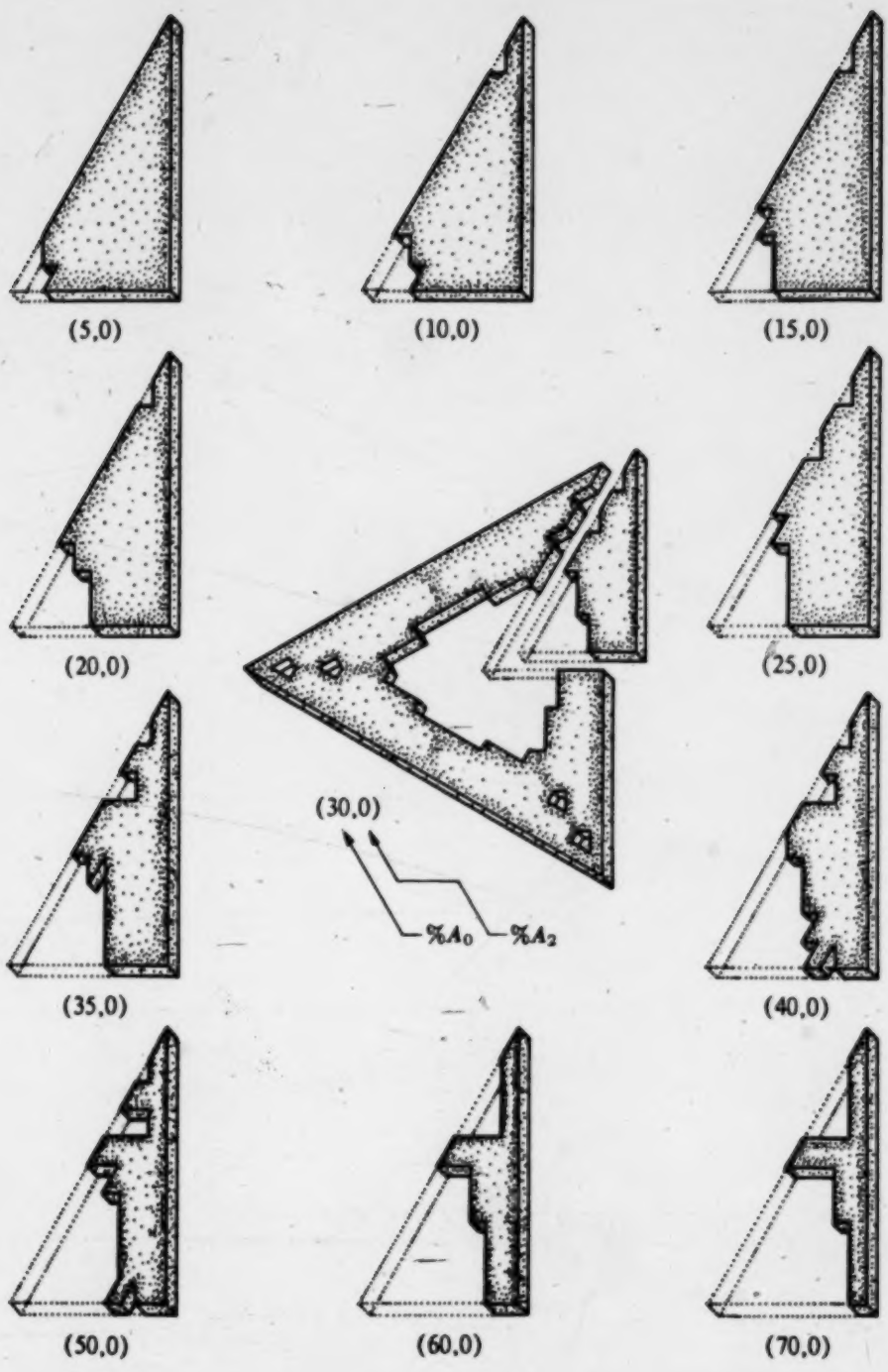

Figure 5.6: Optimal Configuration of the Hollow Homogeneous Equilateral Triangular Cross-Section under Torsion at Various Proportions of the Cavity

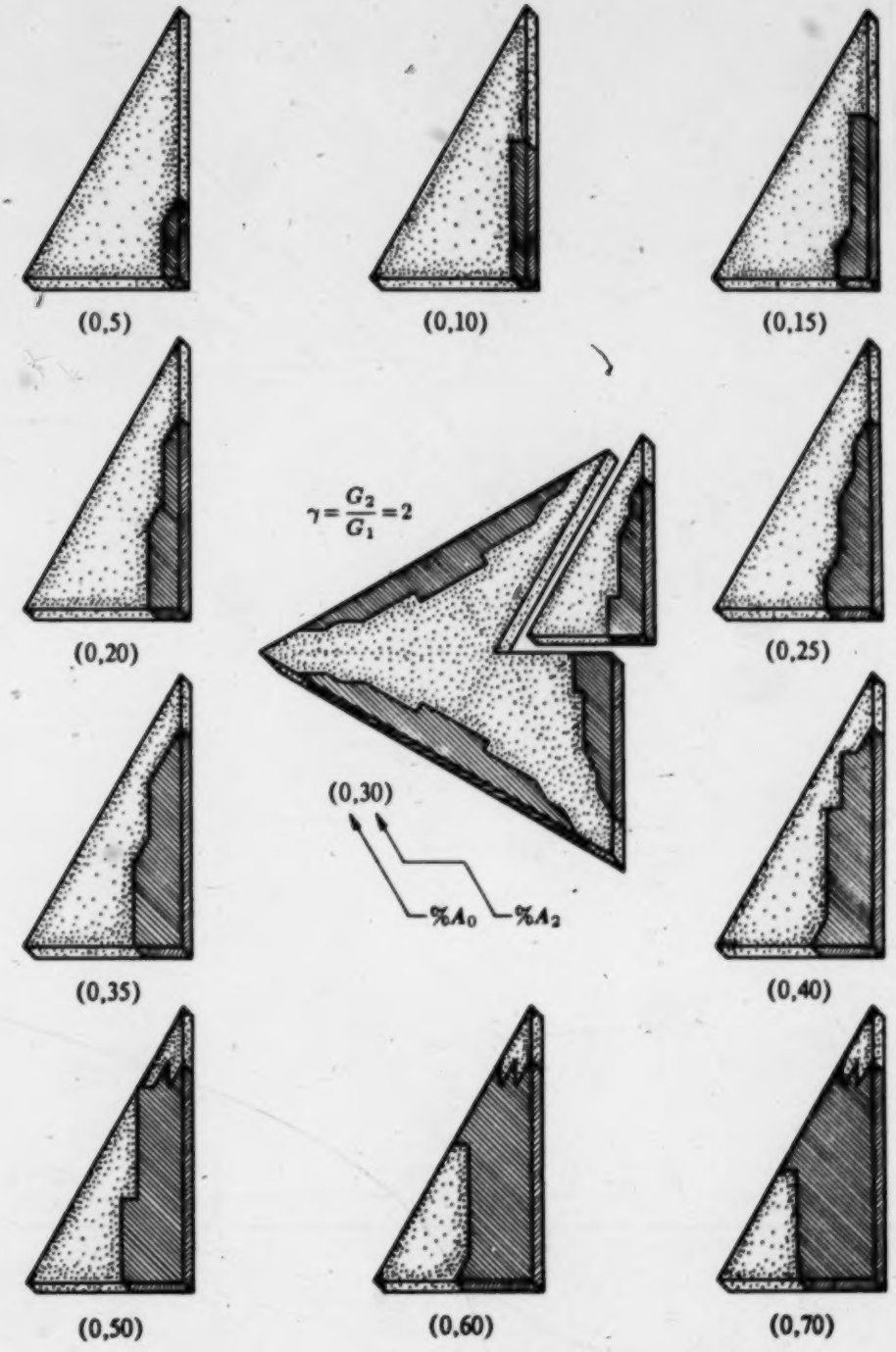

Figure 5.7: Optimal Configuration of the Solid Composite Equilateral Triangular Cross-Section under Torsion at Various Proportions of the Reinforcement ($G_2/G_1=2$)

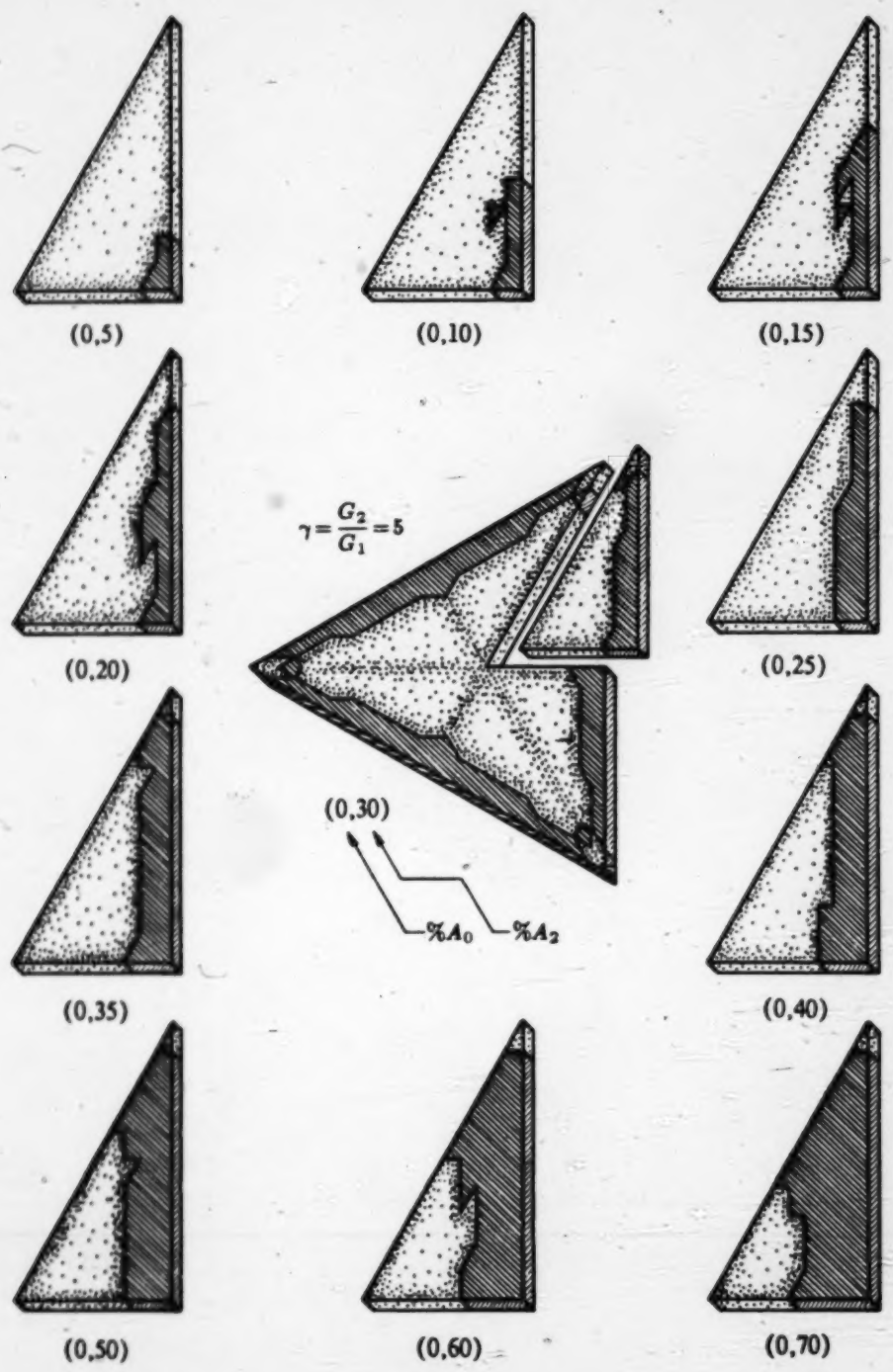

Figure 5.8: Optimal Configuration of the Solid Composite Equilateral Triangular Cross-Section under Torsion at Various Proportions of the Reinforcement ($G_2/G_1=5$)

5.2 THE REGULAR SQUARE CROSS-SECTION

Table 5.3: Optimal Torsional Rigidity for the Hollow Composite Regular Square Cross-Section at Various Proportions of the Cavity and of the Reinforcement

$\%A_2$ / G_2/G_1 / $\%A_1$		0	5	10	15	20	25	30	35	40	50	60	70	80	90	100
0		100.00	-0.61	-1.88	-3.05	-5.44	-8.48	-12.82	-16.77	-24.82	-34.86	-45.68	-62.13	-69.31	-84.65	-100.00
5	2	+10.68														
	5	+19.49														
10	2	+21.83														
	5	+58.98														
15	2	+30.15														
	5	+99.41														
20	2	+37.96														
	5	+125.47														
25	2	+45.38														
	5	+150.08														
30	2	+51.65														
	5	+176.90														
35	2	+57.07														
	5	+221.47														
40	2	+62.56														
	5	+238.45														
50	2	+73.96														
	5	+275.98														
60	2	+82.15														
	5	+320.07														
70	2	+89.55														
	5	+355.31														
80	2	+95.14														
	5	+378.64														
90	2	+98.64														
	5	+393.78														
100	2	+100.00														
	5	+400.00														

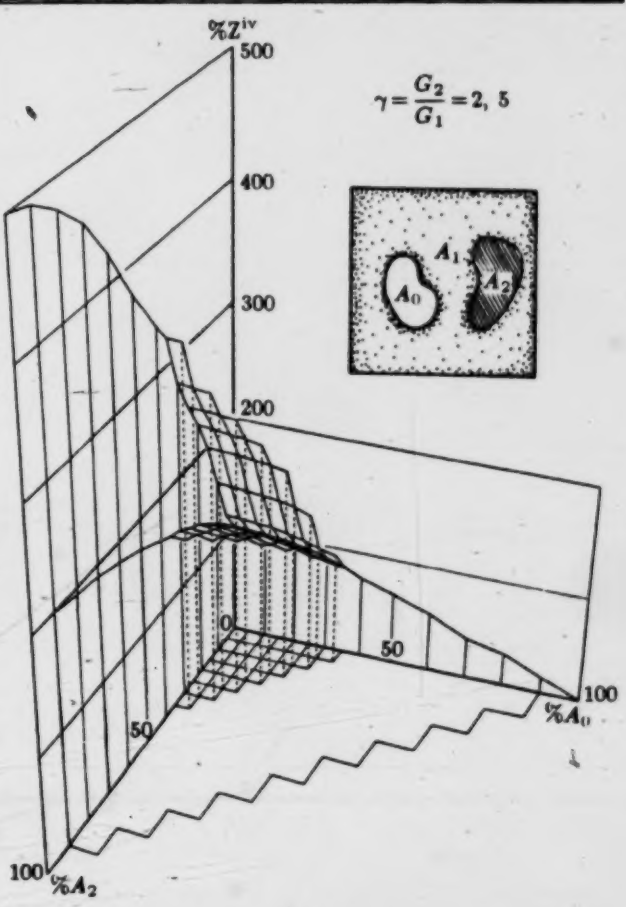

Figure 5.9: Three-Dimensional Display of the Relative Optimal Torsional Rigidity Values for the Hollow Composite Regular Square Cross-Section at Various Proportions of the Cavity and of the Reinforcement ($G_2/G_1=2, 5$)

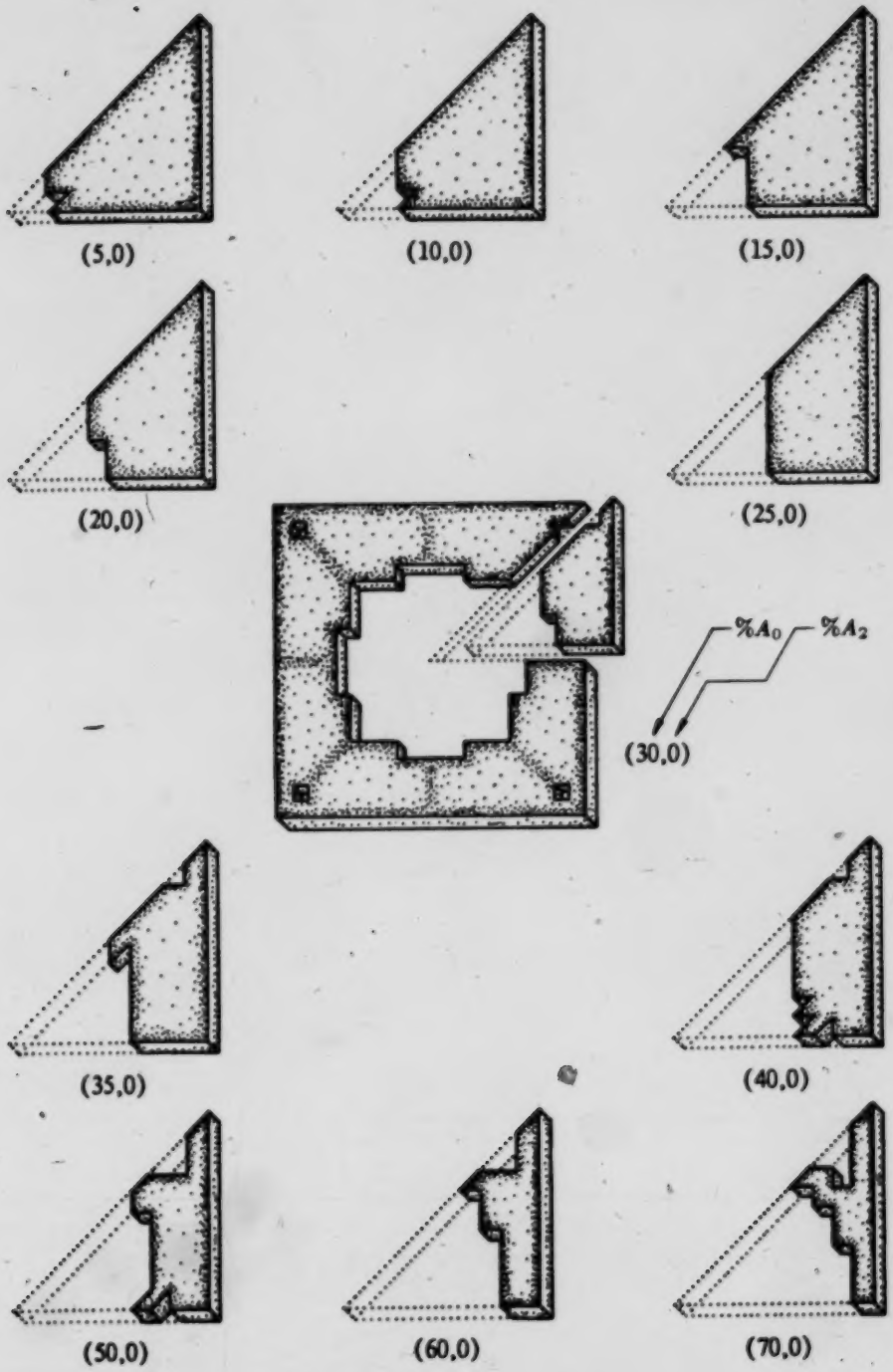

Figure 5.10: Optimal Configuration of the Hollow Homogeneous Regular Square Cross-Section under Torsion at Various Proportions of the Cavity

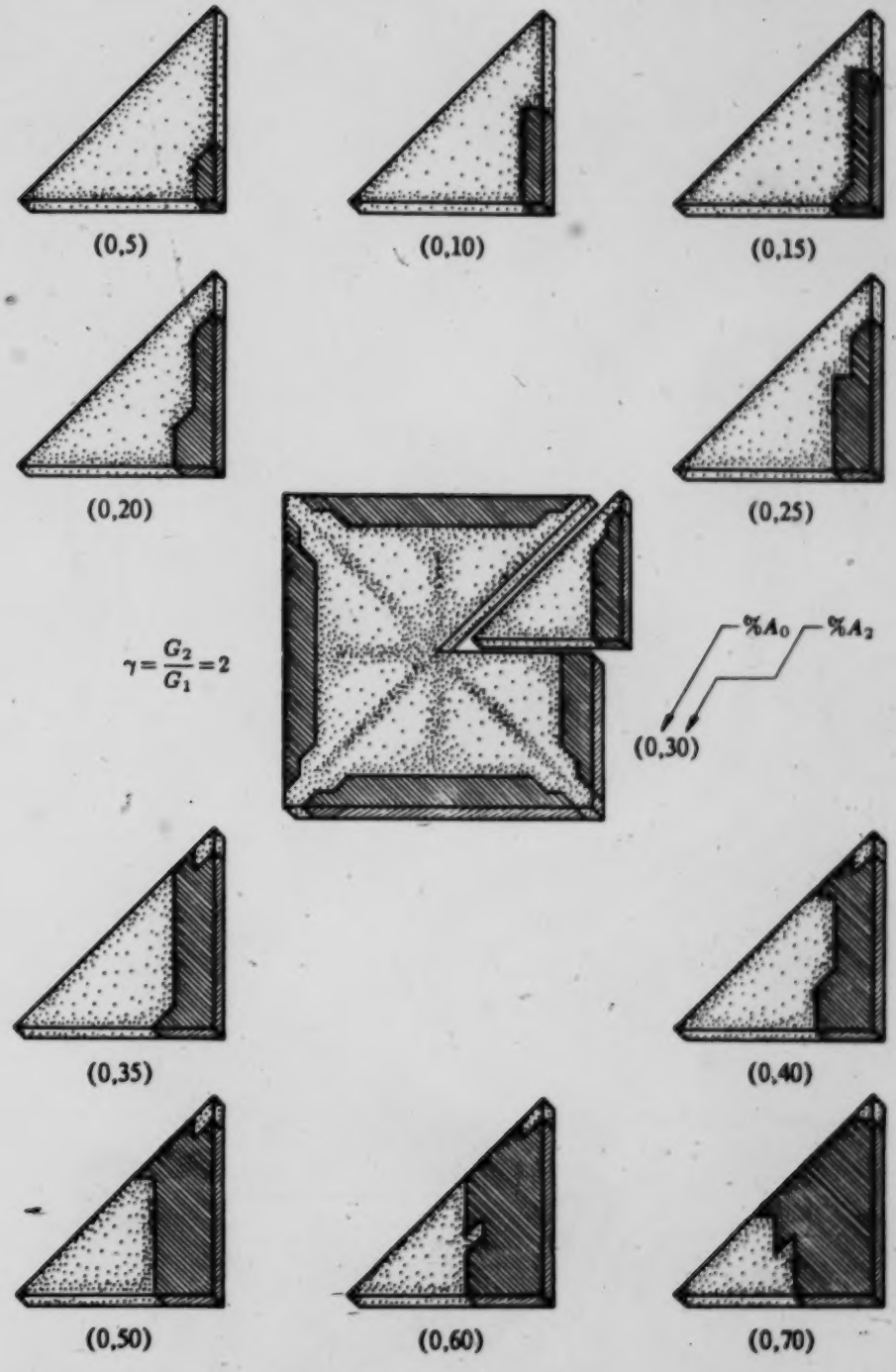

Figure 5.11: Optimal Configuration of the Solid Composite Regular Square Cross-Section under Torsion at Various Proportions of the Reinforcement ($G_2/G_1=2$)

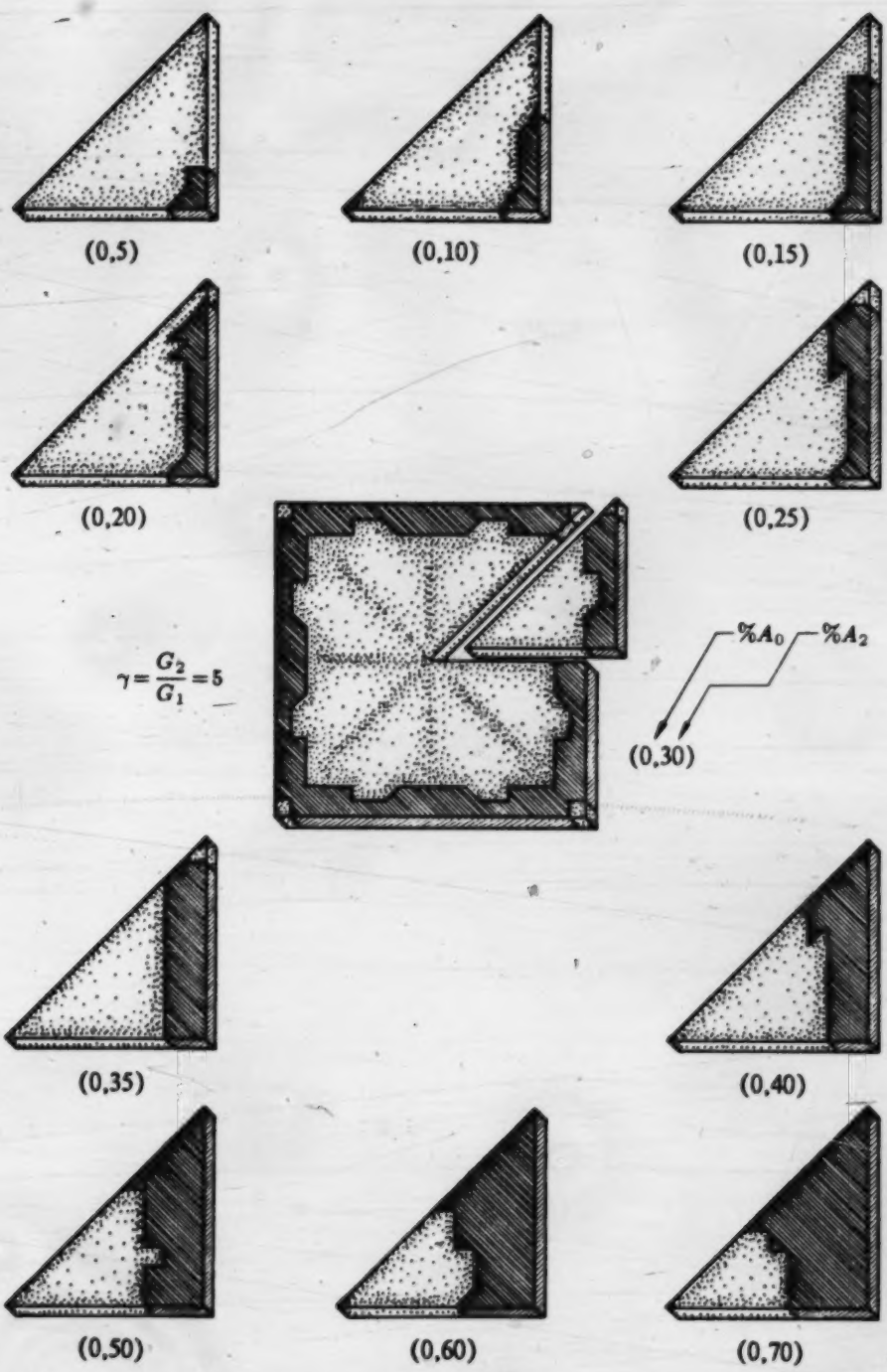

Figure 5.12: Optimal Configuration of the Solid Composite Regular Square Cross-Section under Torsion at Various Proportions of the Reinforcement ($G_2/G_1=5$)

5.3 THE REGULAR HEXAGONAL CROSS-SECTION

Table 5.4: Optimal Torsional Rigidity for the Hollow Composite Regular Hexagonal Cross-Section at Various Proportions of the Cavity and of the Reinforcement

$\%A_0$ / G_2/G_1 / $\%A_2$	0	5	10	15	20	25	30	35	40	50	60	70	80	90	100
0	100.00	-0.66	-1.93	-2.68	-5.27	-6.99	-11.63	-13.73	-28.36	-31.46	-40.91	-63.12	-67.53	-82.83	-100.00
5 — 2	+8.48														
5 — 5	+18.44														
10 — 2	+18.45														
10 — 5	+49.21														
15 — 2	+27.73														
15 — 5	+88.39														
20 — 2	+34.17														
20 — 5	+135.54														
25 — 2	+39.96														
25 — 5	+152.00														
30 — 2	+47.14														
30 — 5	+174.11														
35 — 2	+55.46														
35 — 5	+211.36														
40 — 2	+61.41														
40 — 5	+242.71														
50 — 2	+73.01														
50 — 5	+286.08														
60 — 2	+82.28														
60 — 5	+325.63														
70 — 2	+89.97														
70 — 5	+357.50														
80 — 2	+95.42														
80 — 5	+380.40														
90 — 2	+98.76														
90 — 5	+394.11														
100 — 2	+100.00														
100 — 5	+400.00														

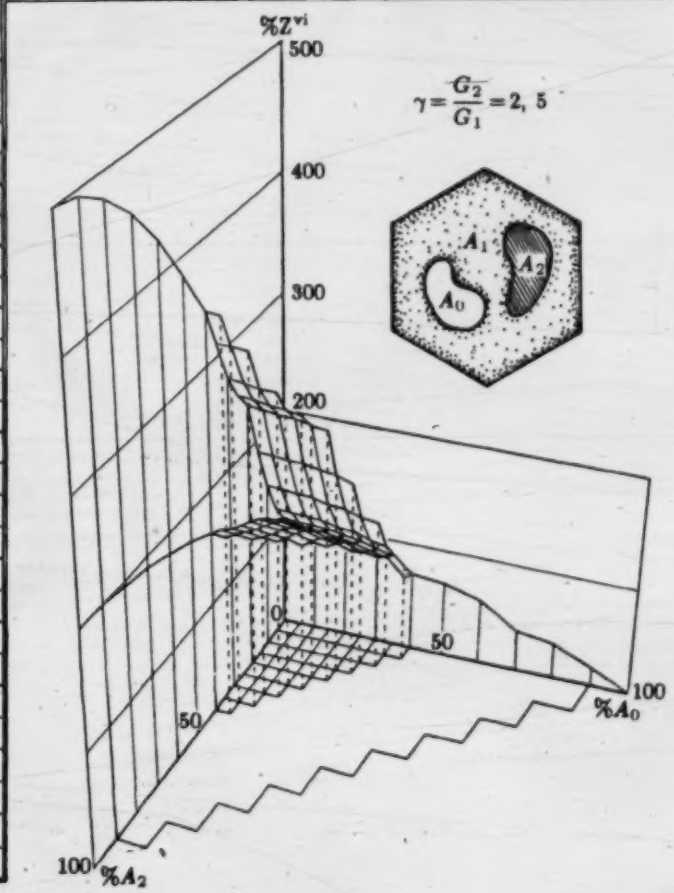

Figure 5.13: Three-Dimensional Display of the Relative Optimal Torsional Rigidity Values for the Hollow Composite Regular Hexagonal Cross-Section at Various Proportions of the Cavity and of the Reinforcement ($G_2/G_1=2, 5$)

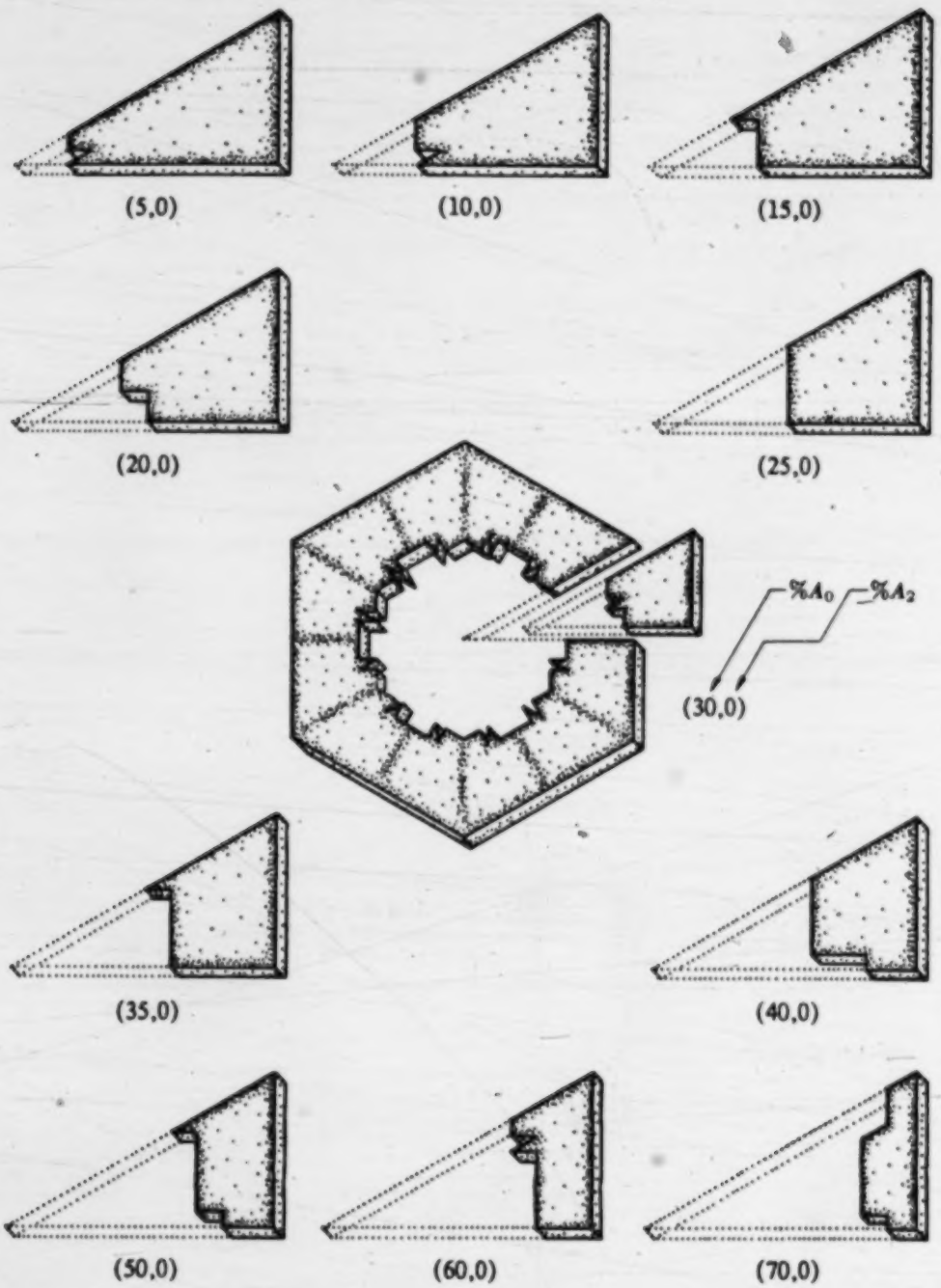

Figure 5.14: Optimal Configuration of the Hollow Homogeneous Regular Hexagonal Cross-Section under Torsion at Various Proportions of the Cavity

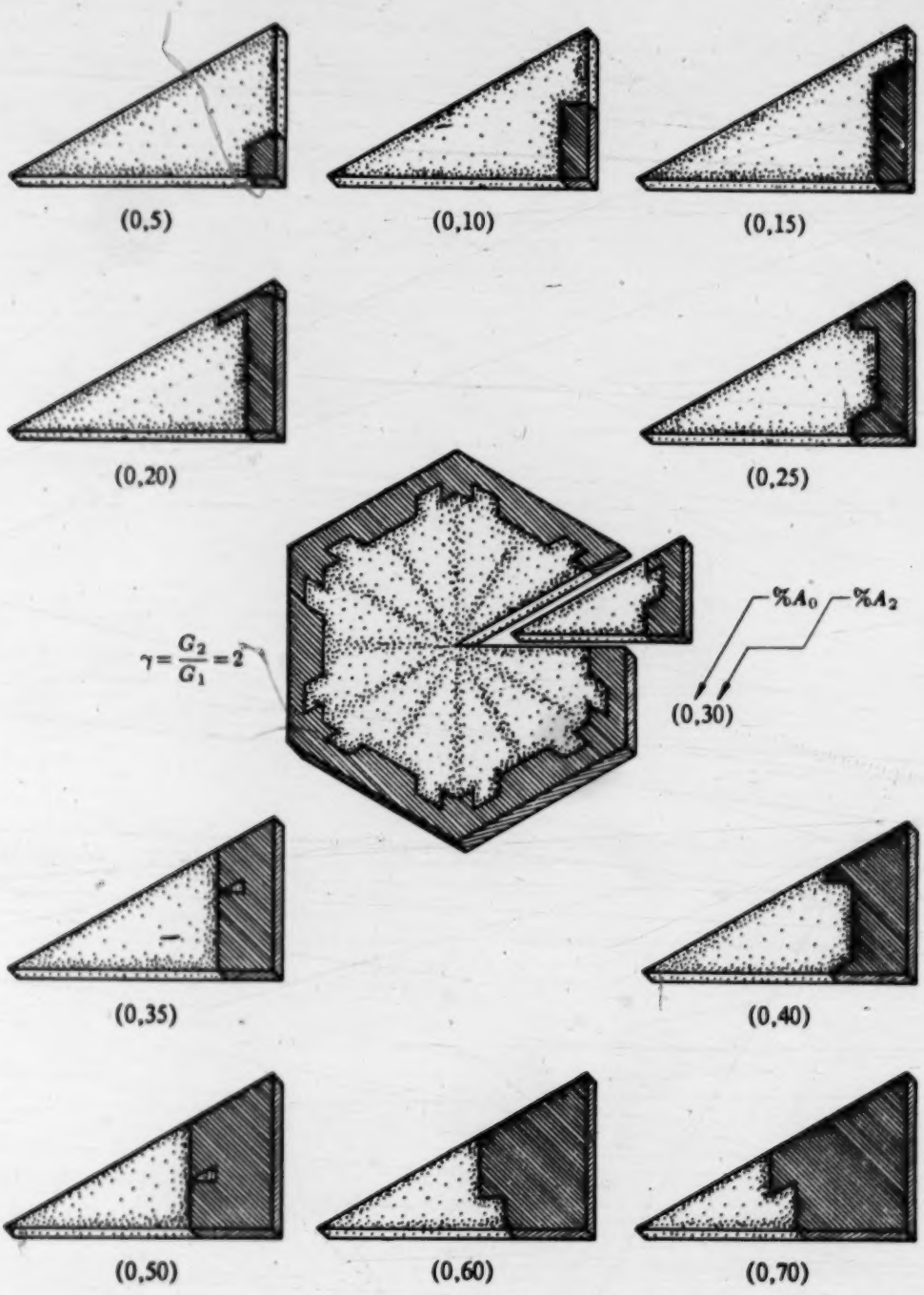

Figure 5.15: Optimal Configuration of the Solid Composite Regular Hexagonal Cross-Section under Torsion at Various Proportions of the Reinforcement ($G_2/G_1=2$)

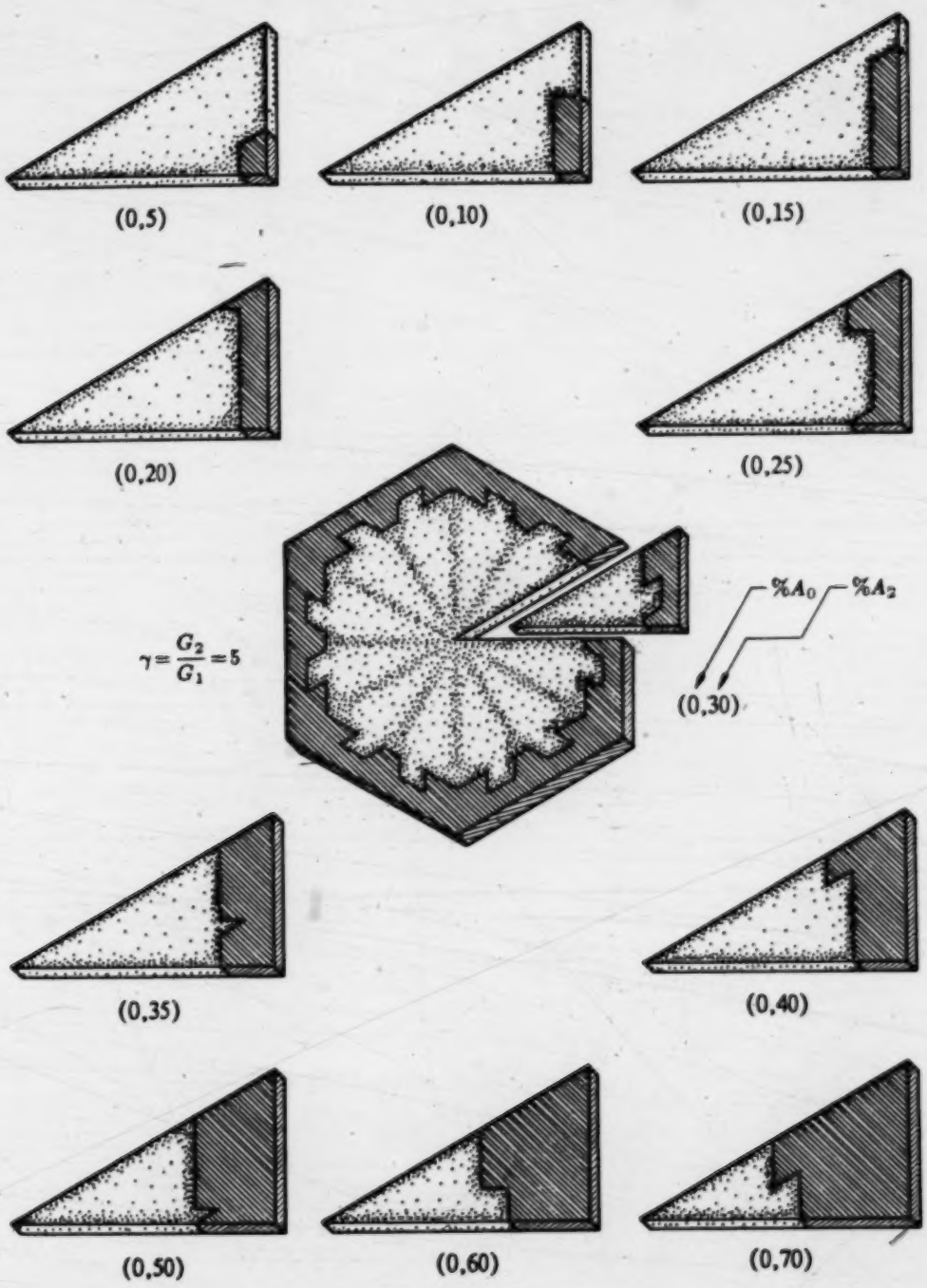

Figure 5.16: Optimal Configuration of the Solid Composite Regular Hexagonal Cross-Section under Torsion at Various Proportions of the Reinforcement ($G_2/G_1=5$)

6 DISCUSSION

6.1 DISCUSSION OF THE NUMERICAL PROCEDURE

[The Stress Function Formulation] The major drawback of the stress function formulation for the torsion problem, which was used in this study, is that it fails to provide a means to satisfy exactly, for the simply-connected problem, the contour integral condition on the external boundary. This particular difficulty may be overcome by using the hybrid or the mixed approach as in [18].

Such a deficiency of the stress function formulation, however, is more than offset by the fact that it is the one that allows consideration of the problem in conjunction with the membrane analogy. Indeed, this analogy is a convenient means for the visual interpretation of not only the whole problem itself but also its solution procedure, especially with the involvement of multiple-connection. This has been well demonstrated by the accuracy of approximation throughout the verification of the numerical procedure.

[The Finite Element Formulation] The finite element equation derived by the use of the weighted residual method in the present formulation is almost identical with what is obtainable from the variational principle.

The simple constant-strain triangular element used in the formulation was found to give excellent results. It was, first of all, very flexible even for extremely large element aspect ratios. For example, one adjacent angle of the element was just as small as 1.8° when a circular cross-section was triangulated, and it still worked stably without resulting in any deterioration in the accuracy of approximation.

The good accuracy and the reasonable rate of convergence of the element were also apparent from the various verifications performed. In fact, values for the torsional

rigidity were all obtained within 0.5% of the known solution when at least 600 elements were used for the whole cross-section.

[**The Transformation Method**] With the transformation method, the shear modulus ratio G_0/G_1 for a good approximation of the cavity element was proved to be of $O(10^{-10})$.

Despite the mathematical incompleteness of disregarding the integral conditions, the transformation method was found to be reliable enough as compared to the superposition method. In fact, the simplicity of this technique furnished a great deal of computational efficiency.

The overall performance of this method was quite stable in most of the cases including those of small cavities and also of thin-walled tubes.

[**The Superposition Method**] From the examination of several other possible forms of the trial solution in the present study, it has been revealed that the additional inclusion of any more linearly dependent mode solutions in the trial function does not affect the final solution at all, as long as the linearly independent ones are all there; in such cases, the magnitude of the weightings are accordingly adjusted to have the original differences in the trial solution compensated. It was in this regard that Shaw's omission [70] of the first mode solution in his trial function in dealing with a doubly-connected problem was found to be incorrect.

The various numerical studies carried out indicated that the trial boundary constants in the superposition method could be chosen quite arbitrarily. For example, any trial boundary values of $O(10^{-1} \sim 10^{+1})$ led to identical final solutions when the exact one was of $O(10^{+4})$. This being the case, there is all the more no reason why it should be other than unity, thereby forming normal mode solutions as has been done in the present study.

One problem observed with this superposition method particularly in conjunction with the finite element procedure, however, was that it became somewhat unstable in its

performance when the cavities were approximated by too small a number of elements: fewer than seven, for instance. In these cases, the contour integral values are so coarsely approximated that the weighting factors obtained through the matrix integral condition are not reasonable, and this eventually affects the final solution. For this reason, the actual solution procedure in the present study employs both the superposition and the transformation methods in combination so as to cover all the possible cases more adequately.

Also as a result of the finite element discretization, there were differences in terms of results between the two methods of obtaining the general solution in the superposition method.

While computationally more expensive to practice because it had to store all the mode solutions, the first alternative—the direct superposition of each of the weighted modes—gave final solutions which satisfied the integral conditions all in an exact sense; in fact, this procedure has been used exclusively in obtaining the present solution.

In contrast, complete satisfaction of the integral conditions was not always possible with the second alternative in which only the exact boundary constants are determined by the linear combination, and the final solution is then obtained by re-solving these boundary values simultaneously with the governing differential equation.

The difference above, however, is not an intrinsic problem of the superposition method, but rather what occurs only when it is used jointly with approximation methods such as the finite element technique. Therefore, in such cases, the difference becomes smaller as the discretization of the solution domain gets finer. It is expected that the two methods eventually give identical results as real continuum problems are approached more closely.

6.2 DISCUSSION OF THE OPTIMIZATION PROCEDURE

As was so suggested for non-circular cases, the three assumptions made in numerically implementing the membrane analogy as an optimization procedure turned out to be not always true in reality.

[The Assumption I] As a way of visualizing the optimization procedure, a homogeneous regular square cross-section was considered. The increment in torsional rigidity caused by replacing each of the base material elements of this cross-section with the reinforcement element is shown in Figure 6.1, while a similar illustration for the decrement with the cavity element is shown in Figure 6.2. In fact, both of these figures illustrate what the optimization procedure does at its very initial stage.

If the linearity condition as stated in the Assumption I were always valid, it would mean that these two plots indicate directly the optimal placement of every possible proportions of either the cavity or the reinforcement. Various numerical studies carried out in this connection, however, show that the linearity in this sense is entirely dependent upon the fineness of the approximation, and therefore that such result tends to get closer to the final optimal solution as the mesh discretization and the approximation of the stress function within the element become more realistic.

For the particular mesh division used (100 linear triangular elements), it has been found that only as many elements as five can be taken as optimal locations at each stage of the optimization procedure. For better precision, however, the steps in the present study were limited only to three elements throughout.

[The Assumption II] The validity of the Assumption II, i.e. the continuity of the optimal torsional rigidity functional, was tested by repeatedly reversing the direction of the optimization procedure. In this case, the forward and the backward movements

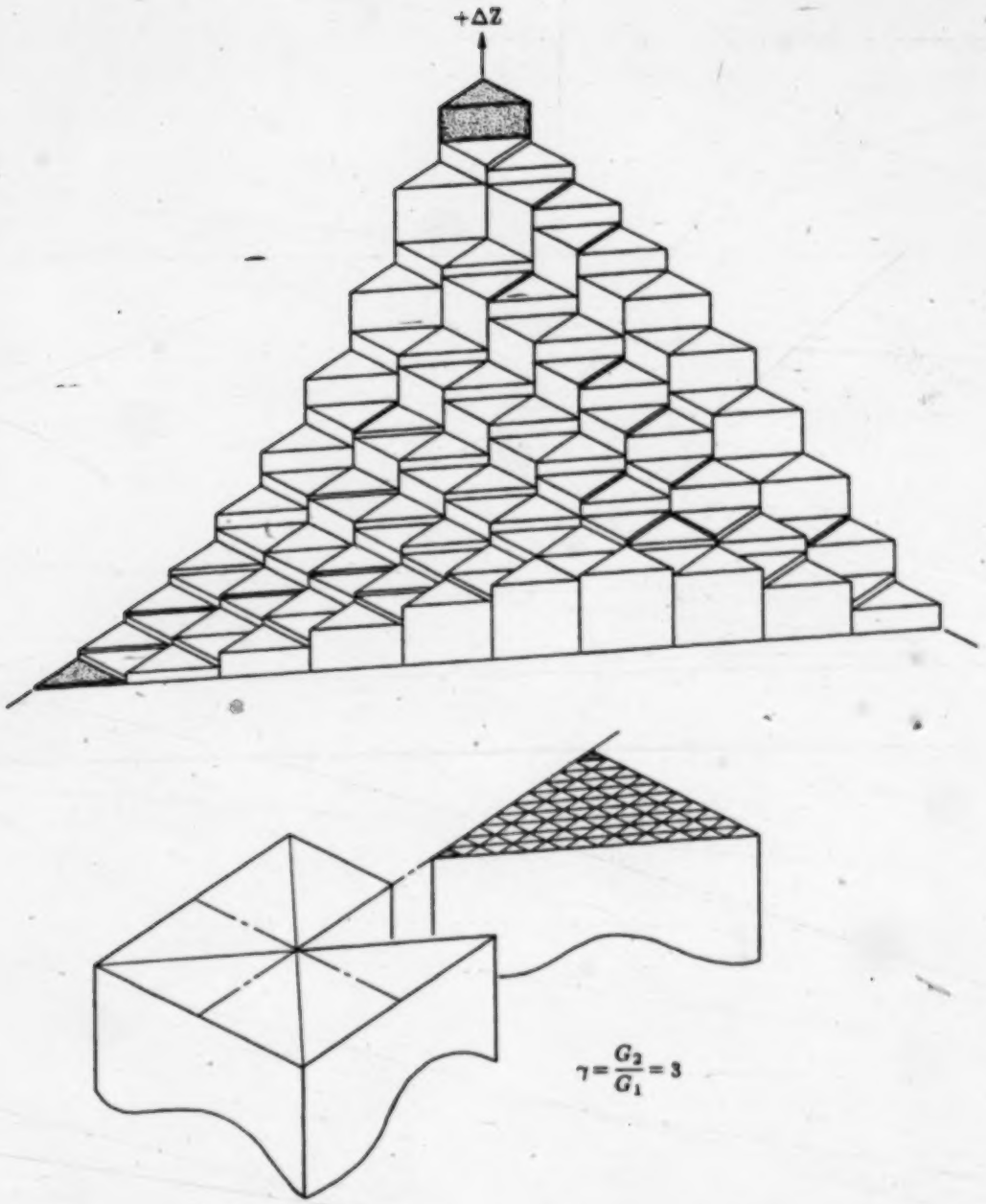

Figure 6.1: Relative Increment in the Torsional Rigidity of a Solid Regular Square Cross-Section with Each of the Constituent Elements Replaced by the Reinforcement ($G_2/G_1=3$)

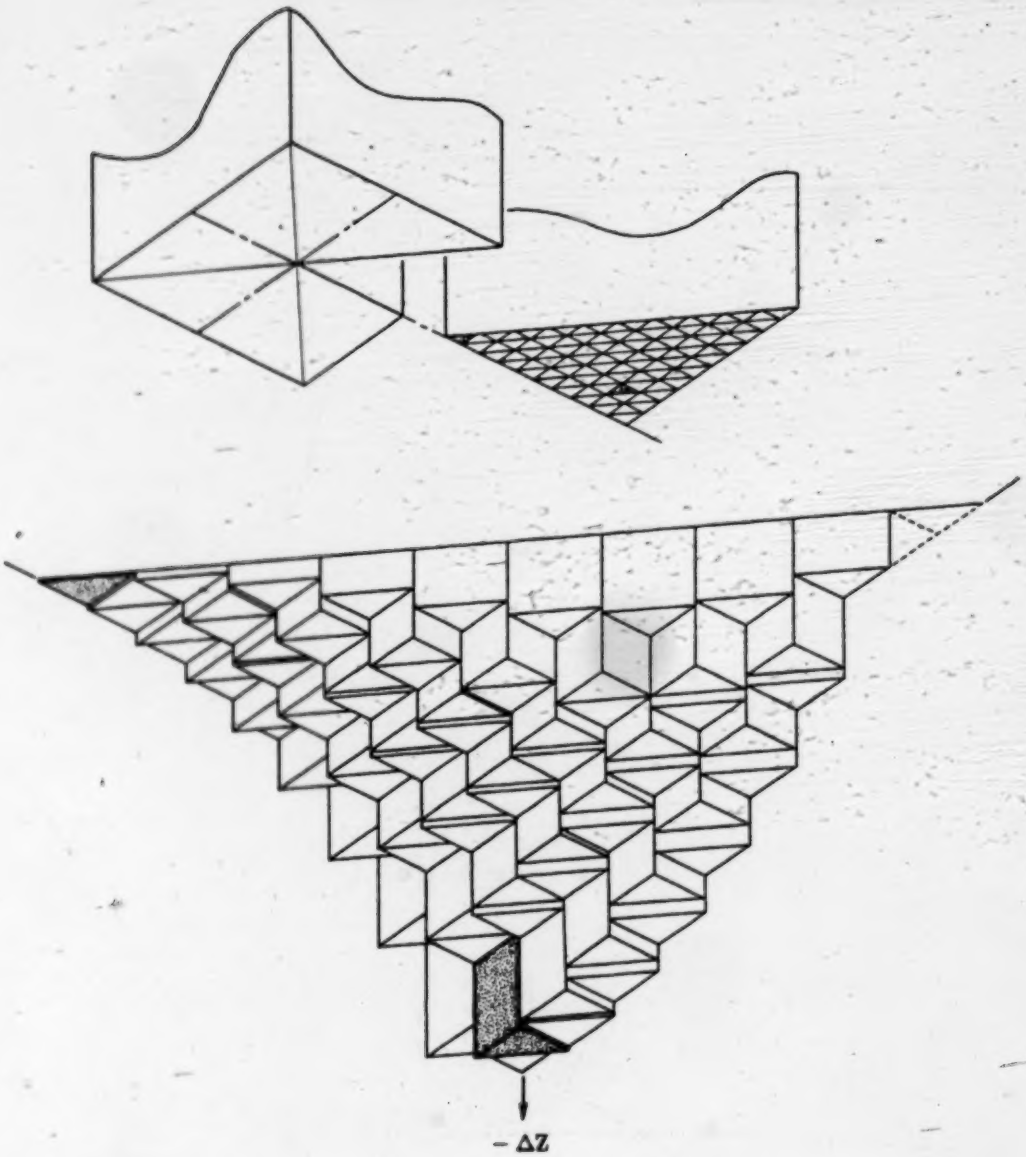

Figure 6.2: Relative Decrement in the Torsional Rigidity of a Homogeneous Regular Square Cross-Section with Each of the Constituent Elements Replaced by the Cavity

correspond, respectively, to the addition of three new elements and the exclusion of one element to and from the existing optimal configuration.

The results obtained through such tests in various situations showed that this assumption is true under most of the practical circumstances, thus making the sequential determination of the optimality possible.

In fact, a similar conclusion can be also drawn from an examination of the previously obtained results by Faulkner, Mioduchowski and Hong [22]. In this case, the three proportions of the reinforcement considered—25, 50 and 75 percents—were treated completely independently, and the obtained optimal solutions appeared such that the 75% fully covered the 50%, while the 50% included all the elements of the 25% case.

[The Assumption III] Finally, for non-circular cross-sections, the Assumption III—the independence of the optimalities of the cavity and the reinforcement—was shown to be valid only when either one of the two parameters was relatively negligible in its influence. The useable range of this weak parameter was found to be somewhere between 0 and 40% of proportion depending on the cross-sectional shape as well as on the shear modulus ratio G_2/G_1; in general, the closer the shape is to the circular cross-section, and also the smaller the value of the shear modulus ratio is, the wider is the range of applicability for this assumption.

It follows, therefore, that the optimality problems of the cavity and the reinforcement, in a strict sense, cannot be treated entirely independently outside the range indicated above.

In summary, the three assumptions established in developing the present optimization procedure are true for the circular cross-section under every possible situations.

For non-circular cases, however, it is only over a certain limited region of the A_0-A_1 plane where these are all simultaneously valid, and unique, path-independent optimal

solutions are thus obtainable by the present procedure of optimization.

It is also in this region only where the optimalities of any non-circular multiply-connected inhomogeneous cross-section can be determined by a simple linear combination of those of the pure cavity and of the pure reinforcement considered separately as with the circular case.

Mathematically, the optimization procedure developed may not be regarded as complete in that the three assumptions upon which it is based are not always true, and therefore that it fails to cover the entire region of the A_0-A_2 plane.

However, in view of the fact that there is, because of the mathematical difficulties involved, no other available method for this sort of three-parameter optimization problem, the method is still useable in an engineering sense.

This is so much the case in that the region where the present optimization procedure is applicable happens to be, fortunately enough, the one in which there is practical interest in composite materials; hence the optimization is most useful; and furthermore its real point exists.

The reliability of the present optimization procedure has also been demonstrated through the improvement in optimal torsional rigidity values as seen in the previous verification.

One particular advantage of the present procedure over others is the fact that it is based on the actual computation and then the comparison of the torsional rigidity values rather than based on the stress values of each of the elements as was done in [22]. In fact, the previous approach turned out to be more vulnerable to the effects of the coarseness of the mesh division and also of large shear modulus ratios between the two constituent materials.

6.3 DISCUSSION OF THE RESULTS

As examples for the application of the developed solution procedure, the present study considered three representative non-circular regular geometries including the triangular, the square and the hexagonal cross-sections. Analysis of the results obtained for these cases reveals some of the typical and general characteristics of the optimal distribution of the cavity and the reinforcement within those prescribed boundaries.

From the optimal torsional rigidity surfaces in Figures 5.5, 5.9 and 5.13, it can be seen, first of all, that the plotted region where the use of the linear combination is possible is larger for the square case as compared with the triangular case's, and larger again for the hexagonal case as compared with the square case's. This, obviously, suggests that the range of the applicability increases as the shape approaches to a circle.

As also can be seen from the various optimal shapes, the configuration and the number of contours inside the cross-section depend notably upon the curvature of the given external boundary. For both the cavity and the reinforcement areas, though, the optimalities are observed to appear in a fashion such that they all tend to become as close as possible in shape to that of the circular case. This can be seen, first, from the observation of the distribution of the optimal cavity over the cross-section for the respective geometries. The optimal triangular cross-section already includes corner cavity at 10% of its proportion, the square at 30%, whereas the hexagon never contains such a cavity at the corner regardless of the proportion; in other words, the further the shape of the cross-section is from that of the circular one, the faster becomes the propagation of the cavity to the corners.

A similar approaching to the circular case can also be seen from Table 6.1 in which the number of contours that appear in the entire optimization procedure are summarized for the four geometries considered.

Table 6.1: Variation of the Number of Contours for Some Typical Optimally-Shaped Hollow Homogeneous Regualr Cross-Sections at Various Proportions of the Cavity

Geometry	NC, Number of Contours within the Entire Cross-Section with the cavity proportion in percentage of										
	0	10	20	30	40	50	60	70	80	90	100
	1	4		7		10	7	4		1	
	1			5		9		5		1	
	1										
	1										

The distribution of the optimal reinforcement also leads, in this regard, to a similar conclusion: the closer the shape of the external boundary of the cross-section is to a circle, the faster is the spread of the optimal reinforcement to the corners. In these cases, the movement of the reinforcement to the corners is even more accelerated by the increase of the shear modulus ratio. This is the same as what was observed by Faulkner, Mioduchowski and Hong in [22].

While the present study is confined only to the range of elastic behaviour of the constituent materials, it is very interesting, although not surprising, to note that the progression of the optimally reinforced region in the present results is quite similar to the development of the plastic region over the cross-section studied by Baba and Kajita [2].

Also, as is immediately noticeable from the striking similarity in variation of the torsional rigidity in Figures 6.1 and 6.2, the optimal location of the cavity on the

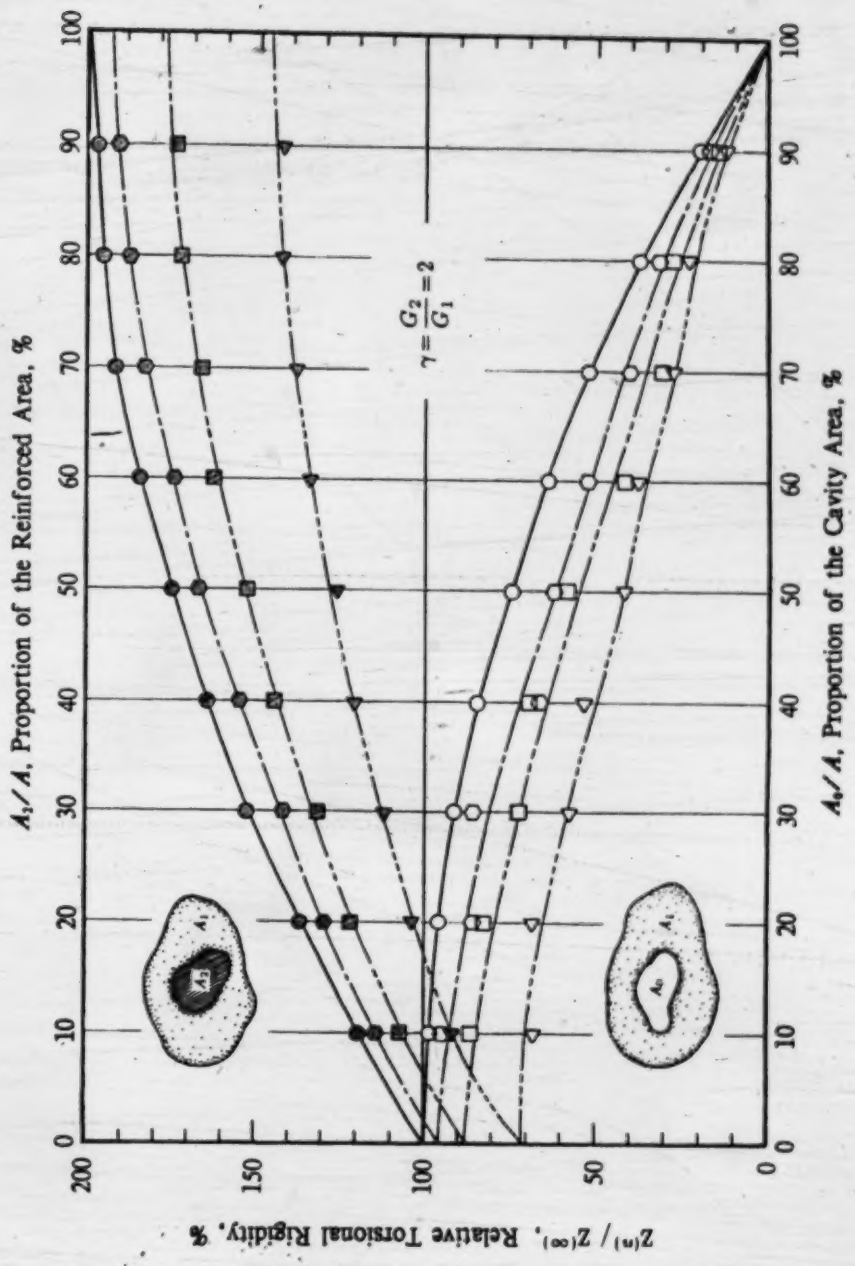

Figure 6.3: Relative Optimal Torsional Rigidity Values for Some Typical Hollow and Composite Equal-Area Regular Cross-Sections at Various Proportions of the Cavity and of the Reinforcement

cross-section is approximately equivalent to the worst place for the addition of the reinforcement, and vice versa. The slight differences in such cases can be attributed to the necessary existence of the wall elements which, to keep the prescribed external boundary shape unchanged, force the optimal cavity to be found inside only.

Shown in Figure 6.3 is the comparison of the optimal torsional rigidity values of the four cases considered in the present study—the triangular, the square, the hexagonal and the circular cross-sections.

The cross-sections in this case have all equal areas, and, for the simultaneous consideration of the effectiveness of the optimalities, the torsional rigidity values are all non-dimensionalized with respect to that of the circular case setting its homogeneous case's to 100%. As for the reinforcement, only the shear modulus ratio of 2 was considered. The lower four and the upper four curves in the plot represent the optimal cavities and the optimal reinforcements, respectively.

As expected, all curves tend toward that of the circular case since it is optimal among all equal-area cross-sections. Because the slopes of the curves for the optimal reinforcement are most steep at the origin, the maximum increase in the torsional rigidity by the same additional amount of the reinforcement occurs at lower proportions of the stiffer material. On the other hand, lower proportions of the cavity also have little effect on the torsional rigidity. It is fortunate that this lower-proportion area happens to be where the optimization procedure developed in the present study functions best.

Figure 6.4 compares the relative torsional rigidity values of various homogeneous regular equal-area cross-sections. The number of sides of the cross-section in this case was increased up to 100, and for each of the cases the torsional rigidity values are non-dimensionalized with respect to that of the circular case. Again, the convergence to the circular case as well as the effectiveness of each of the geometries can be clearly seen.

Figure 6.4: Relative Torsional Rigidity Values for Homogeneous Equal-Area n-Sided Regular Cross-Sections

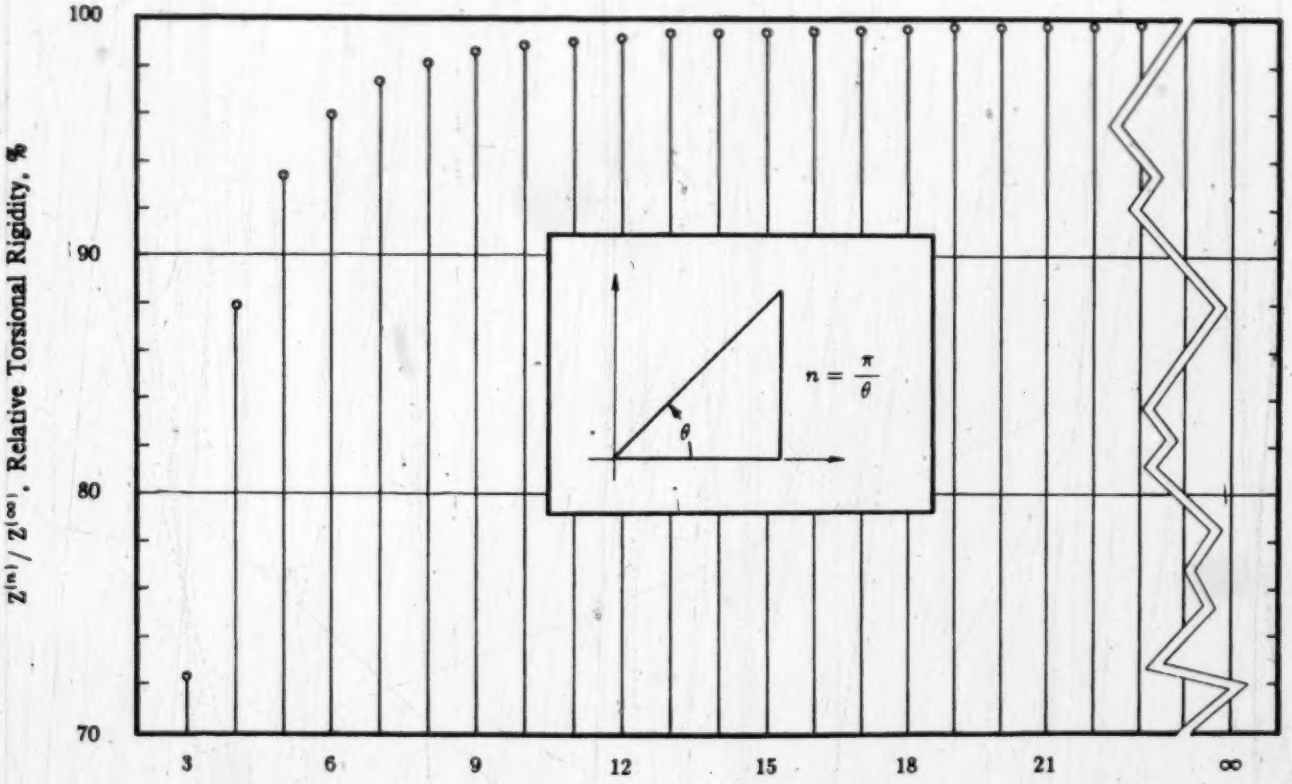

The results obtained in the present study can be used in many different combinations for various purposes of optimization. One of such usage is in design for the determination of the exact optimal configuration and dimension of the cross-section with given the external shape, the shear modulus ratio, the proportions of both the cavity and the reinforcement, and the torsional rigidity value.

As shown earlier, the optimal shape of the cross-section in such cases can be determined by combining the appropriate entries in Figures 5.5 to 5.16. By following proper manipulation, it is also easy to show that the relation below can be used for the determination of the corresponding optimal cross-sectional area A^*:

$$A^* = \sqrt{\frac{2\pi \, \bar{Z}^{n,\gamma}_{A_0,A_2}}{G_1 \left(\frac{Z^{n,\gamma}_{A_0,A_2}}{Z^{n}_{0,0}} \right) \left(\frac{Z^{n}_{0,0}}{Z^{\infty}_{0,0}} \right)}} \tag{6.1}$$

In this equation, $\bar{Z}^{n,\gamma}_{A_0,A_2}$ is the required torsional rigidity value of the given cross-section, $(Z^{n,\gamma}_{A_0,A_2}/Z^{n}_{0,0})$ a non-dimensional parameter which can be determined from one of the Tables 5.2 to 5.4, and $(Z^{n}_{0,0} / Z^{\infty}_{0,0})$ another dimensionless parameter which can be read directly from the graph in Figure 6.4.

7 CONCLUSIONS

The objective of this study was to develop first a suitable solution method that can handle the general multiply-connected inhomogeneous torsion problem, and then an optimization procedure that finds the internal configuration of such cross-sections maximizing the torsional rigidity.

Listed in the following are the major findings and the conclusions drawn from the present investigation:

[1] In formulating the more general class of the torsion problem, the Prandtl stress function approach offers several distinct advantages over others. These include the considerable simplification of the boundary conditions and the availability of various analogies for the visualization of the problem.

[2] With the flexibility in mapping the complicated geometry, the ease of treating the inhomogeneous as well as the multiply-connected situations, the identical satisfaction of the interface conditions, and the variety of choices of elements, the finite element method is the best suited approach available for the analysis of the advanced type of torsion problems.

[3] The rather straightforward transformation technique is, despite its mathematical incompleteness, reliable in most of the multiply-connected situations, and its simplicity furnishes a great deal of computational efficiency. However, this method can be used usually in conjunction with the finite element procedure only.

[4] The superposition technique as developed in this study is capable of dealing with any type of multiply-connected situations regardless of the number of boundary contours

involved, and it is the only known approach determining the boundary constants as simultaneously satisfying all the integral conditions. Its applicability to other types of linear multiple boundary value problem is, as well, apparent.

[5] The method of numerical simulation of the membrane analogy as used for the optimization procedure in the present study is equally applicable to the finding of the optimalities of both the cavity and the reinforcement. Although not mathematically complete especially for general multiply-connected inhomogeneous cases, its performance is sufficiently versatile for many practical situations in composite materials.

[6] In torsion problem, the circular cross-section is special in that it is optimal among all cross-sections of the same area. The optimality condition of this cross-section including both the multiple-connection and the inhomogeneity in it can always be determined by simple linear combination of those of the pure cavity and of the pure reinforcement considered separately. It is also for this case only that the optimal shape is completely independent of the shear modulus ratio. As for non-circular cross-sections, however, the optimalities appear all in a manner that tends to become as close as possible to that of the circular case. Furthermore, for the optimality of a general multiply-connected inhomogeneous case, independent treatment of the multiple-connection and the inhomogeneity as with the circular case is possible only when the proportion of either of the two entries is relatively small with its extend depending on the curvature of the given external boundary and also on the magnitude of the shear modulus ratio.

[7] For all cross-sections of different geometries alike, the appearances of the optimalities of the cavity and the reinforcement are generally opposite to each other, and, in terms of the torsional rigidity, the optimal distributions of both the cavity and the reinforcement at higher proportions are generally not as effective as that at lower proportions.

[8] Although, in the present study, the results have been obtained only for some representative regular cases, both the solution and the optimization procedures developed are completely general and easily applicable with no further difficulties to any irregular cross-sections involving multiple-connections and/or inhomogeneities. The same is also true for the computer program except for the part of the automatic mesh generation subprogram.

[9] Finally, it would be worth noting that the same type of elliptic partial differential equation as in this study describes not only the torsion and the inflated membrane problems, but also a number of other physical phenomena including the potential flow, the seepage, the conduction heat transfer, the electric conduction and the gravitation, etc.. Therefore, it is possible through proper identification of the parameters that the present study find its application to other two-dimensional linear boundary value problems.

REFERENCES

[1] **H. Anthes** — 1906 — *Versuchsmethode zur Ermittlung der Spannungsverteilung der Torsion Prismatischer Stäbe*, Dissertation, Hannover.

[2] **S. Baba and T. Kajita** — 1982 — "Plastic Analysis of Torsion of a Prismatic Beam", *International Journal for Numerical Methods in Engineering*, Vol. 18, pp. 927-944.

[3] **N. V. Banichuk** — 1976 — "Optimization of Elastic Bars in Torsion", *International Journal of Solids and Structures*, Vol. 12, pp. 275-286.

[4] **H. Battenbo and B. H. Baines** — 1975 — "A Boundary Integral Solution to Torsion of Cylinders and Solids of Revolution", *International Journal for Numerical Methods in Engineering*, Vol. 9, pp. 461-476.

[5] **R. D. Bhargava and P. K. Gupta** — 1979 — "Second-Order Torsion Problem of a Cylinder Consisting of Different Isotropic Homogeneous Compressible Elastic Materials", *International Journal of Non-Linear Mechanics*, Vol. 14, pp. 23-33.

[6] **J. R. Booker and S. Kitipornchai** — 1971 — "Torsion of Multi-Layered Rectangular Section", *Proceedings of the American Society of Civil Engineers: Journal of the Engineering Mechanics Division*, Vol. 97, No. EM 5, pp. 1451-1468.

[7] **A. P. Boresi** — 1965 — *Elasticity in Engineering Mechanics*, Prentice-Hall, Inc., Englewood Cliffs, New Jersey.

[8] **J. Boussinesq** — 1871 — *J. de Mathématique*, Vol. 2, No. 16, p. 125.

[9] **Y. K. Cheung and M. F. Yeo** — 1979 — *A Practical Introduction to Finite Element Analysis*, Pitman Publishing Ltd..

[10] **P. C. Chou and N. J. Pagano** — 1967 — *Elasticity: Tensor, Dyadic and Engineering Approaches*, D. Van Nostrand Co., Inc..

[11] **D. G. Christopherson and R. V. Southwell** — 1938 — *Proc. R. Soc.*, London, A 168, p. 317.

[12] **H. D. Cohen** — 1980 — "A Method for the Automatic Generation of Triangular Elements on a Surface", *International Journal for Numerical Methods in Engineering*: Short Communications, Vol. 15, pp. 470-476.

[13] **J. J. Connor and C. A. Brebbia** — 1976 — *Finite Element Techniques for Fluid Flow*, Butterworth & Co. Ltd..

[14] **R. D. Cook** — 1981 — *Concepts and Applications of Finite Element Analysis*, 2nd. Ed., John Wiley & Sons, Inc..

[15] **C. A. Coulomb** — 1784 — *Histoire de l'Académie*, pp. 229-269, Paris.

[16] **R. Courant** — 1943 — "Variational Methods for the Solution of Problems of Equilibrium and Vibrations", *Bull. Am. Math. Soc.*, Vol. 49, pp. 1-23.

[17] **K. Dems** — 1980 — "Multiparameter Shape Optimization of Elastic Bars in Torsion", *International Journal for Numerical Methods in Engineering*, Vol. 15, pp. 1517-1539.

[18] **C. S. Desai** — 1979 — *Elementary Finite Element Method*, Prentice-Hall, Inc..

[19] **D. S. Dugdale and C. Ruiz** — 1971 — *Elasticity for Engineers*, McGraw-Hill Book Co., London.

[20] **J. F. Ely and O. C. Zienkiewicz** — 1960 — "Torsion of Compoound Bars - A Relaxation Solution", *International Journal of Mechanical Sciences*, Vol. 1, pp. 356-365.

[21] **M. G. Faulkner, A. Mioduchowski and D. P. Hong** — 1982 — "Determining the Torsional Rigidity of Square Bars with Jump Nonhomogeneities", *Proceedings of the Joint International Conference on Experimental Mechanics*, pp. 387-391, Honolulu, May 23-28, 1982.

[22] **M. G. Faulkner, A. Mioduchowski and D. P. Hong** — 1984 — "Optimal Jump Nonhomogeneity of Prismatic Bars in Torsion", *Journal of Vibration, Acoustics, Stress and Reliability in Design*, Vol. 106, pp. 547-553.

[23] **J. W. Feldmann** — 1968 — "Direct Numerical Determination of Stresses in Elastic Solids as Illustrated by the Torsion Problem", *International Journal of Solids and Structures*, Vol. 4, pp. 675-688.

[24] **R. T. Fenner** — 1975 — *Finite Element Methods for Engineers*, The MacMillan Press Ltd..

[25] **B. A. Finlayson** — 1972 — *The Method of Weighted Residuals and Variational Principles*, Academic Press, New York & London.

[26] **R. H. Gallagher** — 1975 — *Finite Element Analysis Fundamentals*, Prentice-Hall, Inc., Englewood Cliffs, New Jersey.

[27] **O. D. George** — 1976 — "Torsion of an Elastic Solid Cylinder with a Radial Variation in the Shear Modulus", *Journal of Elasticity*, Vol. 6, No. 3, pp. 229-244, Noordhoff International Publishing.

[28] **C. F. Gerald** — 1978 — *Applied Numerical Analysis*, 2nd. Ed., Addison-Wesley Publishing Co..

[29] **A. E. Green and W. Zerna** — 1954 — *Theoretical Elasticity*, Oxford: At the Clarendon Press.

[30] **G. B. Haggerty** — 1972 — *Elementary Numerical Analysis with Programming*, Allyn and Bacon Inc., Boston.

[31] **C. T. Herakovich and P. G. Hodge Jr.** — 1969 — "Elastic-Plastic Torsion of Hollow Bars by Quadratic Programming", *International Journal of Mechanical Sciences*, Vol. 11, pp. 53-63.

[32] **C. T. Herakovich and R. Y. Itani** — 1976 — "Elastic-Plastic Torsion of Nonhomogeneous Bars", *Proceedings of the American Society of Civil Engineers: Journal of the Engineering Mechanics Division*, Vol. 102, No. EM 4, pp. 757-769.

[33] **L. R. Herrmann** — 1965 — "Elastic Torsional Analysis of Irregular Shapes", *Proceedings of the American Society of Civil Engineers: Journal of the Engineering Mechanics Division*, Vol. 91, No. EM 6, pp. 11-19.

[34] **F. B. Hildebrand** — 1965 — *Methods of Applied Mathematics*, 2nd. Ed., Prentice-Hall, Inc..

[35] **E. Hinton and D. R. J. Owen** — 1979 — *An Introduction to Finite Element Computations*, Pineridge Press Ltd., Swansea, U. K..

[36] **P. G. Hodge Jr.** — 1967 — "Elastic-Plastic Torsion as a Problem in Non-Linear Programming", *International Journal of Solids and Structures*, Vol. 3, pp. 989-999.

[37] **I. Holland and K. Bell** — 1969 — *Finite Element Methods in Stress Analysis*, TAPIR, The Technical University of Norway, Trondheim, Norway.

[38] **D. P. Hong** — 1980 — *Optimal Jump Nonhomogeneity of a Bar in Saint-Venant Torsion*, An M.Sc. Thesis submitted to the Faculty of Graduate Studies and Research, The University of Alberta, Edmonton, Alberta, Canada.

[39] **K. H. Huebner and E. A. Thornton** — 1982 — *The Finite Element Method for Engineers*, 2nd. Ed., John Wiley & Sons, Inc..

[40] **B. Irons and S. Ahmad** — 1980 — *Techniques of Finite Elements*, Ellis Horwood Ltd..

[41] **A. Jennings** — 1977 — *Matrix Computation for Engineers and Scientists*, John Wiley & Sons Ltd..

[42] **L. M. Kachanov** — 1971 — *Foundations of the Theory of Plasticity*, North-Holland Publishing Co., Amsterdam, Netherlands & American Elsevier.

[43] **B. Klosowicz and K. A. Lurie** — 1972 — "On the Optimal Nonhomogeneity of an Elastic Bar in Torsion", *Arch. Mech.*, Vol. 24, pp. 239-249.

[44] **J. L. Krahula and G. F. Lauterbach** — 1969 — "A Finite Element Solution for Saint-Venant Torsion", *AIAA Journal*, Vol. 7, No. 12, pp. 2200-2203.

[45] **Y. M. Kuo and H. D. Conway** — 1974 — "Torsion of Cylinders with Multiple Reinforcement", *Proceedings of the American Society of Civil Engineers: Journal of the Engineering Mechanics Division*, Vol. 100, No. EM 2, pp. 221-234.

[46] **L. M. Kurszin and P. N. Onoprijenko** — 1976 — "Determination of Shape of the Doubly-Connected Cross-Section of Bars of Maximum Torsional Rigidity", *Prik. Math. Mech.*, Vol. 40, pp. 1078-1084.

[47] **S. G. Lekhnitskii** — 1963 — *Theory of Elasticity of an Anisotropic Elastic Body*, Holden-Day Inc., San Francisco, California.

[48] **A. Liniecki and J. Yun** — 1983 — "Finite Element Triangular Meshing Optimization for Pure Torsion" *International Journal for Numerical Methods in Engineering*, Vol. 19, pp. 929-942.

[49] **A. E. H. Love** — 1927 — *A Treatise on the Mathematical Theory of Elasticity*, 4th. Ed., New York Dover Publications.

[50] **A. Mioduchowski** — 1971 — "Optimum Plastic Nonhomogeneity of a Bar under Torsion as a Variational Problem", *Bull. Acad. Polon. Sci.*, Vol. 29, No. 6, pp. 253-259.

[51] **T. Moan** — 1973 — "Finite Element Stress Field Solution of the Problem of Saint-Venant Torsion", *International Journal for Numerical Methods in Engineering*, Vol. 5, pp. 455-458.

[52] **N. I. Muskhelishvili** — 1953 — *Singular Integral Equations*, Translated from the Russian and Edited by J. R. M. Radok, P. Noordhoff N. V. - Groningen, Holland.

[53] **N. I. Muskhelishvili** — 1953 — *Some Basic Problems of the Mathematical Theory of Elasticity: Fundamental Equations, Plane Theory of Elasticity, Torsion and Bending*, Translated from the Russian by J. R. M. Radok, P. Noordhoff Ltd. Groningen, Holland.

[54] **A. Nádai** — 1931 — *Plasticity*, McGraw-Hill Book Co..

[55] **C. L. M. H. Navier** — 1864 — *Résumé des Leçons sur l'Application de la Mécanique*, 3rd. Ed., Paris.

[56] **A. K. Noor and C. M. Andersen** — 1975 — "Mixed Isoparametric Elements for Saint-Venant Torsion", *Computer Methods in Applied Mechanics and Engineering*, Vol. 6, No. 2, pp. 195-218.

[57] **D. H. Norrie and G. de Vries** — 1978 — *An Introduction to Finite Element Analysis*, Academic Press, Inc..

[58] **V. V. Novozhilov** — 1961 — *Theroy of Elasticity*, Translated by J. K. Lusher, Pergamon Press Ltd..

[59] **T. H. H. Pian** — 1965 — "Element Stiffness-Matrices for Boundary Compatibility and for Prescribed Boundary Stresses", *Proc. 1st. Conf. Matrix Meth. Struct. Meth.*, Wright-Patterson Air Force Base, Ohio, AFFDL-TR-66-80, pp. 457-477.

[60] **T. H. H. Pian and P. Tong** — 1969 — "Basis of Finite Element Methods for Solid Continua", *International Journal for Numerical Methods in Engineering*, Vol. 1, pp. 3-28.

[61] **G. Polya and G. Szegö**— 1951 — *Isoparametric Inequalities in Mathematical Physics*, Princeton University Press.

[62] **L. Prandtl** — 1903 — *Phys. Zeitschrift*, Vol. 4, p.758.

[63] **A. K. Rao, I. S. Raju and A. V. Krishna-Murty** — 1971 — "A Powerful Hybrid Method in Finite Element Analysis", *International Journal for Numerical Methods in Engineering*, Vol. 3, pp. 389-403.

[64] **J. N. Reddy** — 1986 — *Applied Functional Analysis and Variational Methods in Engineering*, McGraw-Hill Book Co..

[65] **J. Robinson** — 1973 — *Integrated Theory of Finite Element Methods*, John Wiley & Sons, Ltd..

[66] **J. Rychlewski** — 1965 — "Plastic Torsion of a Rectangular Bar with Jump Nonhomogeneity", *International Journal of Solids and Structures*, Vol. 1, pp. 243-255.

[67] **A. S. Saada** — 1974 — *Elasticity: Theory and Applications*, Pergamon Press Inc..

[68] **M. A. Sadowsky** — 1941 — *J. Appl. Mech.*, Vol. 8, p. 166.

[69] **R. S. Schechter** — 1967 — *The Variational Method in Engineering*, McGraw-Hill Book Co..

[70] **F. S. Shaw** — 1944 — *The Torsion of Solid and Hollow Prisms in the Elastic and Plastic Range by Relaxation Methods*, Australian Council for Aeronautics, Report ACA - 11.

[71] **I. M. Smith** — 1982 — *Programming the Finite Element Method: with Application to Geomechanics*, John Wiley & Sons Ltd.

[72] **I. S. Sokolnikoff** — 1956 — *Mathematical Theory of Elasticity*, 2nd. Ed., McGraw-Hill Book Co..

[73] **R. B. Stout and P. G. Hodge Jr.** — 1970 — "Elastic/Plastic Torsion of Hollow Cylinders", *International Journal of Mechanical Sciences*, Vol. 12, pp. 91-108.

[74] **J. L. Synge and W. F. Cahill** — 1957 — "The Torsion of a Hollow Square", *Quarterly of Applied Mathematics*, Vol. 15, pp. 217-224.

[75] **G. I. Taylor and A. A. Griffith** — 1958 — "The Use of Soap Films in Solving Torsion Problems", *The Scientific Papers of Sir Geoffrey Ingram Taylor*, Edited by G. K. Batchelor, Vol. I; Mechanics of Solids, pp. 1-23, Cambridge: At the University Press.

[76] **G. I. Taylor and A. A. Griffith** — 1958 — "The Application of Soap Films to the Determination of the Torsion and Flexure of Hollow Shafts", *The Scientific Papers of Sir Geoffrey Ingram Taylor*, Vol. I; Mechanics of Solids, pp. 46-60, Cambridge: At the University Press.

[77] **S. P. Timoshenko and J. N. Goodier** — 1970 — *Theory of Elasticity*, 3rd. Ed., McGraw-Hill, Inc..

[78] **I. Todhunter and K. Pearson** — 1886, 1893 — *A History of the Theory of Elasticity and of the Strength of Materials*, Vol. I & II, Cambridge: At the University Press.

[79] **P. Tong** — 1970 — "New Displacement Hybrid Finite Element Models for Solid Continua", *International Journal for Numerical Methods in Engineering*, Vol. 2, pp. 73-83.

[80] **S. Valliappan and V. A. Pulmano** — 1974 — "Torsion of Nonhomogeneous Anisotropic Bars", *Proceedings of the American Society of Civil Engineers: Journal of the Structural Division*, No. ST 1, pp. 287-295.

[81] **K. Washizu** — 1975 — *Variational Methods in Elasticity and Plasticity*, 2nd. Ed., Pergamon Press Ltd., Headington-Hill Hall, Oxford.

[82] **Y. Yamada, S. Nakagiri and K. Takatsuka** — 1972 — "Elastic-Plastic Analysis of Saint-Venant Torsion Problem by a Hybrid Stress Model", *International Journal for Numerical Methods in Engineering*, Vol. 5, pp. 193-207.

[83] **O. C. Zienkiewicz and Y. K. Cheung** — 1965 — "Finite Elements in the Solution of Field Problems", *The Engineer*, Vol. 220, pp. 507-510, London.

[84] **O. C. Zienkiewicz and C. J. Parekh** — 1970 — "Transient Field Problems: Two-Dimensional and Three-Dimensional Analysis by Isoparametric Finite Elements", *International Journal for Numerical Methods in Engineering*, Vol. 2, pp. 61-71.

[85] **O. C. Zienkiewicz** — 1977 — *The Finite Element Method*, 3rd. Ed., McGraw-Hill Book Co., Ltd., U. K..

APPENDIX

```
0001    ****************************************************************
0002    ****************************************************************
0003    *    VS FORTRAN 3.0  /    AMDAHL 5870    /     MTS 1985    *
0004    ****************************************************************
0005    *
0006
0007          PROGRAM  TOROPT
0008
0009    *
0010    * this main program carries out the torsional
0011    * optimization of multiply-connected inhomogeneous prisms!
0012    *
0013
0014          IMPLICIT  DOUBLEPRECISION(  A-H, O-Z  )
0015
0016    *
0017    * AL ------ Angle of Twist per Unit Length of the Prism.
0018    * A$ ------ Cross-Sectional Area of an Element.
0019    * BV ------ Trial Boundary Constant Value.
0020    * (G) ----- Shear Modulus Vector.
0021    * GO ------ Shear Modulus of the Cavity Element.
0022    * G1 ------ Shear Modulus of the Base Material Element.
0023    * G2 ------ Shear Modulus of the Reinforcement Element.
0024    * [M] ----- Node Variable Name Matrix.
0025    * [MO2] --- Torque Addressing Vector.
0026    * MC ------ Maximum Number of Mode Solutions.
0027    * [ME] ---- Element Node Variable Name Matrix.
0028    * (MEC) --- Cavity Element Vector.
0029    * MO ------ Maximum Number of Cavity Elements.
0030    * (MPC) --- Cavity Node Point Vector.
0031    * [MS] ---- Adjacent Element Matrix.
0032    * N ------- Order of the Global Stiffness Matrix.
0033    * NO ------ Number of Cavity Elements.
0034    * N1 ------ Number of Base Material Elements.
0035    * N2 ------ Number of Reinforcement Elements.
0036    * NC ------ Number of Contours.
0037    * ND ------ Number of Dimension.
0038    * NE ------ Number of Elements.
0039    * (NEC) --- Cavity Element Number Vector.
0040    * NF ------ D.O.F. Number per a Node Point.
0041    * NG ------ Number of Corners of the Given Regular Geometry.
0042    * NH ------ Number of Division.
0043    * (NM) ---- Number of Elements Joining at Node Points.
0044    * NN ------ Number of Node Points per an Element.
0045    * NP ------ Number of Node Points for the Whole Region.
0046    * (NPC) --- Cavity Node Point Number Vector.
0047    * NV ------ Number of System Variables.
0048    * NW ------ Number of Wall Elements.
0049    * 'O' ----- Option Parameter.
0050    * (PH) ---- Stress Function Vector.
0051    * [SC] ---- Contour Integral Matrix.
0052    * [SF] ---- Stress Function Matrix.
0053    * [SL] ---- System Load Matrix.
0054    * [SS] ---- Stress Matrix.
0055    * [ST] ---- System Stiffness Matrix.
0056    * TOO ----- Homogeneous Case Torque.
0057    * (TO2) --- Torque Vector.
0058    * [XY] ---- Node Point Coordinate Matrix.
0059    * $ ------- Subscript for the Element.
0060    *
```

```
0061
0062          PARAMETER(   RR=10.D0,  NH=10,  NE=NH*NH,
0063         +     NP=(NH*NH+3*NH+2)/2,  NN=3,  ND=2,
0064         +     NF=1,  N=NP*NF,  NW=2*NH-1,  MO=NE-NW    )
0065
0066          COMMON     GO, A$, AL, BV
0067         +     /$A$/  ST(N,N)          /$B$/  SF(N,0:9)
0068         +     /$C$/  ME(NE,NN)        /$D$/  NM(NP)
0069         +     /$E$/  MS(NE,NN)        /$F$/  XY(NP,ND)
0070         +     /$G$/  G(NE)            /$H$/  M(NP,NF)
0071         +     /$I$/  NEC(9)           /$J$/  MEC(NE)
0072         +     /$K$/  NPC(9)           /$L$/  MPC(NP)
0073
0074          DIMENSION  TO2(NE), MO2(NE), M1(NE)
0075
0076          CHARACTER O*1
0077
0078
0079          READ(5,*)  NG, G1, G2, AL, BV, O
0080          WRITE(6,60)  NG, G1, G2, AL, BV, O
0081
0082          PI= 4.D0*DATAN( 1.D0 )
0083          CO= PI/180.D0
0084
0085          TH= 360.D0/ DFLOAT( 2*NG )
0086          XL= DSQRT(  4.D0/DFLOAT(NG)*DCOTAN(CO*TH)  )*RR
0087          YL= XL*DTAN( CO*TH )
0088
0089          IF(  O .EQ. 'T'  ) THEN
0090              GO= G1*1.D-10
0091          ELSEIF(  O .EQ. 'S'  ) THEN
0092              GO= 0.D0
0093          ELSE
0094              WRITE(6,*) ' *** UNEXPECTED OPTION O IN "TOROPT" '
0095              STOP
0096          ENDIF
0097
0098          CALL  GENMES(  XL, YL,  NC, MC  )
0099
0100          DO 05, NO=0,MO
0101              DO 04, N2=0,NE-NO
0102                IF(  NO.EQ.0 .AND. N2.EQ.0  ) THEN
0103                  DO 01, LE=1,NE
0104                    G(LE)= G1
0105       01           CONTINUE
0106                  CALL  COMPUT(  G, NC, MC,  TOO  )
0107                  WRITE(6,61)  DFLOAT( 2*NG )*TOO
0108                ELSE
0109                  IF(  N2 .EQ. 0  ) THEN
0110                    DO 02, LE=1,NE
0111                      IF(  G(LE) .NE. 0.D0  ) THEN
0112                        G(LE)= G1
0113                      ENDIF
0114       02             CONTINUE
0115                    ME$= MO
0116                    G$= GO
0117                  ELSE
0118                    ME$= NE
0119                    G$= G2
0120                  ENDIF
```

```
0121                  L1= 0
0122                  DO 03, LE=1,ME$
0123                    IF(  G(LE) .EQ. G1  ) THEN
0124                      L1= L1 + 1
0125                      G(LE)= G$
0126                      IF(  G(LE) .EQ. 0.DO  ) THEN
0127                        CALL  DETOUR(  G,  NC, MC  )
0128                      ENDIF
0129                      CALL  COMPUT(  G, NC, MC,  T02(L1)  )
0130                      M02(L1)= LE
0131                      G(LE)= G1
0132                    ENDIF
0133        03          CONTINUE
0134                  CALL  ASSORT(  T02, L1,  M1  )
0135                  L02= M1(L1)
0136                  LG= M02(L02)
0137                  G(LG)= G$
0138                  IF(  G(LG) .EQ. 0.DO  ) THEN
0139                    CALL  DETOUR(  G,  NC, MC  )
0140                  ENDIF
0141                  WRITE(6,62)  NO, N2, T02(L02)/T00, LG
0142                ENDIF
0143        04      CONTINUE
0144        05  CONTINUE
0145
0146
0147            STOP
0148
0149        60  FORMAT(  I5, 4D20.10, A  )
0150        61  FORMAT(  5X, D20.10  )
0151        62  FORMAT(  2I5, D20.10, 5X, I5  )
0152
0153            END
0154
0155    *
0156    ***************************************************************
0157    *
0158
0159            SUBROUTINE  ASSORT(  T, N,  M  )
0160
0161    *
0162    * this subroutine performs the ascending-order sorting!
0163    *
0164
0165            IMPLICIT  DOUBLEPRECISION(  A-H, O-Z  )
0166
0167            DIMENSION  T(N), M(N)
0168
0169
0170            DO 01, L=1,N
0171              M(L)= L
0172        01  CONTINUE
0173
0174            DO 03, I=1,N-1
0175              K= I
0176              DO 02, J=I+1,N
0177                IF(  T( M(J) ) .LT. T( M(K) )  ) THEN
0178                  K= J
0179                ENDIF
0180        02      CONTINUE
```

```
0181              IF( K .NE. I ) THEN
0182                L= M(K)
0183                M(K)= M(I)
0184                M(I)= L
0185              ENDIF
0186        03  CONTINUE
0187
0188
0189          RETURN
0190
0191          END
0192
0193      *
0194      ****************************************************************
0195      *
0196
0197          SUBROUTINE  COMPUT(  G, NC, MC,  T  )
0198
0199      *
0200      * this subroutine hosts computation
0201      * of the torsional rigidity value!
0202      *
0203
0204          IMPLICIT  DOUBLEPRECISION( A-H, O-Z  )
0205
0206          PARAMETER(   NH=10, NE=NH+NH, NP=(NH+NH+3+NH+2)/2,
0207         +    NF=1,  N=NP+NF   )
0208
0209          COMMON     GO, AS, AL, BV
0210
0211          DIMENSION  G(NE), PH(N)
0212
0213
0214          CALL  SYSINI(  MC  )
0215          CALL  SYSASM(  G, MC  )
0216          CALL  SYSCON(  BV, NC, MC,  NV  )
0217          CALL  LEQGEM(  NV, MC  )
0218          CALL  LINCOM(  G, NC, MC,  PH  )
0219          CALL  TORQUE(  PH,  T  )
0220
0221
0222          RETURN
0223
0224          END
0225
0226      *
0227      ****************************************************************
0228      *
0229
0230          SUBROUTINE  CONSTE(  GS, AL, XYS,  STS, SLS  )
0231
0232      *
0233      * this subroutine generates the constant
0234      * strain triangular element stiffness matrix!
0235      *
0236
0237          IMPLICIT  DOUBLEPRECISION(  A-H, O-Z  )
0238
0239          DIMENSION  XYS(6), B(2,3), STSS(3,3), STS(3,3),
0240         +    SLS(3)
```

```
0241
0242
0243          IF(  G$ .EQ. 0.D0  ) THEN
0244              WRITE(6,*) ' *** DIVISION BY ZERO IN "CONSTE" '
0245              STOP
0246          ENDIF
0247
0248          CALL  GENMBC(  XY$, 'B',  B  )
0249          CALL  MATINP(  B, 2, 3,  ST$$  )
0250
0251          DO 02, I=1,3
0252              DO 01, J=1,3
0253                ST$(I,J)= 1.D0/G$*ST$$(I,J)
0254       01       CONTINUE
0255       02   CONTINUE
0256
0257          SL$$= 2.D0/3.D0*AL
0258          DO 03, I=1,3
0259              SL$(I)= SL$$
0260       03   CONTINUE
0261
0262
0263          RETURN
0264
0265          END
0266
0267      *
0268      ****************************************************************
0269      *
0270
0271          DOUBLEPRECISIONFUNCTION  CONSUM(  G, SS, IC  )
0272
0273      *
0274      * this function evaluates the contour integral value!
0275      *
0276
0277          IMPLICIT  DOUBLEPRECISION(  A-H, O-Z  )
0278
0279          PARAMETER(    NH=10, NE=NH*NH, NP=(NH*NH+3*NH+2)/2,
0280         +     NN=3, ND=2    )
0281
0282          COMMON      GO
0283         +     /$C$/  ME(NE,NN)        /$E$/  MS(NE,NN)
0284         +     /$F$/  XY(NP,ND)        /$I$/  NEC(9)
0285         +     /$J$/  MEC(NE)
0286
0287          DIMENSION  G(NE), SS(NE,2)
0288
0289
0290          CONSUM= 0.D0
0291          IF(  IC .EQ. 1  ) THEN
0292              DO 01, LC=NEC(IC),NEC(IC+1)-1
0293                IE= MEC( LC )
0294                IP= ME( IE,2 )
0295                JP= ME( IE,3 )
0296                DX= XY( JP,1 ) - XY( IP,1 )
0297                DY= XY( JP,2 ) - XY( IP,2 )
0298                SC$= (  DX*SS(IE,1) + DY*SS(IE,2)  )/ G(IE)
0299                CONSUM= CONSUM + SC$
0300       01       CONTINUE
```

```
0301            ELSE
0302                DO 03, LC=NEC(IC),NEC(IC+1)-1
0303                  IE= MEC( LC )
0304                  DO 02, LN=1,NN
0305                    JE= MS( IE,LN )
0306                    IF(  JE .NE. 0  ) THEN
0307                      IF(  G(JE) .NE. 0.DO  ) THEN
0308                        IN= LN
0309                        IF(  IN .LT. NN  ) THEN
0310                          JN= IN + 1
0311                        ELSE
0312                          JN= 1
0313                        ENDIF
0314                        IP= ME( IE,IN )
0315                        JP= ME( IE,JN )
0316                        DX= XY( JP,1 ) - XY( IP,1 )
0317                        DY= XY( JP,2 ) - XY( IP,2 )
0318                        SC$= (  DX*SS(JE,1) + DY*SS(JE,2)  )/ G(JE)
0319                        CONSUM= CONSUM + SC$
0320                      ENDIF
0321                    ENDIF
0322          02        CONTINUE
0323          03      CONTINUE
0324            ENDIF
0325
0326
0327            RETURN
0328
0329            END
0330
0331        *
0332        ****************************************************************
0333        *
0334
0335            SUBROUTINE  DETADJ
0336
0337        *
0338        * this subroutine determines the adjacent elements!
0339        *
0340
0341            IMPLICIT  DOUBLEPRECISION(  A-H, O-Z  )
0342
0343            PARAMETER(   NH=10, NE=NH*NH, NP=(NH*NH+3*NH+2)/2,
0344           +    NN=3   )
0345
0346            COMMON
0347           +    /$C$/  ME(NE,NN)        /$D$/  NM(NP)
0348           +    /$E$/  MS(NE,NN)
0349
0350            DIMENSION  NM(NN,5), NM$(NN)
0351
0352            LOGICAL  OK
0353
0354
0355            DO 01, LP=1,NP
0356              NM(LP)= 0
0357          01  CONTINUE
0358
0359            DO 03, LE=1,NE
0360              DO 02, LN=1,NN
```

```
0361                LP= ME(LE,LN)
0362                NM(LP)= NM(LP) + 1
0363          02    CONTINUE
0364          03  CONTINUE
0365
0366              DO 13, IE=1,NE
0367                DO 04, LN=1,NN
0368                  NMS(LN)= 0
0369          04    CONTINUE
0370
0371                DO 08, JE=1,NE
0372                  IF(  JE .NE. IE  ) THEN
0373                    DO 06, IN=1,NN
0374                      DO 05, JN=1,NN
0375                        IF(  ME(JE,JN) .EQ. ME(IE,IN)  ) THEN
0376                          NMS(IN)= NMS(IN) + 1
0377                          NM( IN, NMS(IN) )= JE
0378                        ENDIF
0379          05            CONTINUE
0380          06          CONTINUE
0381                      OK= .TRUE.
0382                      DO 07, IN=1,NN
0383                        OK= OK .AND. ( NMS(IN) .EQ. NM(ME(IE,IN))-1 )
0384          07          CONTINUE
0385                      IF(  OK  ) THEN
0386                        GOTO 09
0387                      ENDIF
0388                  ENDIF
0389          08    CONTINUE
0390
0391          09    DO 12, LN=1,NN
0392                  IN= LN
0393                  IF(  IN .LT. NN ) THEN
0394                    JN= IN + 1
0395                  ELSE
0396                    JN= 1
0397                  ENDIF
0398                  DO 11, IM=1,NMS(IN)
0399                    DO 10, JM=1,NMS(JN)
0400                      IF(  NM(JN,JM) .EQ. NM(IN,IM)  ) THEN
0401                        MS(IE,IN)= NM(IN,IM)
0402                        GOTO 12
0403                      ENDIF
0404          10          CONTINUE
0405          11        CONTINUE
0406                    MS(IE,IN)= 0
0407          12      CONTINUE
0408          13  CONTINUE
0409
0410
0411              RETURN
0412
0413              END
0414
0415      *
0416      ***************************************************************
0417      *
0418
0419              SUBROUTINE  DETOUR(  G,  NC, MC  )
0420
```

```
0421      *
0422      * this subroutine determines
0423      * the status of multiple-connection!
0424      *
0425
0426            IMPLICIT  DOUBLEPRECISION(  A-H, O-Z  )
0427
0428            PARAMETER(    M1=10, ME=M1*M1, MP=(M1*M1+3*M1+2)/2,
0429           +     NN=3    )
0430
0431            COMMON      GO
0432           +     /$G$/  ME(ME,M1)          /$I$/  NEC(9)
0433           +     /$J$/  NEC(ME)            /$K$/  NPC(9)
0434           +     /$L$/  NPC(MP)
0435
0436            DIMENSION  G(ME)
0437
0438
0439            NC= 1
0440
0441            LC= NEC(2)
0442            DO 01, LE=1,NE
0443                IF(  G(LE) .EQ. 0.DO  ) THEN
0444                  NEC(LC)= LE
0445                  LC= LC + 1
0446                ENDIF
0447        01  CONTINUE
0448            NEC(3)= LC
0449
0450        02  IF(  NEC(NC+1) .LT. NEC(NC+2)  ) THEN
0451                N1= NC + 1
0452                N2= NC + 2
0453                N3= NC + 3
0454                NEC(N3)= NEC(N2)
0455                NEC(N2)= NEC(N1) + 1
0456        03      DO 07, IE=NEC(N2),NEC(N3)-1
0457                  IC= NEC(IE)
0458                  DO 06, JE=NEC(N1),NEC(N2)-1
0459                    JC= NEC(JE)
0460                    DO 05, IN=1,NN
0461                      DO 04, JN=1,NN
0462                        IF(  ME(JC,JN) .EQ. ME(IC,IN)  ) THEN
0463                          NEC(IE)= NEC( NEC(N2) )
0464                          NEC( NEC(N2) )= IC
0465                          NEC(N2)= NEC(N2) + 1
0466                          GOTO 03
0467                        ENDIF
0468        04              CONTINUE
0469        05            CONTINUE
0470        06          CONTINUE
0471        07        CONTINUE
0472
0473                  NPC(N2)= NPC(N1)
0474                  DO 10, LE=NEC(N1),NEC(N2)-1
0475                    LC= NEC(LE)
0476                    DO 09, LN=1,NN
0477                      IP= ME(LC,LN)
0478                      DO 08, JP=NPC(N1),NPC(N2)-1
0479                        IF(  NPC(JP) .EQ. IP  ) THEN
0480                          GOTO 09
```

```
0481                    ENDIF
0482          08        CONTINUE
0483                    MPC( MPC(N2) )= IP
0484                    MPC(N2)= MPC(N2) + 1
0485          09      CONTINUE
0486          10    CONTINUE
0487                NC= NC + 1
0488                GOTO 02
0489            ENDIF
0490
0491            IF(  NC .EQ. 1  ) THEN
0492                NC= 0
0493            ELSE
0494                NC= NC
0495            ENDIF
0496
0497
0498            RETURN
0499
0500            END
0501
0502      *
0503      *****************************************************************
0504      *
0505
0506            SUBROUTINE  GENMBC(  XY$, $,  BC  )
0507
0508      *
0509      * this subroutine generates the [B]
0510      * or the [C] transformation matrix
0511      *
0512
0513            IMPLICIT  DOUBLEPRECISION(  A-H, O-Z  )
0514
0515            DIMENSION  XY$(6), BC(2,3)
0516
0517            CHARACTER  $
0518
0519
0520            X1= XY$(1)
0521            Y1= XY$(2)
0522
0523            X2= XY$(3)
0524            Y2= XY$(4)
0525
0526            X3= XY$(5)
0527            Y3= XY$(6)
0528
0529            B1= Y2-Y3
0530            B2= Y3-Y1
0531            B3= Y1-Y2
0532
0533            C1= X3-X2
0534            C2= X1-X3
0535            C3= X2-X1
0536
0537            A$= TRIARE(  XY$  )
0538            IF(  A$ .EQ. 0.DO  ) THEN
0539                WRITE(6,*) ' *** DIVISION BY ZERO IN "GENMBC" '
0540                STOP
```

```
0541          ENDIF
0542
0543          CO= 1.D0/2.D0/A$
0544
0545          IF(  $ .EQ. 'B'  ) THEN
0546              BC(1,1)=  CO*B1
0547              BC(1,2)=  CO*B2
0548              BC(1,3)=  CO*B3
0549              BC(2,1)=  CO*C1
0550              BC(2,2)=  CO*C2
0551              BC(2,3)=  CO*C3
0552          ELSEIF(  $ .EQ. 'C'  ) THEN
0553              BC(1,1)=  CO*C1
0554              BC(1,2)=  CO*C2
0555              BC(1,3)=  CO*C3
0556              BC(2,1)= -CO*B1
0557              BC(2,2)= -CO*B2
0558              BC(2,3)= -CO*B3
0559          ELSE
0560              WRITE(6,*) ' *** UNEXPECTED OPTION $ IN "GENMBC" '
0561              STOP
0562          ENDIF
0563
0564
0565          RETURN
0566
0567          END
0568
0569      *
0570      ******************************************************************
0571      *
0572
0573          SUBROUTINE  GENMES(  XL, YL,  NC, MC  )
0574
0575      *
0576      * this subroutine generates the mesh information!
0577      *
0578
0579          IMPLICIT  DOUBLEPRECISION(  A-H, O-Z  )
0580
0581          PARAMETER(   NH=10, NE=NH*NH, NP=(NH*NH+3*NH+2)/2,
0582         +    NN=3, ND=2, NF=1   )
0583
0584          COMMON      GO, A$
0585         +    /$C$/  ME(NE,NN)        /$F$/  XY(NP,ND)
0586         +    /$H$/  M(NP,NF)         /$I$/  NEC(9)
0587         +    /$J$/  MEC(NE)          /$K$/  NPC(9)
0588         +    /$L$/  MPC(NP)
0589
0590
0591          LE= 1
0592          DO 02, IN=1,NH
0593              NOB= ( IN*IN - IN + 2 )/2
0594              NPB= NOB + IN
0595              DO 01, JN=1,IN
0596                NOO= NOB + JN - 1
0597                NOP= NOO + 1
0598                NPO= NPB + JN - 1
0599                NPP= NPO + 1
0600
```

```
0601                ME(LE,1)= NOO
0602                ME(LE,2)= NPO
0603                ME(LE,3)= NPP
0604                LE= LE + 1
0605
0606                IF(  NOP .NE. NPB  ) THEN
0607                  ME(LE,1)= NOO
0608                  ME(LE,2)= NPP
0609                  ME(LE,3)= NOP
0610                  LE= LE + 1
0611                ENDIF
0612          01      CONTINUE
0613          02  CONTINUE
0614
0615              CALL  DETADJ
0616
0617              DX= XL/ DFLOAT( NH )
0618              DY= YL/ DFLOAT( NH )
0619
0620              LP= 1
0621              DO 04, IH=0,NH
0622                  X= DX*DFLOAT( IH )
0623                  DO 03, JH=0,IH
0624                    Y= DY*DFLOAT( JH )
0625                    XY(LP,1)= X
0626                    XY(LP,2)= Y
0627                    LP= LP + 1
0628          03        CONTINUE
0629          04  CONTINUE
0630
0631              A$= ( XL*YL/2.D0 )/ DFLOAT( NE )
0632
0633              LV=1
0634              DO 06, LP=1,NP
0635                  DO 05, LF=1,NF
0636                    M(LP,LF)= LV
0637                    LV= LV + 1
0638          05        CONTINUE
0639          06  CONTINUE
0640
0641              NEC(1)= 1
0642              LC= NH*NH - 2*NH + 2
0643              DO 07, LE=1,NH
0644                  NEC(LE)= LC
0645                  LC= LC + 2
0646          07  CONTINUE
0647              NEC(2)= NH + 1
0648
0649              NPC(1)= 1
0650              LC= ( NH*NH + NH + 2 )/2
0651              DO 08, LP=1,NH+1
0652                  NPC(LP)= LC
0653                  LC= LC + 1
0654          08  CONTINUE
0655              NPC(2)= NH + 2
0656
0657              NC= 1
0658              NC= 0
0659
0660
```

```
0661          RETURN
0662
0663          END
0664
0665      *
0666      ****************************************************************
0667      *
0668
0669          SUBROUTINE  GETCOR(  LE,  COR$  )
0670
0671      *
0672      * this subroutine returns element coordinate information!
0673      *
0674
0675          IMPLICIT  DOUBLEPRECISION(  A-H, O-Z  )
0676
0677          PARAMETER(   NH=10, NE=NH*NH,  NP=(NH*NH+3*NH+2)/2,
0678         +    NN=3, ND=2   )
0679
0680          COMMON
0681         +    /$C$/  ME(NE,NN)       /$F$/  COR(NP,ND)
0682
0683          DIMENSION  COR$(NN*ND)
0684
0685
0686          DO 02, LN=1,NN
0687              LP= ME( LE,LN )
0688              L$= ( LN-1 )*ND
0689              DO 01, LD=1,ND
0690                COR$( L$+LD )= COR( LP,LD )
0691       01     CONTINUE
0692       02 CONTINUE
0693
0694
0695          RETURN
0696
0697          END
0698
0699      *
0700      ****************************************************************
0701      *
0702
0703          SUBROUTINE  GETVAN(  LE,  M$  )
0704
0705      *
0706      * this subroutine returns element node variable names!
0707      *
0708
0709          IMPLICIT  DOUBLEPRECISION(  A-H, O-Z  )
0710
0711          PARAMETER(   NH=10, NE=NH*NH,  NP=(NH*NH+3*NH+2)/2,
0712         +    NN=3, NF=1, N$=NN*NF   )
0713
0714          COMMON
0715         +    /$C$/  ME(NE,NN)       /$H$/  M(NP,NF)
0716
0717          DIMENSION  M$(N$)
0718
0719
0720          DO 02, LN=1,NN
```

```
0721              LP= ME( LE,LN )
0722              L$= ( LN-1 )*NF
0723              DO 01, LF=1,NF
0724                M$( L$+LF )= M( LP,LF )
0725        01    CONTINUE
0726        02  CONTINUE
0727
0728
0729          RETURN
0730
0731          END
0732
0733      *
0734      ***********************************************************************
0735      *
0736
0737          SUBROUTINE  LEQGEM(  NV, MC  )
0738
0739      *
0740      * this subroutine solves a system of
0741      * multiple-right-hand-sided linear equations performing
0742      * Gaussian Elimination!
0743      *
0744
0745          IMPLICIT  DOUBLEPRECISION(  A-H, O-Z  )
0746
0747          PARAMETER(   NH=10,  NP=(NH*NH+3*NH+2)/2,  NF=1,
0748         +    N=NP*NF   )
0749
0750          COMMON
0751         +    /$A$/  ST(N,N)       /$B$/  SL(N,0:9)
0752
0753          DIMENSION  SF(N,0:9)
0754
0755          EQUIVALENCE  (  SL, SF  )
0756
0757
0758          DO 04, LV=1,NV
0759              IF(  ST(LV,LV) .EQ. 0.DO  ) THEN
0760                WRITE(6,*) ' *** DIVISION BY ZERO IN "LEQGEL" '
0761                STOP
0762              ENDIF
0763              DO 03, IV=LV+1,NV
0764                CO= ST(IV,LV) / ST(LV,LV)
0765                DO 01, JV=LV+1,NV
0766                  ST(IV,JV)= ST(IV,JV) - CO*ST(LV,JV)
0767        01        CONTINUE
0768                DO 02, JC=0,MC
0769                  SL(IV,JC)= SL(IV,JC)- CO*SL(LV,JC)
0770        02        CONTINUE
0771        03      CONTINUE
0772        04  CONTINUE
0773
0774          DO 07, IV=NV,1,-1
0775              DO 06, JC=0,MC
0776                CU= 0.DO
0777                DO 05, KV=IV+1,NV
0778                  CU= CU + ST(IV,KV)*SF(KV,JC)
0779        05        CONTINUE
0780                SF(IV,JC)= ( SF(IV,JC)-CU )/ ST(IV,IV)
```

```
0781        08      CONTINUE
0782        07  CONTINUE
0783
0784
0785            RETURN
0786
0787            END
0788
0789        *
0790        ****************************************************************
0791        *
0792
0793            SUBROUTINE  LINCOM(  G, NC, MC,  PH  )
0794
0795        *
0796        * this subroutine performs the linear combination!
0797        *
0798
0799            IMPLICIT  DOUBLEPRECISION(  A-H, O-Z  )
0800
0801            PARAMETER(    NH=10, NE=NH+NH, NP=(NH+NH+3+NH+2)/2,
0802           +    NF=1, N=NP+NF    )
0803
0804            COMMON      GO, A$, AL, BV
0805           +    /$A$/  SC(N,N)          /$B$/  SF(N,0:9)
0806           +    /$I$/  NEC(9)
0807
0808            DIMENSION  SR(N), SW(N), SS(NE,2), PH(N), G(NE)
0809
0810            EQUIVALENCE  (  SF, SR, SW  )
0811
0812
0813            IF(  NC .EQ. 1  ) THEN
0814                DO 01, IV=1,N
0815                  PH(IV)= SF(IV,0)
0816        01      CONTINUE
0817            ELSE
0818                DO 04, JC=0,MC
0819                  IF(  JC .EQ. 0  ) THEN
0820                    DO 02, IC=1,NC
0821                      IF(  IC .EQ. 1  ) THEN
0822                        AR= A$*DFLOAT( NE )
0823                      ELSE
0824                        AR= A$*DFLOAT(  NEC(IC+1) - NEC(IC)  )
0825                      ENDIF
0826                      SR(IC)= 2.DO*AL*AR
0827        02            CONTINUE
0828                    ELSE
0829                      CALL  STRESS(  SF(1,JC),  SS  )
0830                      DO 03, IC=1,NC
0831                        SC(IC,JC)= CONSUM(  G, SS, IC  )
0832        03            CONTINUE
0833                    ENDIF
0834        04        CONTINUE
0835                  CALL  LEQGEM(  NC, 0  )
0836                  PH$= SW(1)*BV
0837                  DO 08, IV=1,N
0838                    PH(IV)= 0.DO
0839                    DO 05, JC=1,MC
0840                      PH(IV)= PH(IV) + SW(JC)*SF(IV,JC)
```

```
0841       05         CONTINUE
0842                  PH(IV)= PH(IV) - PH$
0843       06       CONTINUE
0844           ENDIF
0845
0846
0847           RETURN
0848
0849           END
0850
0851       *
0852       ****************************************************************
0853       *
0854
0855           SUBROUTINE  MATINP(  A$$, N$$, N$,  A$  )
0856
0857       *
0858       * this subroutine performs matrix inner-production!
0859       *
0860
0861           IMPLICIT  DOUBLEPRECISION(  A-H, O-Z  )
0862
0863           DIMENSION  A$$(N$$,N$), A$(N$,N$)
0864
0865
0866           DO 03, I$=1,N$
0867               DO 02, J$=1,N$
0868                 A$(I$,J$)= 0.DO
0869                 DO 01, K$=1,N$$
0870                   A$(I$,J$)= A$(I$,J$) + A$$(K$,I$)*A$$(K$,J$)
0871       01        CONTINUE
0872       02      CONTINUE
0873       03  CONTINUE
0874
0875
0876           RETURN
0877
0878           END
0879
0880       *
0881       ****************************************************************
0882       *
0883
0884           SUBROUTINE  MATRAL(  A, NI, NJ, XI,  XO  )
0885
0886       *
0887       * this subroutine performs matrix linear transformation!
0888       *
0889
0890           IMPLICIT  DOUBLEPRECISION(  A-H, O-Z  )
0891
0892           DIMENSION  A(NI,NJ), XI(NJ), XO(NI)
0893
0894
0895           DO 02, I=1,NI
0896               XO(I)= 0.DO
0897               DO 01, J=1,NJ
0898                 XO(I)= XO(I) + A(I,J)*XI(J)
0899       01      CONTINUE
0900       02  CONTINUE
```

```
0901
0902
0903            RETURN
0904
0905            END
0906
0907      *
0908      ***********************************************************************
0909      *
0910
0911            SUBROUTINE  STRESS(  SF,  SS  )
0912
0913      *
0914      * this subroutine computes element stress components!
0915      *
0916
0917            IMPLICIT  DOUBLEPRECISION(  A-H, O-Z  )
0918
0919            PARAMETER(    NH=10, NE=NH*NH, NP=(NH*NH+3*NH+2)/2,
0920           +    NN=3,  NF=1,  N=NP*NF,  N$=NN*NF    )
0921
0922            DIMENSION  SF(N), XY$(8), C(2,3), M$(N$), SF$(N$),
0923           +    SS$(2), SS(NE,2)
0924
0925
0926            DO 01, LE=1,NE
0927                CALL  GETCOR(  LE,  XY$  )
0928                CALL  GENMBC(  XY$, 'C',  C  )
0929                CALL  GETVAN(  LE,  M$  )
0930                CALL  VECOMP(  SF, N, M$, N$,  SF$  )
0931                CALL  MATRAL(  C, 2, 3, SF$,  SS$  )
0932                SS(LE,1)= SS$(1)
0933                SS(LE,2)= SS$(2)
0934          01  CONTINUE
0935
0936
0937            RETURN
0938
0939            END
0940
0941      *
0942      ***********************************************************************
0943      *
0944
0945            SUBROUTINE  SYSASM(  G, MC  )
0946
0947      *
0948      * this subroutine assembles the system matrices!
0949      *
0950
0951            IMPLICIT  DOUBLEPRECISION(  A-H, O-Z  )
0952
0953            PARAMETER(    NH=10, NE=NH*NH, NP=(NH*NH+3*NH+2)/2,
0954           +    NN=3,  ND=2,  NF=1,  N=NP*NF,  N$=NN*NF    )
0955
0956            COMMON      GO, A$, AL
0957           +    /$A$/  ST(N,N)          /$B$/  SL(N,0:8)
0958
0959            DIMENSION  G(NE), XY$(NN*ND), ST$(N$,N$), SL$(N$),
0960           +    M$(N$)
```

```
0961
0962
0963            DO 04, LE=1,NE
0964                IF(  G(LE) .NE. 0.D0  ) THEN
0965                  CALL  GETCOR(  LE,  XY$  )
0966                  CALL  CONSTE(  G(LE), AL, XY$,  ST$, SL$  )
0967                  CALL  GETVAN(  LE,  M$  )
0968                  DO 03, IV$=1,N$
0969                    IV= M$( IV$ )
0970                    DO 01, JV$=1,N$
0971                      JV= M$( JV$ )
0972                      ST(IV,JV)= ST(IV,JV) + ST$(IV$,JV$)
0973          01          CONTINUE
0974                    DO 02, JC=0,MC
0975                      SL(IV,JC)= SL(IV,JC) + SL$(IV$)
0976          02          CONTINUE
0977          03        CONTINUE
0978                ENDIF
0979          04  CONTINUE
0980
0981
0982            RETURN
0983
0984            END
0985
0986        *
0987        ****************************************************************
0988        *
0989
0990            SUBROUTINE  SYSCON(  BV, NC, MC,  NV  )
0991
0992        *
0993        * this subroutine applies system constraints!
0994        *
0995
0996            IMPLICIT  DOUBLEPRECISION(  A-H, O-Z  )
0997
0998            PARAMETER(   NH=10, NP=(NH+NH+3*NH+2)/2, NF=1,
0999           +    N=NP*NF   )
1000
1001            COMMON
1002           +    /$A$/  ST(N,N)          /$B$/  SL(N,0:9)
1003           +    /$H$/  M(NP,NF)         /$K$/  NPC(9)
1004           +    /$L$/  NPC(NP)
1005
1006            DIMENSION  SF$(0:9), SF(N,0:9)
1007
1008            EQUIVALENCE  (  SL, SF  )
1009
1010
1011            NV= N - (  NPC(2)-NPC(1)  )*NF
1012
1013            DO 11, IC=1,NC
1014                DO 01, JC=0,MC
1015                  IF(  JC .EQ. IC  ) THEN
1016                    SF$(JC)= BV
1017                  ELSE
1018                    SF$(JC)= 0.D0
1019                  ENDIF
1020          01      CONTINUE
```

```
1021                IF(  IC .EQ. 1  ) THEN
1022                  DO 05, LC=NPC(IC),NPC(IC+1)-1
1023                    LP= MPC(LC)
1024                    DO 04, LF=1,NF
1025                      LV= M(LP,LF)
1026                      DO 03, JC=0,MC
1027                        DO 02, IV=1,NV
1028                          SL(IV,JC)= SL(IV,JC) - ST(IV,LV)*SF$(JC)
1029        02                CONTINUE
1030                          SF(LV,JC)= SF$(JC)
1031        03                CONTINUE
1032        04              CONTINUE
1033        05            CONTINUE
1034                ELSE
1035                  DO 10, LC=NPC(IC),NPC(IC+1)-1
1036                    LP= MPC(LC)
1037                    DO 09, LF=1,NF
1038                      LV= M(LP,LF)
1039                      DO 07, IV=1,NV
1040                        ST(LV,IV)= 0.D0
1041                        DO 06, JC=0,MC
1042                          SL(IV,JC)= SL(IV,JC) - ST(IV,LV)*SF$(JC)
1043        06                CONTINUE
1044                          ST(IV,LV)= 0.D0
1045        07                CONTINUE
1046                        ST(LV,LV)= 1.D0
1047                        DO 08, JC=0,MC
1048                          SF(LV,JC)= SF$(JC)
1049        08                CONTINUE
1050        09              CONTINUE
1051        10            CONTINUE
1052                ENDIF
1053        11    CONTINUE
1054
1055
1056              RETURN
1057
1058              END
1059
1060        *
1061        ****************************************************************
1062        *
1063
1064              SUBROUTINE  SYSINI(  MC  )
1065
1066        *
1067        * this subroutine initializes the system matrices!
1068        *
1069
1070              IMPLICIT  DOUBLEPRECISION(  A-H, O-Z  )
1071
1072              PARAMETER(   NH=10, NP=(NH*NH+3*NH+2)/2, NF=1,
1073             +    N=NP*NF   )
1074
1075              COMMON
1076             +    /$A$/  ST(N,N)          /$B$/  SL(N,0:9)
1077
1078
1079              DO  03, IV=1,N
1080                  DO 01, JV=1,N
```

```
1081                ST(IV,JV)= 0.D0
1082        01      CONTINUE
1083                DO 02, JC=0,MC
1084                  SL(IV,JC)= 0.D0
1085        02      CONTINUE
1086        03  CONTINUE
1087
1088
1089            RETURN
1090
1091            END
1092
1093        *
1094        ***********************************************************************
1095        *
1096
1097            SUBROUTINE  TORQUE(  PH,  T  )
1098
1099        *
1100        * this subroutine returns the torque value!
1101        *
1102
1103            IMPLICIT  DOUBLEPRECISION(  A-H, O-Z  )
1104
1105            PARAMETER(   NH=10, NP=(NH+NH+3+NH+2)/2, NF=1,
1106           +    N=NP+NF    )
1107
1108            COMMON     GO, A$
1109           +    /$D$/  NM(NP)
1110
1111            DIMENSION  PH(N)
1112
1113
1114            T$= 0.D0
1115            DO 01, L=1,NP
1116                T$= T$ + DFLOAT( NM(L) )*PH(L)
1117        01  CONTINUE
1118
1119            T= 2.D0/3.D0 * A$ * T$
1120
1121
1122            RETURN
1123
1124            END
1125
1126        *
1127        ***********************************************************************
1128        *
1129
1130            DOUBLEPRECISIONFUNCTION  TRIARE(  XY$  )
1131
1132        *
1133        * this function returns the area of a triangular element!
1134        *
1135
1136            IMPLICIT  DOUBLEPRECISION(  A-H, O-Z  )
1137
1138            DIMENSION  XY$(6)
1139
1140
```

```
1141            X1= XY$(1)
1142            Y1= XY$(2)
1143
1144            X2= XY$(3)
1145            Y2= XY$(4)
1146
1147            X3= XY$(5)
1148            Y3= XY$(6)
1149
1150            D= X1*( Y2-Y3 ) + X2*( Y3-Y1 ) + X3*( Y1-Y2 )
1151            TRIARE=  D/2.DO
1152
1153
1154            RETURN
1155
1156            END
1157
1158      *
1159      ****************************************************************
1160      *
1161
1162            SUBROUTINE  VECOMP(  SF, N, M$, N$,  SF$  )
1163
1164      *
1165      * this subroutine returns vector components!
1166      *
1167
1168            IMPLICIT  DOUBLEPRECISION(  A-H, O-Z  )
1169
1170            DIMENSION  SF(N), M$(N$), SF$(N$)
1171
1172
1173            DO 01, I$=1,N$
1174                SF$( I$ )= SF(  M$(I$)  )
1175         01 CONTINUE
1176
1177
1178            RETURN
1179
1180            END
End of file
```